NASA/TM—2003–212633

Determination of Significant Composite Processing Factors by Designed Experiment

(MSFC Center Director's Discretionary Fund Final Report, Project No. 95–23)

J.L. Finckenor
Marshall Space Flight Center, Marshall Space Flight Center, Alabama

July 2003

The NASA STI Program Office...in Profile

Since its founding, NASA has been dedicated to the advancement of aeronautics and space science. The NASA Scientific and Technical Information (STI) Program Office plays a key part in helping NASA maintain this important role.

The NASA STI Program Office is operated by Langley Research Center, the lead center for NASA's scientific and technical information. The NASA STI Program Office provides access to the NASA STI Database, the largest collection of aeronautical and space science STI in the world. The Program Office is also NASA's institutional mechanism for disseminating the results of its research and development activities. These results are published by NASA in the NASA STI Report Series, which includes the following report types:

- TECHNICAL PUBLICATION. Reports of completed research or a major significant phase of research that present the results of NASA programs and include extensive data or theoretical analysis. Includes compilations of significant scientific and technical data and information deemed to be of continuing reference value. NASA's counterpart of peer-reviewed formal professional papers but has less stringent limitations on manuscript length and extent of graphic presentations.

- TECHNICAL MEMORANDUM. Scientific and technical findings that are preliminary or of specialized interest, e.g., quick release reports, working papers, and bibliographies that contain minimal annotation. Does not contain extensive analysis.

- CONTRACTOR REPORT. Scientific and technical findings by NASA-sponsored contractors and grantees.

- CONFERENCE PUBLICATION. Collected papers from scientific and technical conferences, symposia, seminars, or other meetings sponsored or cosponsored by NASA.

- SPECIAL PUBLICATION. Scientific, technical, or historical information from NASA programs, projects, and mission, often concerned with subjects having substantial public interest.

- TECHNICAL TRANSLATION. English-language translations of foreign scientific and technical material pertinent to NASA's mission.

Specialized services that complement the STI Program Office's diverse offerings include creating custom thesauri, building customized databases, organizing and publishing research results...even providing videos.

For more information about the NASA STI Program Office, see the following:

- Access the NASA STI Program Home Page at ***http://www.sti.nasa.gov***

- E-mail your question via the Internet to help@sti.nasa.gov

- Fax your question to the NASA Access Help Desk at (301) 621–0134

- Telephone the NASA Access Help Desk at (301) 621–0390

- Write to:
  NASA Access Help Desk
  NASA Center for AeroSpace Information
  7121 Standard Drive
  Hanover, MD 21076–1320
  (301)621–0390

NASA/TM—2003–212633

Determination of Significant Composite Processing Factors By Designed Experiment
(MSFC Center Director's Discretionary Fund Final Report, Project No. 95–23)

J.L. Finckenor
Marshall Space Flight Center, Marshall Space Flight Center, Alabama

National Aeronautics and
Space Administration

Marshall Space Flight Center • MSFC, Alabama 35812

July 2003

Acknowledgments

This work was funded by the Center Director's Discretionary Fund of NASA Marshall Space Flight Center (MSFC). It would not have been possible without the work of many people. Programming and coordination of sample manufacturing was done by Bill McMahon (MSFC/ED34), Gary Smith (Thiokol), and Stephen Richardson and Bob Huff (formerly Thiokol). Sample layup and machining was performed by Scott Chambers, Greg Young, and Sam McGee (Thiokol). Sample testing was done by Andy Hodge (MSFC/ED34). Thanks to Drs. Alton Highsmith, John Jackson, and William Nichols of the University of Alabama, Tuscaloosa, for their assistance and technical expertise. Since this work also comprised my Master's thesis, thanks to my wife, Miria, for giving me the support needed to complete my degree.

Available from:

NASA Center for AeroSpace Information
7121 Standard Drive
Hanover, MD 21076–1320
(301) 621–0390

National Technical Information Service
5285 Port Royal Road
Springfield, VA 22161
(703) 487–4650

TABLE OF CONTENTS

LIST OF FIGURES

LIST OF FIGURES (Continued)

LIST OF FIGURES (Continued)

LIST OF TABLES

LIST OF ACRONYMS AND SYMBOLS

A	autoclave cure
ANOVA	analysis of variance (statistical evaluation tool for the designed experiment)
ASTM	American Society for Testing and Materials
ATL	automated tape layer
BMI	bismaleimide (resin)
CNC	computer numerical control
DOF	degree of freedom
H	hand layup
Hg	mercury
MS	mean square (equals SS/DOF)
MTS	Mechanical Testing Simulation Systems Corporation
O	oven cure
PEEK	polyetheretherketone
PMR	polymerization of monomeric reactants
SS	sum of squares
T	tape-laying machine
TM	Technical Memorandum

NOMENCLATURE

*	wildcard (sample identifier)
$\mathbf{A}$	regression matrix
a	number of levels for cure, two—oven cure and autoclave cure
$\mathbf{B}$	array of sample values for regression
b	number of levels for layup, two—hand and tape-laying machine
C	cure, autoclave versus oven (as a factor in the ANOVA)
c	number of levels for thickness, two—8 and 52 plies
DOF_E	degree of freedom of the error
DOF_F	degree of freedom of the factor
E	error
E_1	0° elastic modulus
E_2	90° elastic modulus
E_{1C}	0° elastic modulus, compressive
E_{2C}	90° elastic modulus, compressive
F	F (test value) ($F=MS/MS_E$)
G_{12}	shear modulus
Int	intercept
i	incremental counter
L	layup, hand versus tape-laying machine (as a factor in the ANOVA)
$\mathbf{M}$	relative magnitude of the regression coefficients

NOMENCLATURE (Continued)

MS	mean square (sum of squares for each term divided by degrees of freedom)
MS_E	mean square for error
n	number of replicates in the experiment (two for material properties, six for ply thickness)
P	applied load
P_s	probability of being significant
$\mathbf{R}$	array of regression coefficients
R	regression coefficient
R_{Int}	average of all the data points
S	shear strength
SS	sum of squares
SS_C	cure sum of squares
SS_{C-L}	cure-layup interaction sum of squares
SS_{C-L-T}	cure-layup-thickness interaction sum of squares
SS_{C-T}	cure-thickness interaction sum of squares
SS_{corr}	correction sum of squares
SS_E	error evaluaion sum of squares
SS_L	layup sum of squares
SS_{L-T}	layup-thickness interaction sum of squares
SS_T	thickness sum of squares
SS_{Total}	total sum of squares (each individual value squared and summed, and correction term subtracted)

NOMENCLATURE (Continued)

T	thickness, 8 ply versus 52 ply (as a factor in the ANOVA)
t	specimen thickness
t_{ply}	ply thickness
w	specimen width
X	material property
X_c	0° compressive strength
X_T	0° tensile strength
Y_c	90° compressive strength
Y_T	90° tensile strength
ε_1	axial strain
ε_2	transverse strain
γ	shear strain
ν_{12}	Poisson's ratio
τ	shear stress

TECHNICAL MEMORANDUM

DETERMINATION OF SIGNIFICANT COMPOSITE PROCESSING FACTORS BY DESIGNED EXPERIMENT

(MSFC Center Director's Discretionary Fund Final Report, Project No. 95–23)

1. INTRODUCTION

Structural applications of composite materials are becoming increasingly important to the aerospace industry. A long-term goal of composite material research is to reduce the cost of using composites by simplifying manufacturing. This need is made more imperative by the ever-greater importance being placed on cost in aerospace applications.

The typical method of aerospace composite fabrication is laying up a part by hand or by automated machinery and curing the part in an autoclave. The autoclave pressure provides consolidation of the plies during cure to generate a "good" part. Unfortunately, automated machinery and large autoclaves can be extremely expensive to start up and operate. If there are changes in material properties due to different manufacturing processes and if they can be quantified, it may be possible to reduce manufacturing costs. For example, if a part can be made by hand layup and oven cure while maintaining acceptable safety margins, cost can be reduced and the number of capable vendors can be greatly increased.

This study used a statistically designed experiment, a 2^3 factorial analysis of variation (ANOVA), to determine whether processing variables affect material properties. The variables studied were method of layup (hand versus tape-laying machine), method of cure (oven versus autoclave), and part thickness (8 plies versus 52 plies). Since variations in processing have a more significant effect on the resin than the fiber, fiber-dominated properties, such as 0° tension properties, would not be expected to show much variation. Compression tests would be more likely to show changes or flaws in the parts that might be masked by tension tests. For this reason, and also to reduce the size of the test matrix, tension properties were not included.

To help correlate the material properties studied in the designed experiment, void content was also measured. Voids were measured by microscope and qualitatively compared for each of the processes and materials. The presence of voids was then related back to the indication of property changes.

2. LITERATURE SURVEY

2.1 Composite Material Processing

Yoon et al.[1] studied laminate compaction (thickness) as a real-time function of temperature and pressure. For 16-ply laminates, they found that the same amount of ply compaction could be reached for cure temperatures between 90 °C (195 °F) and 120 °C (250 °F), but the time required to reach full compaction varied. Cure pressures were also varied through 0, 30, and 60 psig with a 90 °C cure and a vacuum bag pulling 29 in. of mercury (Hg). Again, each pressure achieved full compaction but over 50, 70, and 90 min, respectively. They warned that for thicker laminates, higher pressure may be needed to achieve full compaction before the resin gels. Based on compaction alone, this study implied that oven-cured laminates can be just as high quality as autoclaved laminates.

In *Composite Manufacturing Technology*,[2] vacuum pressure and autoclave, or force-action pressure, were treated separately. The application of vacuum is to remove air and volatiles, to give reliable contact to the molding fixture, and to squeeze out excess resin. The force action of the autoclave pressure helps shape forming and facilitates squeezing out excess binder. Bratukhin and Bogolyubov[2] concluded that it is best to have no autoclave pressure if the formed shape is simple enough to allow molding without it. Autoclave pressure on a complicated part can give an uneven and undesirable force distribution over the surface.

Carpenter[3] addressed the interrelationships of volatiles, physiochemical, and mechanical properties of AS4/3501–6. One aspect of testing placed 3501–6 resin at 95 °C (203 °F) at a vacuum of 29 in. of Hg. When placed under vacuum, a large quantity of bubbles formed in the viscous fluid. Water was considered the most likely volatile since most of the bubbles formed after reducing the pressure on the resin below water's vapor pressure. The conclusion from this test was that to produce low void composites, processing conditions must be controlled to either remove the volatiles or retain them in solid solution.

Johnson[4] studied the effect of both areal size as well as thickness on coupon material properties for AS4/3502 and APC–2 graphite/polyetheretherketone. His results showed that quasi-isotropic layups were stiffer for thicker layups, at least at higher stress levels where plies were exhibiting damage. The effect of thickness on strength depended on the relative amount of 0° plies in the layup. He concluded that scaling effects could be linked directly to damage propagation in plies that contributed the most to the strength and stiffness of the laminate. This made scaling effects more pronounced in layups with matrix-dominated properties.

Camponeschi's dissertation[5] included a review of the wide variety of compression test setups that have been used. The conclusion was that no single test fixture is adequate for all specimens. He also stated that the modulus of elasticity is not affected by the loading method. The greater concern is with material strength. He studied AS4/3501–6 at 48, 96, and 192 plies with layups of $[0]_n$ and $[0_2/90]_n$. Results did not show significant changes for modulus. The data showed significant drops in strength as thickness increased, but this was attributed to end effects from the test fixture. He concluded that failures in thick composites, as previously postulated for thin composites, initiate at a local stress concentration at a point of geometric or material inhomogeneity. This leads to a shear-dominated instability which propagates through the part.

Gipple[6] compared thick and thin properties of wet and dry AS4/3501–6 $[0_2/90]_{ns}$ laminates. The $[0_2/90]$ layup was used to help alleviate brooming of the ends of end-loaded, unidirectional compression samples. The fiber-dominated layups had no difference in strength when dry, but the thick samples lost strength when saturated. The modulus was not affected by either thickness or moisture.

Vannucci[7] studied the affect of autoclave pressure as well as degree of resin advancement and heating rate on the mechanical properties of polymerization of monomeric reactant polyimide composites. When originally developed, polyimides required autoclave cure pressures between 500 and 1,000 lb/in^2. This has been dropped to 200 lb/in^2. Vannucci cured samples at 50, 100, and 200 lb/in.^{2} Strength decreased as cure pressure decreased, with greater differences between the 50 and 100 lb/in.^{2} samples and small changes from 100 to 200 lb/in^2. It was also noted that void content increased significantly as cure pressure went down.

A joint NASA/General Dynamics composite intertank study[8] baselined oven curing because of the cost required for a 30-ft-diameter autoclave facility. Most of the material properties studies were for T300/934 graphite/epoxy, but some data were included for the toughened epoxy resin system T300/8553–50. Layups using combined hand-layed, filament-wound laminates had significant air entrapment from gaps left during the layup process. The reduced pressure of oven curing was unable to remove the air. To reduce the amount of air trapped in the part during the layup process, filament winding was replaced by automated tape laying. Oven curing did not affect the tensile properties, but the matrix-dominated properties of compression and shear were somewhat degraded from the autoclave-cured properties. Tape laying was significantly beneficial over the filament-wound, hand-layed process and increased compression strength by 20 percent and in-plane shear strength by 10 percent.

2.2 Design of Experiments[9]

Designed experiments are used to determine how changes in controls or inputs affect the response of a process or system. Since there is a natural variation in material properties and testing, a statistically designed experiment is required. This means the data must be collected in a manner that lends itself to statistical analysis.

A factorial design is an experiment in which all the possible combinations of the factors that can be varied are studied. It is possible to have partial factorial experiments, which reduce the number of individual tests to be run, but this study used a full factorial experiment. In this study, all the factors had two levels, so this is called a 2^n factorial experiment. Since there were three factors, it was a 2^3 factorial experiment with 2*2*2=8 possible combinations for any given material property. To gain statistical significance and a measure of the error (natural deviations), two replicates were run of each combination for a total of 16 tests for each given material and property.

3. EXPERIMENTAL PROCEDURE

In a study such as this, the designed experiment is used as a screen to determine which properties are particularly sensitive to the manufacturing processes. To complete the ANOVA, 16 samples were needed for each material property. Studying four materials and performing three sets of tests for each material (thick compression, thin compression, and tension shear) produced a large amount of data. Of course, for any new material or manufacturing process, the properties used in the analysis of the structure should be developed with coupons manufactured using the same techniques as the part.

A 0° compression test, a 90° compression test, and a shear test were used to provide E_{1C}, E_{2C}, G_{12}, and ν_{12}. Since part thickness was a factor, the standard American Society for Testing and Materials (ASTM) tests, D3410[10] for compression and D3518[11] for shear, could not be used since they define specific thicknesses. Because the specimens were nonstandard, many of the failures occurred near the sample ends or inside the grips and cannot be considered valid. A brief discussion of the strength results for X_C, Y_C, and S is included in appendix A.

Since the experiment is a statistical evaluation, it was important to remove as many extraneous variables as possible. Toward this end, all layups were made by a single technician and all testing was performed by a single operator.

Void content was measured by cutting 1-in. ends off the shear specimens, polishing them, and observing the cross section under a microscope. The microscope was connected to a computer which was used to digitize the image. The number of pixels in the darkest areas, the voids, were summed up by the computer and compared against the total pixels in the image. This was not a rigorous analysis and does not conform to ASTM D2734[12] for determination of void content but was intended as a qualitative comparison of the voids between the different processes. Even the reliability of ASTM D2734 is unclear in that it "does not yet contain a numerical precision and bias statement and it shall not be used as a referee method in case of dispute" (p. 3, sec. 11.1).

3.1 Materials

AS4/3501–6 is an older graphite/epoxy system that has been used in many applications. The material used was Hercules AS4/3501–6 automated tape layer (ATL) grade prepreg tape with a 62-percent fiber volume and a fiber areal weight of 4.4 oz/yd^2.

IM7/8551–7 is a common, high-performance graphite/epoxy system using the stronger, stiffer IM7 fiber and toughened 8551–7 epoxy resin. The material used was Hercules Magnamite IM7/8551–7 prepreg tape with a fiber volume of 62 percent and a fiber areal weight of 4.25 oz/yd^2.

IM7/F655 has the IM7 fiber and a bismaleimide (BMI) matrix allowing operational temperatures >400 °F and single-use temperatures >700 °F. The graphite/BMI used was Hexcel T9A 145 3-in. HX 1568 ATL grade with a fiber areal weight of 4.25 oz/yd^2.

IM7/F584 uses a resin chemically similar to 3501–6 with the stiffer fiber. Because of material availability, only the shear tests were performed on IM7/F584. The material used was Hercules IM7/F584 with a fiber areal weight of 4.25 oz/yd^2.

The honeycomb for the series sample tests labeled AA and AB was Hexcel CRIII–1/4–5052–0.0015P–3.4, 1.5 in. thick, and was bonded in place using 3M AF–191K, 0.080 lb/ft^2 weight structural adhesive film.

3.2 Test Samples

Six different types of specimens were used, as detailed in the sample drawings in appendix B. Vacuum debulks were applied to the first ply of every sample and every eighth ply for the thick specimens. Cure cycles for the different materials are shown in appendix C.

To stabilize the 8-ply samples during compression tests, they were bonded to a honeycomb core after cure. This was a nonstandard test configuration; however, Kim and Crasto[13] cured composite material onto a partially cured resin plate which became a sandwich core and performed compression tests per ASTM D3410. Also, test standard ASTM D5467[14] obtains compression properties by bonding cured skins onto a high-density core which is then tested in bending.

The 8-ply compression tests were labeled AA for the 0° specimens and AB for the 90° specimens. The first specimens tested were potted into channels and then placed between platens of the test machine. It became apparent that the potted samples were not providing good failure data and the potting was eliminated for the following tests. The samples were placed directly between the platens of the test machine. This variation in testing would have invalidated strength data, but based on the previously referenced work by Camponeschi,[5] modulus data are unaffected by loading method.

The 52-ply tests were similar to ASTM D695.[15] Small samples of the thick laminates were made and placed directly between the platens of the testing machine. AC indicated 0° specimens and AD indicated 90° specimens.

Except for the thickness, the shear tests were by ASTM D3518 (which refers to ASTM D3039[16] for specimen geometry and testing). These samples were ±45° layups which were tested in tension to provide shear data. AE indicated the 8-ply specimens and AF was for the 52-ply specimens.

3.3 Specimen Identification

The specimens are identified by a code string which identifies test series, material, cure method, layup method, thickness, and replicate. Test series identifiers are AA, AB, AC, AD, AE, and AF as indicated in section 3.2 on test samples. Material identifiers are "3" for AS4/3501–6, "8" for IM7/8551–7, "B" for IM7/F655 (BMI), and "4" for IM7/F584. Cure identifiers are "O" for oven cure (using vacuum bag pressure only) and "A" for autoclave cure. Layup identifiers are "H" for hand layup and "T" for layup by tape-laying machine. Thickness identifiers are "8" for 8-ply laminates and "52" for 52-ply laminates. The thickness is redundant since all samples within a given test are the same thickness, but including the thickness identifier makes it easier to quickly identify a specific property. Replicate identifiers are the serial numbers "1" and "2."

As an example, AF–8–O–T–52–2 is the second sample of test series AF (thick tension-shear test) using IM7/8551–7, oven-curing, tape-laying, 52 plies thick.

3.4 Manufacturing Equipment

The tape-laying machine was a Cincinnati Milicron, 10-axis Gantry-type model AE with A975 computer numerical code control. The oven used for curing was built for NASA by the Despatch Oven Company, has a 20 × 30 × 20 ft working space, and is equipped with a Molytech data recorder and dimensions controller. The autoclave used for curing, built by the Harvick Manufacturing Corporation, is 12 ft deep with a diameter of 9 ft and has 150 lb/in.^{2} and 600 °F maximums. The tape-laying machine, oven, and autoclave are all located in building 4707 at NASA Marshall Space Flight Center.

3.5 Test Equipment

The strain gauges used for the AA, AB, AE, and AF tests were CEA–05–125UW–350 and CEA–05–125UT–350. The AC and AD test series used extensometers made by the Mechanical Testing and Simulation (MTS) Systems Corporation, Ext 632.26E–30, with a 0.3-in.-gauge length.

AC and AD samples were tested in an MTS model No. 310.50, 1,000-kip machine. All other samples were tested in an Instron® model No. 4507, 40-kip machine. The signal conditioner was a Sig Con 2311. Test rates were 0.05 in./min for all tests.

The void content samples were 1-in. ends cut off by a bandsaw from the tabbed ends of the AE and AF samples. All had been tested to failure except the AF BMI samples which were cut from excess material. The cross section was polished using 600-grit silicon carbide grinding paper on a Buehler Ecomet® 3 grinder/polisher. The samples were observed using a Leica WILD M420 stereo microscope with a WILD 400076APO zoom 1:6 lens. Images were scanned using a Pulnix progressive scan camera and Media Cybernetics® Image-Pro® Plus 3.0.01.00 for Microsoft Windows® 95/NT.

4. ANALYSIS

4.1 Modulus and Strength Data

All of the raw data were read into Microsoft® Excel (version 7.0 for Windows 95) spreadsheets. Plots of the stress-strain curves are shown in appendix D. Raw data were provided as load versus strain. Load was converted to stress using individually measured specimen dimensions.

The curves were plotted and the largest stress range in which all the samples provided good data was identified. The low end of the range is the lowest stress which is past the startup noise for all the samples. The high end of the range is the highest possible stress that remained in the linear portion of the curve for all samples except for the shear samples discussed below. The low and high stress values were determined by inspection and comparison of the plotted data. Ranges were kept constant for each material and property. The modulus was determined from this range of data points using the Excel Slope spreadsheet function which returns the slope of the linear regression line through the data. Strengths were taken as the peak value for stress.

In series AA and AC, ν_{12} was calculated by dividing the slope of the axial stress-strain curve by the slope of the transverse stress-strain curve. In series AC and AD, the second available data channel measured the output from a redundant axial strain gauge on the back side of the sample. The average of the two moduli, which typically agreed to within a few percent, was used as the E_2 value for that specimen. In series AE and AF, the shear stress and shear strain were calculated from the axial and transverse strain data according to ASTM D3518. The equations for shear stress and shear strain are

$$\tau = \frac{P}{2 * w * t} \tag{1}$$

and

$$\gamma = \varepsilon_1 - \varepsilon_2 \ . \tag{2}$$

G_{12} is the slope of the shear stress versus shear strain curve, but this curve is nonlinear with a gradual flattening of the curve as stress increases. Since there is no linear region on the curve, the Excel Slope function was used to calculate modulus for data from 0.5 to 1 ksi, 0.5 to 3 ksi, 0.5 to 7 ksi, and 0.5 to 10 ksi. This approach results in four different shear modulus values that can highlight differences occurring at varying stress levels. It would have been equally valid to calculate modulus in four contiguous segments; e.g., 0.5 to 1 ksi, 1 to 3 ksi, 3 to 7 ksi, and 7 to 10 ksi. However, this approach was not chosen because it would have tended to artificially magnify differences in slope, particularly between 7 and 10 ksi.

4.2 Statistical Evaluation, ANOVA

Once all the strengths and moduli were calculated from the raw data, they were compiled into Excel spreadsheets for statistical evaluation. These spreadsheets are shown in appendix E.

The actual strength and moduli values were tabulated along with the individual sample average ply thicknesses. All of the values, except for ν_{12}, were also normalized to a single-ply thickness in an attempt to evaluate the properties for a nominal design ply thickness. The properties were normalized by

$$X_{\text{normalized}} = X_{\text{actual}} * \frac{t_{\text{ply(actual)}}}{t_{\text{ply(nominal)}}} \ . \tag{3}$$

The statistical evaluation of the data was done by an ANOVA. A typical material property ANOVA is shown in table 1. The number of levels was two for all three factors—*a*, *b*, and *c*. For the material property ANOVA's, the number of replicates, *n*, was two; and for the ply thickness ANOVA's, *n* was six. Since there were three types of samples for each thickness, the number of replicates was tripled. For the thickness ANOVA table, the error degrees of freedom (DOF's) was 40 and the total DOF's was 47. The primary input to the ANOVA table was the sum of squares (SS). Equations (4)–(14) were used for each material and property. The values were identified by the cure (*C*), layup (*L*), and thickness (*T*) sample identifiers.

Table 1. Material property ANOVA

Factor	DOF	*SS*	*MS=SS*/DOF	*F* Test
C	$1 = a-1$	SS_C	$SS_C/1$	MS_C/MS_E
L	$1 = b-1$	SS_L	$SS_L/1$	MS_L/MS_E
T	$1 = c-1$	SS_T	$SS_T/1$	MS_T/MS_E
C–L	$1 = (a-1)*(b-1)$	SS_{C-L}	$SS_{C-L}/1$	MS_{C-L}/MS_E
C–T	$1 = (a-1)*(c-1)$	SS_{C-T}	$SS_{C-T}/1$	MS_{C-T}/MS_E
L–T	$1 = (b-1)*(c-1)$	SS_{L-T}	$SS_{L-T}/1$	MS_{L-T}/MS_E
C–L–T	$1 = (a-1)*(b-1)*(c-1)$	SS_{C-L-T}	$SS_{C-L-T}/1$	MS_{C-L-T}/MS_E
E	$8 = a*b*c*(n-1)$	SS_E	$SS_E/8$	
Total	$15 = a*b*c*n-1$	SS_{Total}		

The correction SS, SS_{corr}, was used in the calculation of the individual SS values:

$$SS_{corr} = \frac{\left(\sum_{i=1}^{n}\left(X_{\text{OH8}i} + X_{\text{AH8}i} + X_{\text{OT8}i} + X_{\text{AT8}i} + X_{\text{OH52}i} + X_{\text{AH52}i} + X_{\text{OT52}i} + X_{\text{AT52}i}\right)\right)^2}{a*b*c*n} \ . \tag{4}$$

The cure SS, SS_C, was

$$SS_C = \frac{\left(\sum_{i=1}^{n}\left(X_{\mathrm{OH8}i} + X_{\mathrm{OT8}i} + X_{\mathrm{OH52}i} + X_{\mathrm{OT52}i}\right)\right)^2}{b * c * n}$$

$$+ \frac{\left(\sum_{i=1}^{n}\left(X_{\mathrm{AH8}i} + X_{\mathrm{AT8}i} + X_{\mathrm{AH52}i} + X_{\mathrm{AT52}i}\right)\right)^2}{b * c * n} - SS_{corr} \; . \tag{5}$$

The layup SS, SS_L, was

$$SS_L = \frac{\left(\sum_{i=1}^{n}\left(X_{\mathrm{OH8}i} + X_{\mathrm{AH8}i} + X_{\mathrm{OH52}i} + X_{\mathrm{AH52}i}\right)\right)^2}{a * c * n}$$

$$+ \frac{\left(\sum_{i=1}^{n}\left(X_{\mathrm{OT8}i} + X_{\mathrm{AT8}i} + X_{\mathrm{OT52}i} + X_{\mathrm{AT52}i}\right)\right)^2}{a * c * n} - SS_{corr} \; . \tag{6}$$

The thickness SS, SS_T, was

$$SS_T = \frac{\left(\sum_{i=1}^{n}\left(X_{\mathrm{OH8}i} + X_{\mathrm{AH8}i} + X_{\mathrm{OT8}i} + X_{\mathrm{AT8}i}\right)\right)^2}{a * b * n}$$

$$+ \frac{\left(\sum_{i=1}^{n}\left(X_{\mathrm{OH52}i} + X_{\mathrm{AH52}i} + X_{\mathrm{OT52}i} + X_{\mathrm{AT52}i}\right)\right)^2}{a * b * n} - SS_{corr} \; . \tag{7}$$

The cure-layup interaction SS, SS_{C-L}, was

$$SS_{C-L}=\frac{\left(\sum_{i=1}^{n}\left(X_{\mathrm{OH8}i}+X_{\mathrm{OH52}i}\right)\right)^2}{c*n}+\frac{\left(\sum_{i=1}^{n}\left(X_{\mathrm{AH8}i}+X_{\mathrm{AH52}i}\right)\right)^2}{c*n}$$

$$+\frac{\left(\sum_{i=1}^{n}\left(X_{\mathrm{OT8}i}+X_{\mathrm{OT52}i}\right)\right)^2}{c*n}+\frac{\left(\sum_{i=1}^{n}\left(X_{\mathrm{AT8}i}+X_{\mathrm{AT52}i}\right)\right)^2}{c*n}-SS_{corr}-SS_C-SS_L\ . \qquad (8)$$

The cure-thickness interaction SS, SS_{C-T}, was

$$SS_{C-T}=\frac{\left(\sum_{i=1}^{n}\left(X_{\mathrm{OH8}i}+X_{\mathrm{OT8}i}\right)\right)^2}{b*n}+\frac{\left(\sum_{i=1}^{n}\left(X_{\mathrm{AH8}i}+X_{\mathrm{AT8}i}\right)\right)^2}{b*n}+\frac{\left(\sum_{i=1}^{n}\left(X_{\mathrm{OH52}i}+X_{\mathrm{OT52}i}\right)\right)^2}{b*n}$$

$$+\frac{\left(\sum_{i=1}^{n}\left(X_{\mathrm{AH52}i}+X_{\mathrm{AT52}i}\right)\right)^2}{b*n}-SS_{corr}-SS_C-SS_T\ . \qquad (9)$$

The layup-thickness interaction SS, SS_{L-T}, was

$$SS_{L-T}=\frac{\left(\sum_{i=1}^{n}\left(X_{\mathrm{OH8}i}+X_{\mathrm{AH8}i}\right)\right)^2}{a*n}+\frac{\left(\sum_{i=1}^{n}\left(X_{\mathrm{OT8}i}+X_{\mathrm{AT8}i}\right)\right)^2}{a*n}+\frac{\left(\sum_{i=1}^{n}\left(X_{\mathrm{OH52}i}+X_{\mathrm{AH52}i}\right)\right)^2}{a*n}$$

$$+\frac{\left(\sum_{i=1}^{n}\left(X_{\mathrm{OT52}i}+X_{\mathrm{AT52}i}\right)\right)^2}{a*n}-SS_{corr}-SS_L-SS_T\ . \qquad (10)$$

The cure-layup-thickness interaction SS, SS_{C-L-T}, was

$$SS_{C-L-T} = \frac{\left(\sum_{i=1}^{n} X_{\mathrm{OH8}i}\right)^2}{n} + \frac{\left(\sum_{i=1}^{n} X_{\mathrm{AH8}i}\right)^2}{n} + \frac{\left(\sum_{i=1}^{n} X_{\mathrm{OT8}i}\right)^2}{n} + \frac{\left(\sum_{i=1}^{n} X_{\mathrm{AT8}i}\right)^2}{n}$$

$$+ \frac{\left(\sum_{i=1}^{n} X_{\mathrm{OH52}i}\right)^2}{n} + \frac{\left(\sum_{i=1}^{n} X_{\mathrm{AH52}i}\right)^2}{n} + \frac{\left(\sum_{i=1}^{n} X_{\mathrm{OT52}i}\right)^2}{n} + \frac{\left(\sum_{i=1}^{n} X_{\mathrm{AT52}i}\right)^2}{n}$$

$$-SS_{corr} - SS_C - SS_L - SS_T - SS_{C-L} - SS_{C-T} - SS_{L-T} \ . \tag{11}$$

The total SS, SS_{Total}, was each individual value squared and summed, and the correction term subtracted:

$$SS_{\mathrm{Total}} = X_{\mathrm{OH81}}{}^2 + X_{\mathrm{OH82}}{}^2 + X_{\mathrm{AH81}}{}^2 + X_{\mathrm{AH82}}{}^2 + X_{\mathrm{OT81}}{}^2$$

$$+ X_{\mathrm{OT82}}{}^2 + X_{\mathrm{AT81}}{}^2 + X_{\mathrm{AT82}}{}^2 + X_{\mathrm{OH521}}{}^2 + X_{\mathrm{OH522}}{}^2 + X_{\mathrm{AH521}}{}^2$$

$$+ X_{\mathrm{AH522}}{}^2 + X_{\mathrm{OT521}}{}^2 + X_{\mathrm{OT522}}{}^2 + X_{\mathrm{AT521}}{}^2 + X_{\mathrm{AT522}}{}^2 - SS_{corr} \ . \tag{12}$$

The SS for the error evaluation, SS_E, was used to quantify the scatter in the data:

$$SS_E = SS_{\mathrm{Total}} - SS_C - SS_L - SS_T - SS_{C-L} - SS_{C-T} - SS_{L-T} - SS_{C-L-T} \ . \tag{13}$$

The DOF's were determined by the number of samples in the experiment and were used in evaluating the probability of differences caused by the given factor. Interaction DOF's were the products of the individual DOF's. The total DOF's was one less than the total number of samples run. The error DOF's was the difference between the total DOF and the DOF's claimed by the factors and their interactions.

The mean square (MS) was the SS for each term divided by the DOF. The F-test evaluation was each factor's MS divided by the MS for error, MS_E. A large MS_E indicates a lot of variation in the samples and makes it more difficult to find differences. A large MS for a factor indicates a strong difference between the levels of the factor.

The F-test evaluation was then used to determine P_s, the probability that the given factor was significant. This was done using the Excel FDIST spreadsheet function. FDIST returns the F probability distribution. F is the F-test value, and DOF_F and DOF_E are the degrees of freedom of the factor of interest and the error, respectively:

$$P_S = 1 - \mathrm{FDIST}(F, \mathrm{DOF}_F, \mathrm{DOF}_E) \ . \tag{14}$$

4.3 Statistical Evaluation, Regression

The ANOVA defines the confidence of there being differences between the levels of a factor but gives no indication of the direction or magnitude of the difference. To find this information, a multivariate regression analysis was applied. For this, the lower levels, oven cure, hand layup, and 8 plies were identified with a –1. The upper levels, autoclave cure, tape-laying machine, and 52 plies, were identified with a 1. Using these levels, the regression matrix, equation (15), was established. "Int" is the intercept column, and is set to 1. "C" is for cure, "L" is for layup, and "T" is for thickness. The interaction terms are the products of their factors. The same method is applied to the ply thickness data by increasing the rows of **A** and **B** and including all six data points for each variation:

$$\mathbf{A} = \begin{array}{c} \begin{array}{cccccccc} Int & C & L & T & CL & LT & CT & CLT \end{array} \\ \begin{bmatrix} 1 & -1 & -1 & -1 & 1 & 1 & 1 & -1 \\ 1 & -1 & -1 & -1 & 1 & 1 & 1 & -1 \\ 1 & 1 & -1 & -1 & -1 & 1 & -1 & 1 \\ 1 & 1 & -1 & -1 & -1 & 1 & -1 & 1 \\ 1 & -1 & 1 & -1 & -1 & -1 & 1 & 1 \\ 1 & -1 & 1 & -1 & -1 & -1 & 1 & 1 \\ 1 & 1 & 1 & -1 & 1 & -1 & -1 & -1 \\ 1 & 1 & 1 & -1 & 1 & -1 & -1 & -1 \\ 1 & -1 & -1 & 1 & 1 & -1 & -1 & 1 \\ 1 & -1 & -1 & 1 & 1 & -1 & -1 & 1 \\ 1 & 1 & -1 & 1 & -1 & -1 & 1 & -1 \\ 1 & 1 & -1 & 1 & -1 & -1 & 1 & -1 \\ 1 & -1 & 1 & 1 & -1 & 1 & -1 & -1 \\ 1 & -1 & 1 & 1 & -1 & 1 & -1 & -1 \\ 1 & 1 & 1 & 1 & 1 & 1 & 1 & 1 \\ 1 & 1 & 1 & 1 & 1 & 1 & 1 & 1 \end{bmatrix} \end{array} \qquad \mathrm{B} = \begin{bmatrix} X_{\mathrm{OH81}} \\ X_{\mathrm{OH82}} \\ X_{\mathrm{AH81}} \\ X_{\mathrm{AH82}} \\ X_{\mathrm{OT81}} \\ X_{\mathrm{OT82}} \\ X_{\mathrm{AT81}} \\ X_{\mathrm{AT82}} \\ X_{\mathrm{OH521}} \\ X_{\mathrm{OH522}} \\ X_{\mathrm{AH521}} \\ X_{\mathrm{AH522}} \\ X_{\mathrm{OT521}} \\ X_{\mathrm{OT522}} \\ X_{\mathrm{AT521}} \\ X_{\mathrm{AT522}} \end{bmatrix} \ . \tag{15}$$

The coefficient array is calculated by

$$\mathbf{R} = (\mathbf{A}^{\mathbf{T}} * \mathbf{A})^{-1} * \mathbf{A}^{\mathbf{T}} * \mathbf{B} = \begin{bmatrix} R_{Int} \\ R_C \\ R_L \\ R_T \\ R_{CL} \\ R_{CT} \\ R_{LT} \\ R_{CLT} \end{bmatrix} . \tag{16}$$

The resulting regression equation, where C, L, and T are –1 or 1, is

$$X_{\text{Estimated}} = R_{Int} + R_C * C + R_L * L + R_T * T + R_{CL} * C * L$$

$$+ R_{CT} * C * T + R_{LT} * L * T + R_{CLT} * C * L * T \ . \tag{17}$$

Since the factor inputs are –1 and 1, R_{Int} becomes the average of all the data points. The magnitudes of each change are related to the intercept value. **R** was doubled since the factor inputs span –1 to 1:

$$\mathbf{M} = \frac{2 * \mathbf{R}}{R_{Int}} \ . \tag{18}$$

5. RESULTS

5.1 Observations of Failures

5.1.1 Series AA, 0°, 8 Ply

Most of the AS4/3501 samples failed in the skin-to-honeycomb bond, with a small amount of brooming/crushing at the very end of the sample. Sample AA–3–A–H–8–1 did not debond from the honeycomb and had significantly more brooming than the other samples. AA–3–A–T–8–2 had one face completely debond from the core. Figure 1 shows sample AA–3–A–H–8–2 with a typical AS4/3501–6 debond failure.

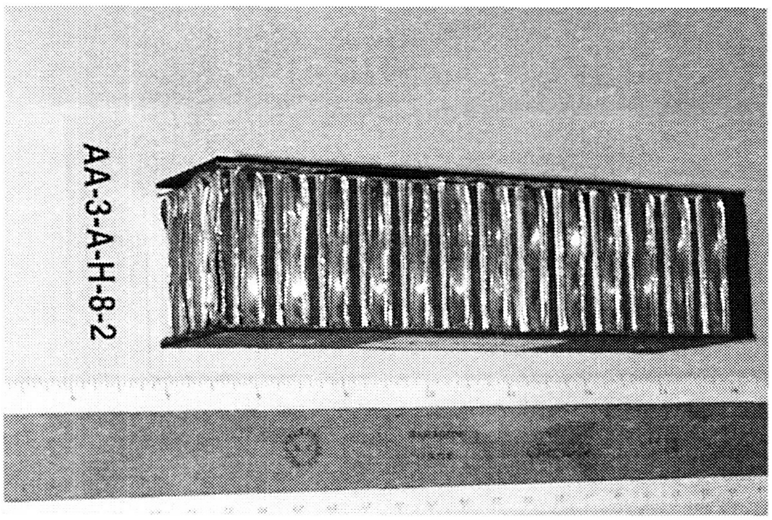

Figure 1. Failed sample AA–3–A–H–8–2.

Most of the IM7/BMI samples failed with at least one skin debonding completely from the honeycomb and a small amount of brooming/crushing at the ends. Samples AA–B–A–H–8–1 and AA–B–O–T–8–2 did not debond and showed greater crushing damage at the ends. Figure 2 shows sample AA–B–A–H–8–2 with a typical IM7/BMI debond failure.

The IM7/8551 samples were the first ones tested. AA–8–A–H–8 and AA–8–O–H–8 were potted in epoxy-filled aluminum channels, but it was determined that this added a great deal of complexity to the tests and very little value. All of the potted samples had the faces debond from the core, but AA–8–O–H–8–1 had greater damage to the faces, with breaks occuring over the length of the face in the 0° direction. All of the unpotted samples failed by crushing/brooming at the ends with no evidence of core debonding. Figure 3 shows sample AA–8–O–H–8–1 potted in the aluminum channel.

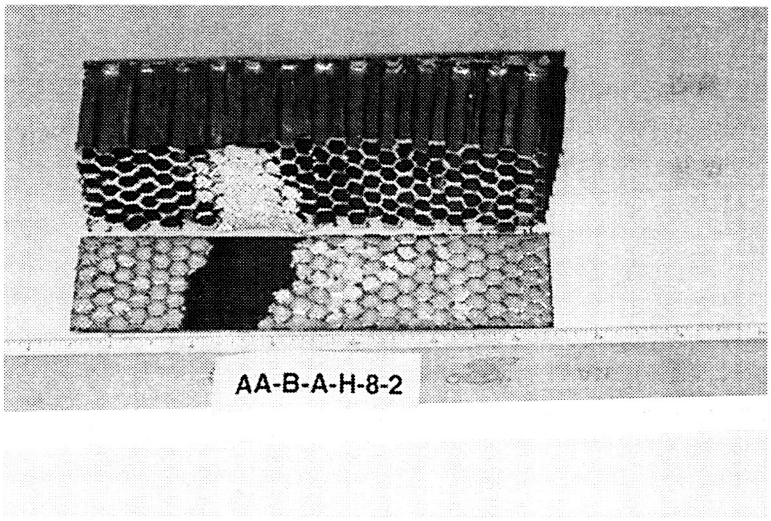

Figure 2. Failed sample AA–B–A–H–8–2.

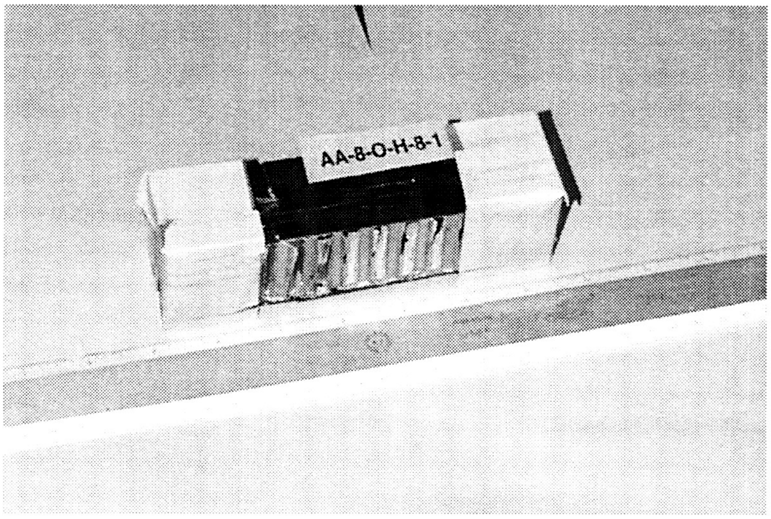

Figure 3. Failed sample AA–8–O–H–8–1.

Failures within a given material were relatively consistent. Between materials, the IM7/BMI failed consistently by debonding; the AS4/3501 debonded, but there was some brooming on the ends; and the IM7/8552 showed very little evidence of debonding.

5.1.2 Series AB, 90°, 8 Ply

All of the AS4/3501 failures were near an end. All samples exhibited very localized crushing of the faces, while several (OH82, AT82, AH81, and AH82) also had small pieces break off within 0.75 in. of the ends. These breaks were parallel to the fiber, as would be expected. Figure 4 shows the local crushing on sample AB–3–O–T–8–2.

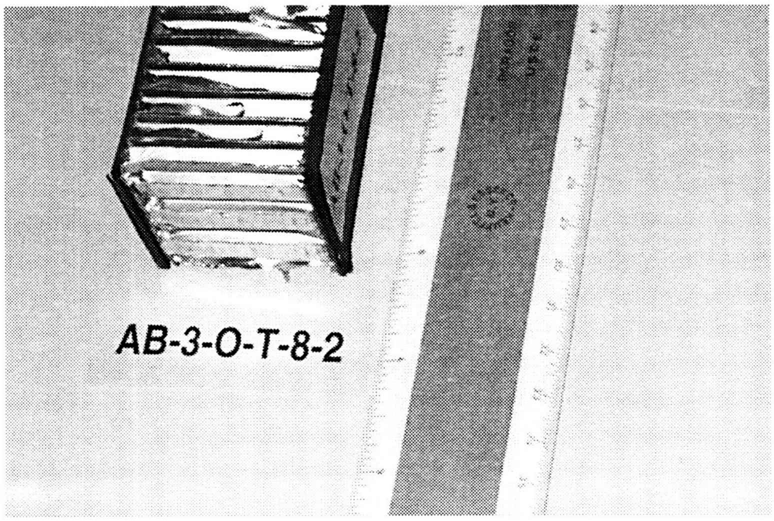

Figure 4. Failed sample AB–3–O–T–8–2.

All of the IM7/BMI failures were breaks parallel to the fiber at some distance in from the edge. The closest failures to the edge were on the A–T–8 samples, with the breaks ≈0.5 in. from the edge. Figure 5 shows the fiber parallel break on sample AB–B–A–H–8–1.

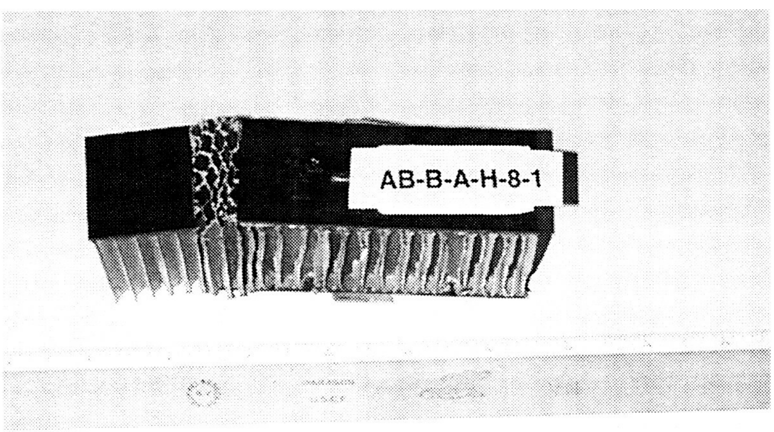

Figure 5. Failed sample AB–B–A–H–8–1.

The IM7/8551 failures were all at the ends and parallel to the fibers. The IM7/BMI samples failed closer to the centers than both the IM7/8551 and AS4/3501 samples. The 3501 samples showed crushing on the ends.

5.1.3 Series AC, 0°, 52 Ply

All of the AS4/3501 samples had cracks running the full length of the sample, parallel to the fibers. There was also crumbling of the samples at one end. This was particularly clear on the A–H–52 samples, to a lesser extent on A–T–52 and O–T–52, and least on O–H–52. The O–T–52 samples had multiple full-length cracks which were not clearly seen in the other samples. Figure 6 shows sample AC–3–A–H–52 with the axial cracks and the crumbled end.

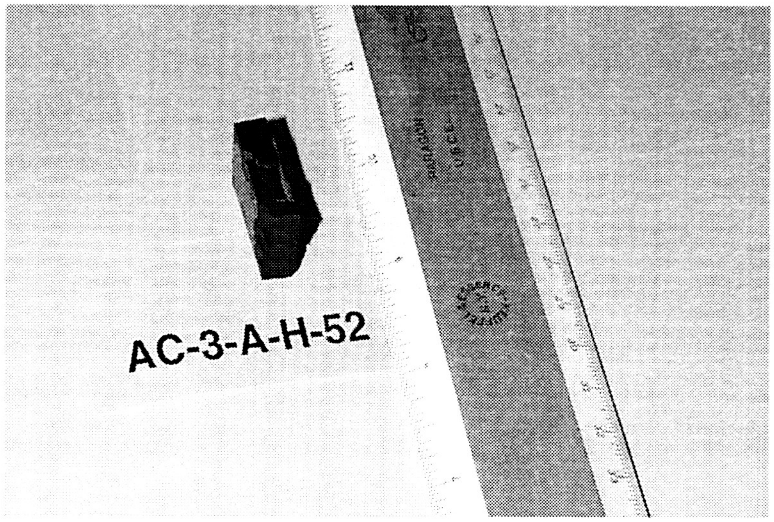

Figure 6. Failed sample AC–3–A–H–52.

All of the IM7/BMI samples had lengthwise cracks, but exhibited very little edge crumbling. The AC–B–O–T–52 samples, similar to the AC–3–O–T–52 samples, had multiple lengthwise cracks. AC–B–O–T–52–2 is shown in figure 7.

The IM7/8551 samples had lengthwise cracks with very little edge crumbling. However, for at least one sample of each factor group, a dislocation near an end was visible. That is, there was a lengthwise crack intersecting through the thickness crack, shown in figure 8.

There were clear material differences for the AC tests. The AS4/3501 samples crumbled on the ends, the IM7/8551 samples had transverse as well as longitudinal cracks, and the IM7/BMI samples had very little end damage. The OT samples for AS4/3501 and IM7/BMI had multiple interlaminar cracks, but this trend did not continue to the IM7/8551 samples.

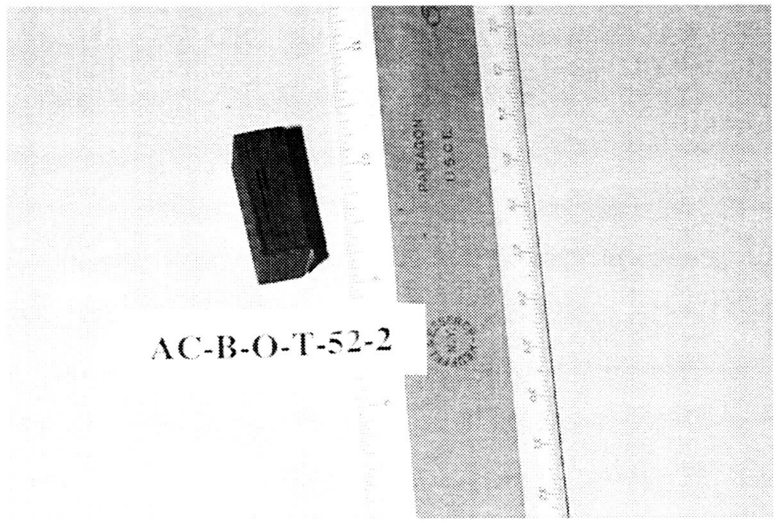

Figure 7. Failed sample AC–B–O–T–52–2.

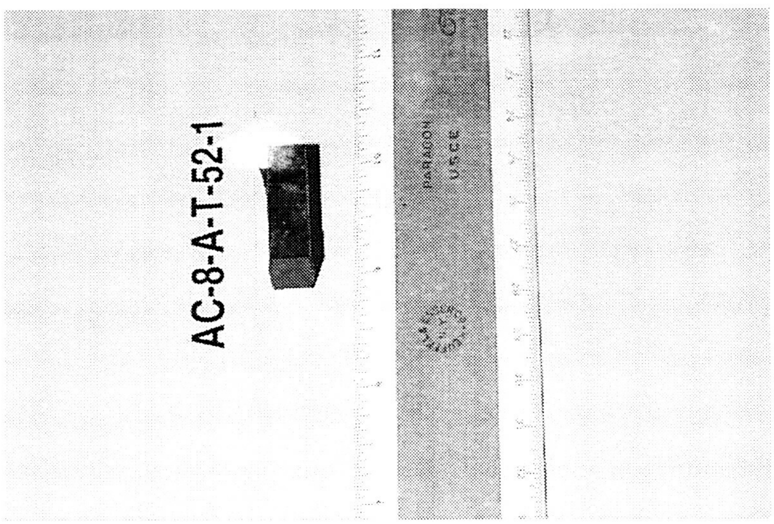

Figure 8. Failed sample AC–8–A–T–52–1.

5.1.4 Series AD, 90°, 52 Ply

The AD sample failures were consistent between materials and factors. They all had multiple cracks through the width of the sample with no clear affinity for interlaminar failures. A typical failure is shown in figure 9 with sample AD–8–A–T–52–1.

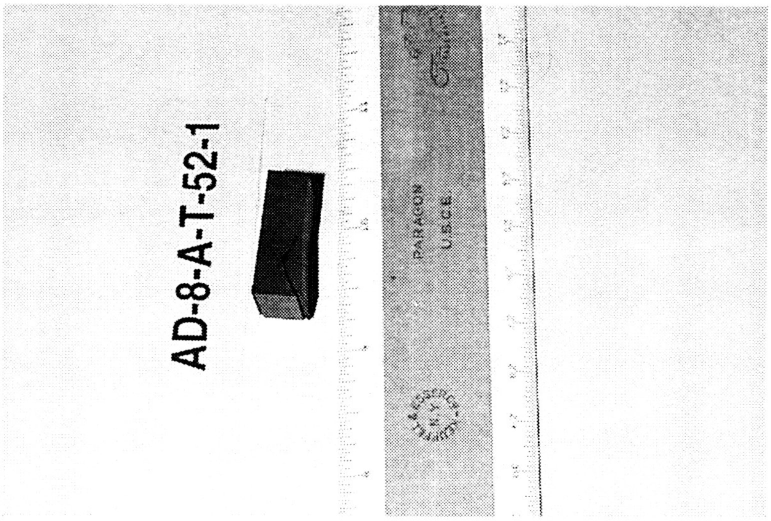

Figure 9. Failed sample AD–8–A–T–52–1.

5.1.5 Series AE, Shear Samples, 8 Ply

Failures for all materials and factors appeared as expected. Many of the failures occurred in or near the tapered grip tabs. Similar tests made and tested by the same people showed much better failure results (in the gauge region) with square tabs, indicating that tapered tabs as shown in ASTM D3039 are ineffective. Figures 10 and 11 show a failure in the gauge length, AE–3–O–H–8, and within the tabs, AE–B–O–H–8–2.

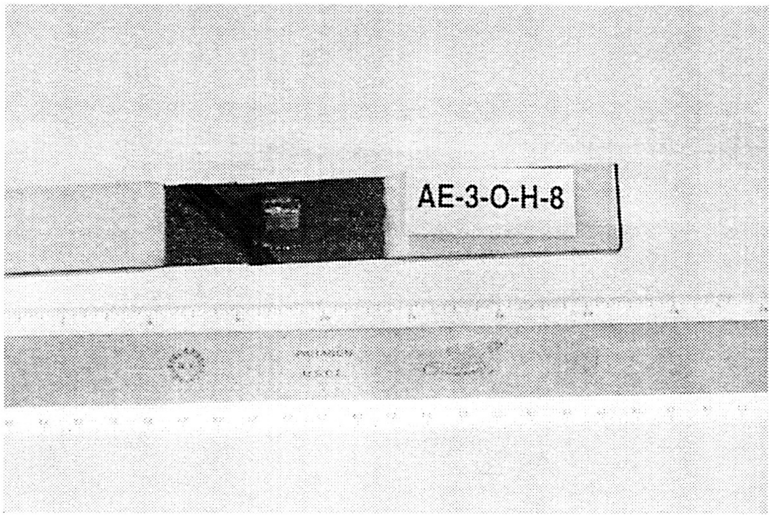

Figure 10. Failed sample AE–3–O–H–8.

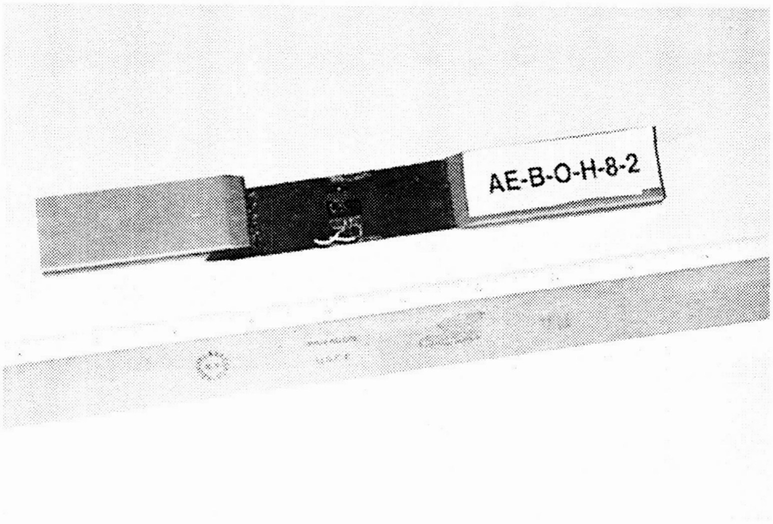

Figure 11. Failed sample AE–B–O–H–8–2.

5.1.6 Series AF, Shear Samples, 52 Ply

The AS4/3501 and IM7/F584 samples failed with extreme violence, fracturing most of the surface of the sample, as shown in figure 12, sample AF–3–A–H–52. The IM7/BMI and IM7/8551 samples looked much more coherent, shown in figure 13, sample AF–B–O–H–52–1. On most of the samples, the centerline was clearly visible as a long crack.

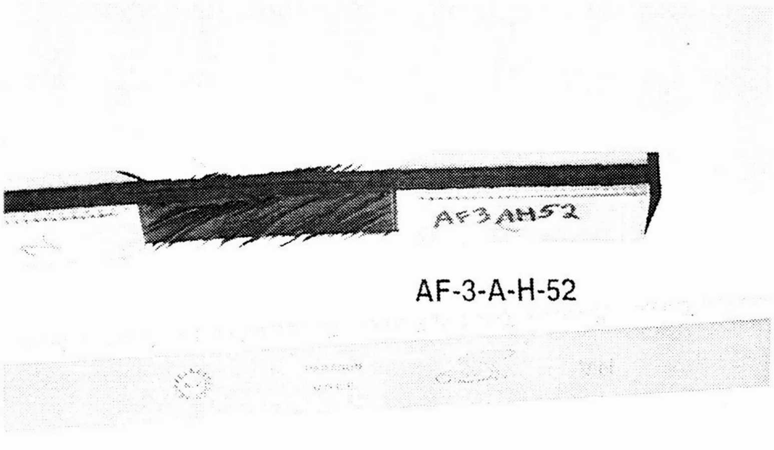

Figure 12. Failed sample AF–3–A–H–52.

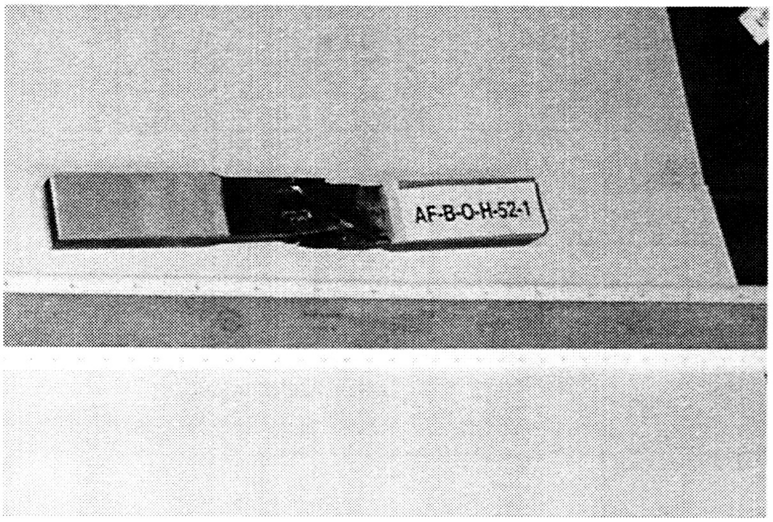

Figure 13. Failed sample AF–B–O–H–52–1.

5.2 Data Presentation and Interpretation

The raw data from the testing machines were brought into Excel spreadsheets for plotting and analysis. All of the individual stress-strain plots are included in appendix D. The detailed material property values and statistical calculations are tabulated in appendix E. The acceptable linear range was 15–25 ksi for all of the AA and AC (0°) samples and 3–7 ksi for the AB and AD (90°) samples.

The large volume of data is condensed into table 2, showing the significant factors and the magnitude of their effects on the stiffnesses and thickness for each material. Appendix A has a similar table for strengths (table 5) that is not included in the main body of this TM, since very few of the samples failed in the gauge length. In the following discussion, different combinations are referred to by their sample identifiers, using "*" as a wildcard. O–H–* specifies oven cure, hand layup, and either 8- or 52-ply thickness.

The factors are listed for each material as well as the interaction terms. Values are given for ply thickness, Poisson's ratio, the one- and two-direction moduli, and the shear stiffnesses.

The ply thickness column was calculated using all the samples of each thickness, both the unidirectional and the shear samples. This gives the ANOVA 48 data points for 47 total DOF's as opposed to 15 DOF for the material property ANOVA's.

The shear stiffnesses are slopes of least-squares curve fit lines over different ranges of the same data. The different ranges were chosen to see if there were variations between high and low strain levels. G_{12}–1K used data points between 0.5 and 1 ksi shear stress. G_{12}–3K used data points between 0.5 and 3 ksi. G_{12}–7K and G_{12}–10K used points between 0.5 and 7 ksi, and 0.5 and 10 ksi, respectively.

The "actual" column is for properties calculated from the as-measured specimen thicknesses, and the "normal" column uses values normalized to nominal average ply thickness. The normalized

Table 2. Effect of factors based on linear regression.

Confidence (97%)		G_{12}–1K Actual (%)	G_{12}–1K Normal (%)	G_{12}–3K Actual (%)	G_{12}–3K Normal (%)	G_{12}–7K Actual (%)	G_{12}–7K Normal (%)	G_{12}–10K Actual (%)	G_{12}–10K Normal (%)	E_1 Actual (%)	E_1 Normal (%)	E_2 Actual (%)	E_2 Normal (%)	ν_{12} Actual (%)	t_{ply} (%)
C	AS4/	14.5	–	12.8	–	16.4	–	22.4	12.6	–	–	13.9	9.7	–	–5.2
L	3501–6	–	–	–	7.8	–	6.9	–	–	–	–	–	–	–	6.3
T		–25.5	–13.3	–23.9	–11.8	–23.9	–12.0	–27.0	–15.2	–	–	–16.6	–23.2	–	–
C–T		–	–	–	–	–	–	–	–	–	–	–	–	–	–
C–T		–	–	–	–	–	–	–	–	–	–	–	1.8	–	–
L–T		–	–	–	–	–	–	–	–	–	–	–	–	–	–
C–L–T		–	–	–	–	–	–	–	–	–	–	–	–	–	–
C	IM7/	–	4.6	–	3.4	–	–	–	–	–	–	–	–	–	–
L	8551–7	–	–	–	–	–	–	–	–	–	–	–4.3	–	–	–
T		–17.2	–11.0	–10.0	–3.8	–7.1	–	–24.7	–18.7			–18.0	–12.6		5.3
C–T		–	–	–	–3.9	–	–	–	–	–	–	–	–	–	–
C–T		–	–	–	–	–	–	–	–			–	–		–
L–T		–	–	–	–	–	–	–	–			–	–		–1.4
C–L–T		–	–	–	–	–	–	–	–			–	–		–
C	IM7/	–	–	–	–	–	–	–	–	–	–	13.2	6.5	–29.0	–6.3
L	F655	–	–	–	–	–	–	–	–	–	–24.8	–	–7.3	–	–
T		–	–	–	–	–	–	–	–	–	–	–25.6	–28.8	–51.8	–
C–T		–	–	–	–	–	–	–	–	–	–	–	–	–29.4	–
C–T		–	–	–	–	–	–	–1.1	–0.6	–	–	–2.7	7.3	–	–5.4
L–T		–	–	–	–	–	–	–	–	–	–	–	9.5	–	6.9
C–L–T		–	–	–	–	–	–	–	–	–	–	–	3.8	–	–
C	IM7/	–	–	–	–	–	–	–	–						–
L	F584	–	–	–	–	–	–	–	–						–
T		–11.2	–	–13.6	–7.2	–	–	–14.1	–						6.4
C–T		5.7	6.0	–	7.1	–	–	–	–						–
C–T		–	–	–	–	–	–	–	–						–
L–T		–	–	–	–	–	–	–	–						–
C–L–T		–	–	–	–	–	–	–	–						–

value would be more applicable to design work since only a single-ply thickness must be assumed. Increases in thickness may be caused by voids or by less resin bleeding off during cure. A higher-than-expected resin fraction will result in a weight penalty. Values in table 2 are listed only if the confidence that they cause a difference is >97 percent. The value shown, in percent format, is the factor's coefficient divided by the intercept from the regression analysis. The designed experiment is used to determine significant variables, while the regression is used to indicate the direction and magnitude of change caused by that factor. Since the factor levels used in the regression were –1 and 1 (–1 for hand layup, oven cured, and 8 ply; 1 for tape layed, autoclave cured, and 52 ply), the intercept is the average of all the samples.

5.2.1 IM7/8551–7

For IM7/8551, thickness was a significant factor with losses in stiffness as more plies were added. The 52-ply layup did make the ply thickness 6 percent larger, indicating less compaction of the material. When the properties were normalized to a constant ply thickness, the loss of stiffness was still evident but not as severe. Autoclave versus oven curing had no effect on most of the properties, but did indicate a small increase in shear strength for low loads. Layup technique had no effect except for a slight decrease in E_2 for tape laying.

A cure-layup interaction was indicated for G_{12}–3K, and a layup-thickness interaction for ply thickness. The cure-layup interaction for G_{12} from 0.5–3 ksi is probably an anomaly, since it is unsupported by the other shear properties. The small layup-thickness interaction occurred for thickness, probably because the extra pressure from the tape-laying machine helped compaction for the thick part, while the thinner samples compacted well when layed either by hand or tape.

For IM7/8551, thickness had a major effect on reducing stiffness properties. Cure and layup techniques have not demonstrated any indication of affecting most material properties.

5.2.2 IM7/F584

Only shear stiffnesses and thickness data were gathered for IM7/F584. Of the primary factors, only part thickness had any effect on properties. Thicker parts had a reduction in stiffness of a little over 10 percent. However, once the variations in ply thickness were taken into account, it could not be clearly stated that there were material property differences. The only indication of interaction was for cure-layup, and only at the lower shear stress levels. O–H–* and A–T–* were stiffer than O–T–* and A–H–*.

5.2.3 AS4/3501–6

For the 8551 epoxy, an increase in the number of plies gave a consistent, significant reduction in G_{12} and E_2. However, for the 3501 material, the number of plies did not have an effect on the average ply thickness. E_1 and ν_{12} were unaffected by any of the factors. Layup technique seemed to have a small effect on midrange shear stiffnesses, and using the tape-laying machine actually increased the thickness 6 percent over hand layups. Autoclave curing had a beneficial effect on G_{12} and E_2 as well as reducing the average ply thickness. There was an indication of a very small cure-thickness interaction effect on E_2, where stiffness was higher for 0–*–8 and A–*–52 than for A–*–52 and O–*–8.

This was the only material that showed a consistent benefit from the autoclave cure. Since the AS4 fiber is not as stiff as the IM7, the contributions of the resin on the overall material properties are more significant. This indicated that there is a benefit from autoclave over oven cures, but when using a stiff enough fiber, the difference becomes small.

5.2.4 IM7/F655

This is a BMI resin and is the only material in the study that is not an epoxy. It displayed significant differences from the others. G_{12} was unaffected by any of the factors, including thickness, except for a very slight cure-thickness interaction indication. Normalized E_1 lost stiffness when the tape layer was used.

Ply thickness decreased with an autoclave cure and was subject to cure-thickness and layup-thickness interactions. Oddly, A–*–8 and O–*–52 were thicker than O–*–8 and A–*–52. Also, *–T–8 and *–H–52 were thicker than *–T–52 and *–H–8.

E_2 showed significant changes due to every factor and most of the interactions. Table 3 summarizes the combinations that made E_2 stiffer or softer. The autoclave cure and 8-ply samples would be expected to be stiffer, but not the hand-layed samples. The 8-ply, autoclave samples had similar lower stiffness to the 52-ply, oven-cured samples. The 8-ply, tape-layed samples had similar lower stiffness to the 52-ply, hand-layed samples. The three-way interaction also placed the A–T–8 samples in the softer group than the O–H–52 samples.

Table 3. IM7/F655, factors and interactions affecting E_2.

	Stiffer	Softer
Individual Factors	A–*–* *–H–* *–*–8	O–*–* *–T–* *–*–52
Two-Factor Interactions	O–*–8, A*–52 *–H–8, *–T–52	O–*–52, A–*–8 *–T–8, *–H–52
Three-Factor Interactions	O–H–52, O–T–8, A–H–8, A–T–52	O–H–8, O–T–52, A–H–52, A–T–8

Poisson's ratio for the BMI showed dependence on several factors where the epoxies were completely unaffected. ν_{12} decreased significantly with an autoclave cure and greater thickness. It was also susceptible to cure-layup interactions.

The BMI material behaved much differently than the epoxies, and in several counterintuitive ways. This, along with the two-direction interactions, indicated that the optimization of the BMI cure cycle can be complicated. While testing of components is always wise for composite structures, this reinforces the need when using BMI materials.

5.3 Void Content Results

The percentage of void content in the observed cross sections are shown in table 4. Most of the values were <1 percent, considered by ASTM D2734 to be a quality part. A few of the values were quite high and are marked in bold. All of the autoclave-cured samples had excellent compaction, which would be expected.

Table 4. Void content by material and process.

Process	AS4/3501-6 (%)	IM7/8551-7 (%)	IM7/F655 (%)	IM7/F584 (%)
A-T-8	<0.1	<0.1	<0.1	<0.1
A-H-8	<0.1	<0.1	<0.1	<0.1
A-T-52	<0.1	<0.1	<0.1	<0.1
A-H-52	<0.1	<0.1	<0.1	<0.1
O-T-8	0.7	0.2	<0.1	0.3
O-H-8	0.7	<0.1	<0.1	<0.1
O-T-52	**3.6**	0.3	**3.4**	1.0
O-H-52	**3.2**	0.8	**4.1**	0.8

The BMI material had very good compaction except for the thick oven-cured samples that had a very high void content. This was consistent with the cure-thickness interaction sensitivity seen for G_{12} at the 10-ksi stress level, E_2, and the ply thickness. The other factors which E_2 and ν_{12} were sensitive to cannot be related to void content. A typical high void content micrograph is shown in figure 14.

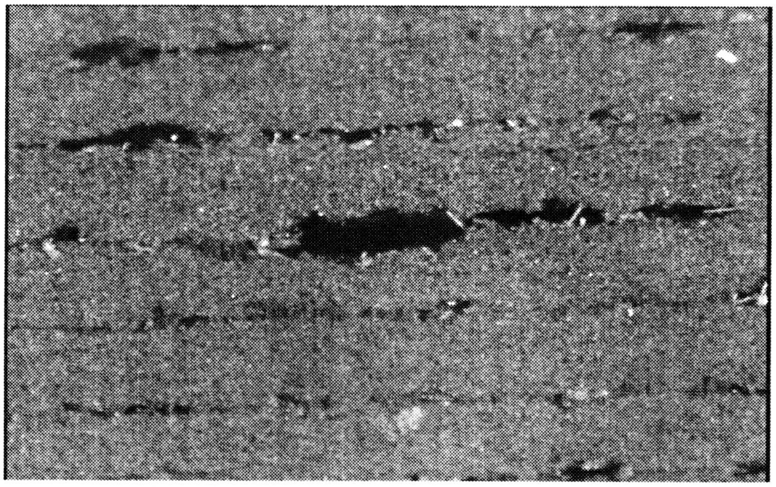

Figure 14. Micrograph of AF–B–O–T–52, 3.4-percent void content.

The AS4/3501–6 had good, though not excellent, compaction for the thin oven-cured samples and many voids in the thick samples. This related to the cure effect on every property measured except E_1 and ν_{12}. The high void content for the thick oven-cured samples might imply a cure-thickness interaction similar to the BMI material, but there was only a small indication of this interaction in E_2. The strong thickness dependence of AS4/3501–6 did not seem to be related to void content, since the thick autoclaved samples had excellent compaction. A micrograph of a typical sample with excellent consolidation is shown in figure 15.

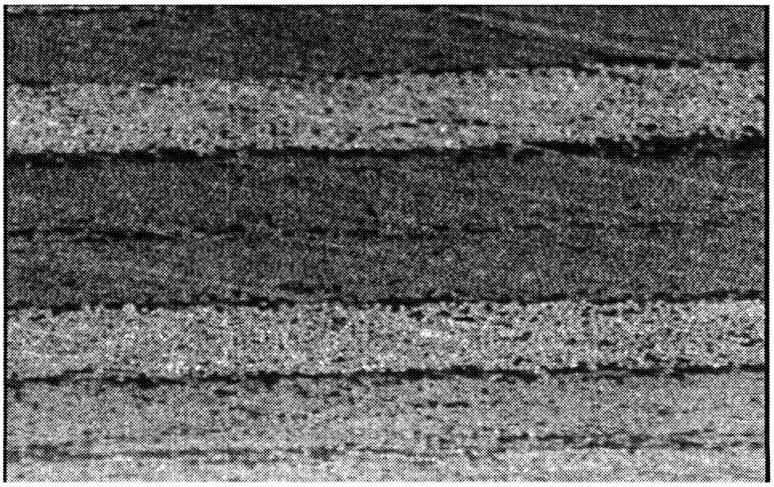

Figure 15. Micrograph of AE–3–A–T–8, <0.1-percent void content.

The IM7/8551–7 had a low but measurable void content in most of the oven-cured samples that may relate to the small cure dependency for G_{12} at the 1- and 3-ksi stress levels. The strong thickness dependence of IM7/8551–7 did not relate to void content. A micrograph of a sample with void content approaching 1 percent is shown in figure 16.

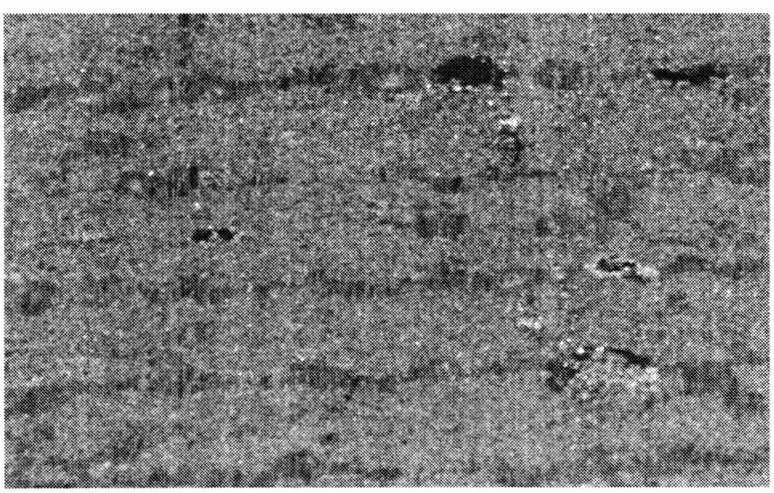

Figure 16. Micrograph of AF–8–O–H–52, 0.8-percent void content.

The IM7/F584, like the IM7/8551–7, had low but measurable void content in most of the oven-cured samples. However, in this case, there was no dependence on cure in the material properties. Because of the difference in the thick oven and autoclaved samples, a cure-thickness interaction might be expected. This was not seen in the results; but for the BMI material, there was only slight evidence of a cure-thickness interaction in G_{12} (the only data available for the IM7/F584). IM7/F584 had a fairly strong thickness dependence which did not correlate with the void data. A typical micrograph of a sample with void content >0.1 percent is shown in figure 17.

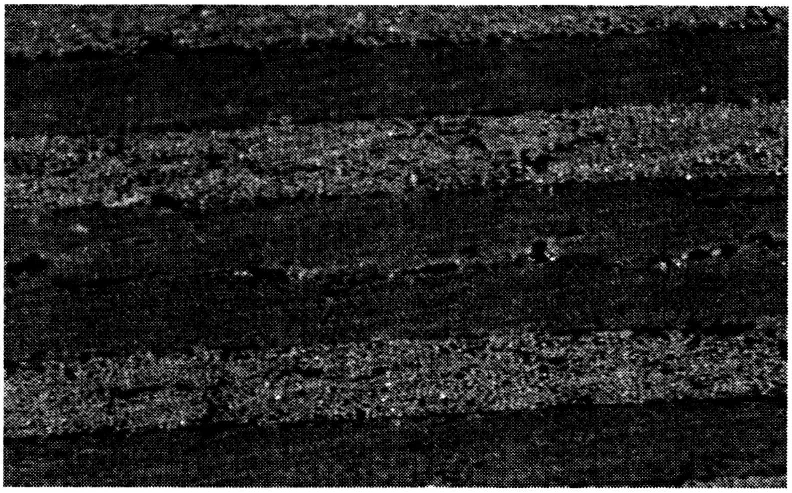

Figure 17. Micrograph of AE–4–O–T–8, 0.3-percent void content.

5.4 Relationship to Literature Survey

Yoon et al.[1] showed that full compaction can be reached over a range of temperatures and pressures, but cautioned that for thicker parts, more cure time might be required. The most consistent differences in this study were due to part thickness. G_{12} and E_2 consistently dropped by a significant amount for all the epoxies.

Bratukhin and Bogolyubov[2] stated that the ideal for high-quality parts is an absence of autoclave pressure, though this is often impractical for the molding of other than simple shapes. The flat plate coupon samples used here are simple shapes. Autoclave curing offered some benefits for the lower modulus fibers and for the two-direction properties of the BMI material, but otherwise had little effect.

Carpenter[3] showed that low-pressure processing could result in the formation of voids. He stated that cures could be controlled to either remove the volatiles or retain them in solid solution. Data presented here indicate that high void content can be related to reduced properties, but that it is not the only factor.

Johnson's study[4] of scaled laminates showed a higher stiffness for thicker laminates. The higher stiffness, though, did not exhibit itself until the laminates were suffering damage, meaning the stiffness change was more a function of the laminate than the unidirectional properties. He did state that the scaling effects are dependent on the relative amount of 0° plies in the layup. As the 0° plies fail, differences due to the remaining plies become more apparent.

Camponeschi's testing review[5] supported the validity of these tests for modulus and stated that adequately determining strength is difficult. His results did not show changes in stiffness for $[0_2/90]$ layups, which was consistent with the E_1 properties of this study. Strength and stiffness of the $[0_2/90]$ layup will be dominated by the 0° plies. He also supported the contention that compression tests are more valuable than tension tests for variations in the matrix, since all compression failures progress through a shear-dominated (and therefore matrix-dominated) instability.

Gipple[6] addressed the problem of brooming for end-loaded specimens by using the same $[0_2/90]$ layup as Camponeschi.[5] While she concentrated on differences due to dry/wet conditions, she also found no modulus difference between thick and thin specimens. As with Camponeschi, this agreed with the 0° data presented here.

Vannucci[7] varied autoclave pressure, although on a chemically different polyimide resin. His results showed a correlation between strength and cure pressure, though there was a stronger relationship between strength and voids. Void content ranged as high as 13 percent for some of the low-pressure cure specimens. As in this study, high void content has an effect on the mechanical properties. Elimination of the voids through cure optimization may restore the property losses.

In the NASA/General Dynamics study,[8] strength was significantly increased by going from a wound/hand-layed part to a tape-layed part, both with oven cures. The effect of the tape layer was to increase compaction and reduce voids that were inherent in the first process. Oven curing did not affect the tensile properties but did have some effect on the matrix-dominated properties. The properties were not affected severely enough to prevent the production of high-quality composite components. In fact, autoclave curing (30 lb/in.^{2}) of end joints with a honeycomb transition resulted in lesser quality parts due to impressing core discontinuities into the composite facesheets.

6. CONCLUSIONS

While there are differences due to the different processing factors, the largest differences being due to thickness, high-quality parts can be made using inexpensive manufacturing techniques. Materials with the higher stiffness fiber, IM7, are relatively insensitive to cure and layup variations. The material with the AS4 fiber did see some significant stiffness improvements with an autoclave cure. The material with BMI resin is sensitive to many of the experimental factors for E_2 and ν_{12}, implying that BMI resins are more sensitive to processing. High void content can be related to a loss in material properties, but there is not a void content relationship with many of the detected property variations. Careful cure optimization may be able to reduce many of the variations which did show up.

The only material with a consistent improvement for autoclave curing in G_{12} and E_2 was AS4/3501–6. Since the AS4 fiber is of lower stiffness than the IM7 fiber, the matrix made a greater contribution to the overall properties. Since F584 is chemically similar to 3501, the lack of a cure effect in IM7/F584 implied that the higher stiffness fiber reduced the effect. This indicated that there was some benefit to autoclave curing over oven curing, but that effect was smaller when higher performance fibers were used.

Average ply thickness results were inconsistent between the different graphite/epoxies. The ply thickness for IM7/8551 and IM7/F584 both increased with the number of plies while AS4/3501 was unaffected. AS4/3501 was the only material affected by cure and thinned with an autoclave cure. It was also the only material affected by layup, getting unexpectedly thicker with tape laying.

For the graphite/epoxies, E_1 and ν_{12} were unaffected by any of the factors. They also showed a consistent loss of G_{12} and E_2 when the number of plies was increased.

The graphite/BMI behaved differently. The BMI shear stiffnesses were relatively unaffected by any of the factors. E_1 decreased when tape layed. E_2 was affected by all factors and most of the interactions. Ply thickness decreased with autoclave curing and was subject to interaction effects. ν_{12} varied strongly with cure, thickness, and cure-layup interaction. If the high void content of the thick oven-cured samples could be reduced by optimization of the cure cycle, the cure-thickness interaction sensitivity might be eliminated.

All of the autoclave-cured samples had extremely low void content while the oven-cured samples had higher void content. Except for the thick oven-cured 3501–6 and BMI samples, the void content was still low and would be considered a good part. The high void content values correlated with changes in material properties, but many of the other material property changes were not related.

Oven cures and hand layups can give high-quality parts, especially when using high-performance fibers. It is likely that the oven-cured properties can be improved even more by optimization of the cure cycle for lower cure pressure, making sure that void content is minimized. Since part thickness is such a significant factor, and some properties such as E_2 for BMI are highly dependent on the whole manufacturing process, design layups must be tested to give accurate allowables for stress analysis.

APPENDIX A—STRENGTH RESULTS

Since most of the failures were not in the gauge length of the samples, the strength data cannot be considered valid. Additionally, since the thick and thin samples were of significantly different configuration, thickness must be considered as a driving factor, which can be seen in table 5. Nonetheless, since all the samples were tested the same way, some insight can be gained by looking at the results. Note that these results may be more indicative of a change in failure mode rather than an actual change in strength.

Table 5. Significance of factors on strength.

Confidence (97 %)		S		X_c		Y_c	
		Actual (%)	Normal (%)	Actual (%)	Normal (%)	Actual (%)	Normal (%)
C	AS4/3501–6	17.8	–	9.2	–	28.1	23.4
L		–	–	–	–	–	–
T		42.2	53.6	80.0	80.6	46.2	39.3
C–L		–	–	–	–	–	–
C–T		–	–	–	–	–2.1	–1.0
L–T		–	–	–	–	–	–
C–L–T		–	–	–10.9	–	–	–
C	IM7/8551–7	6.2	6.6	–	–	5.5	6.4
L		–	–1.1	–	–	–	–
T		32.7	38.7	30.8	35.4	17.0	22.4
C–L		–	–1.1	–	–	–5.3	–5.3
C–T		1.1	–0.6	–	–	–	–
L–T		–2.5	–	–	–	–2.0	–1.7
C–L–T		–	–	–	–	–	–
C	IM7/F655	11.7	10.4	–	–34.4	48.9	41.9
L		–	–	–30.5	31.7	–12.5	–17.9
T		12.1	16.4	33.0	–	–	–
C–L		–	–	–	–	–	–
C–T		3.3	3.5	–	–	3.8	12.4
L–T		–	–	–	–	–	35.5
C–L–T		–	–	–	–	16.7	16.9
C	IM7/F584	–	6.6				
L		–	–				
T		44.1	50.2				
C–L		–	–				
C–T		–	–				
L–T		–	–				
C–L–T		–	–				

Shear strength consistently improved with an autoclave cure by ≈10 percent. The improvement was significantly higher for the material with the AS4 fiber. The IM7/8551–7 showed several interaction effects, but these effects are small values, as is the case with the effect from layup. The IM7/F655 (BMI) again showed that it is different from the epoxies by having a cure-thickness interaction.

X_C did not seem strongly affected by cure method except for some sensitivity of AS4/3501–6. The BMI appeared to get significantly weaker for tape-layed parts. This is counterintuitive but is consistent with the reduction of E_1 in tape-layed samples.

Y_C showed varying increases in strength for autoclave cures. The epoxies were unaffected by layup but increased in strength with thickness. The BMI was unaffected by thickness but lost strength when tape layed. Interactions were indicated for all the materials, with the most significant being the BMI.

The thickness showed up as a significant factor in almost every case, which was to be expected due to the different sample configurations. For the epoxies, X_C was essentially unaffected by the other factors, while S and Y_C had some sensitivity to cure. The BMI was again different, having been affected by layup for both X_C and Y_C.

As for the stiffnesses, thickness seemed to be a very important factor. Autoclave curing provided strength benefits, but the benefits were small in many cases. The few indications of layup effect showed a decrease in strength for tape-layed samples.

APPENDIX B—TEST SAMPLE DRAWINGS

Test sample drawings are shown in figures 18–23.

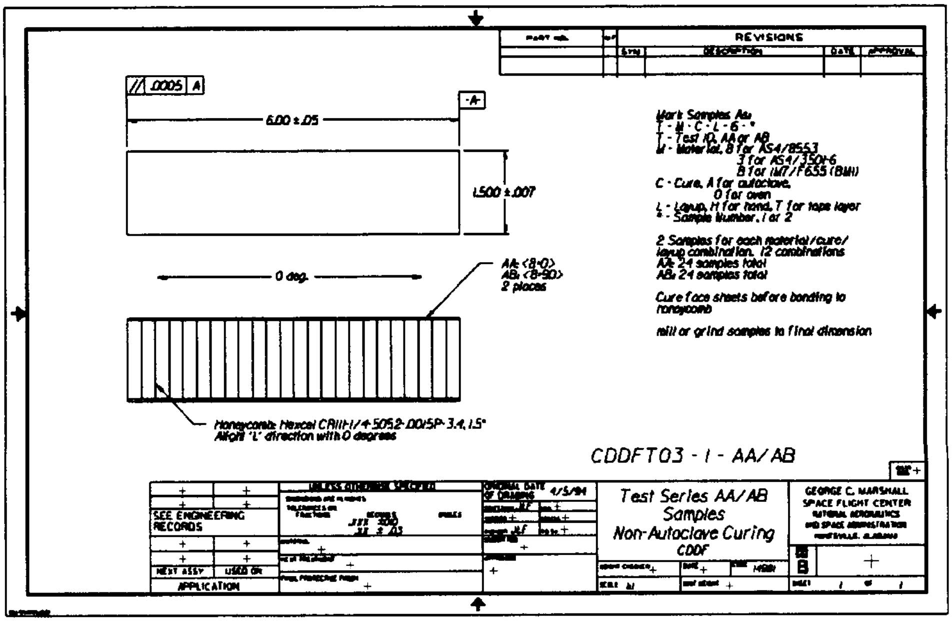

Figure 18. Eight-ply test samples AA and AB.

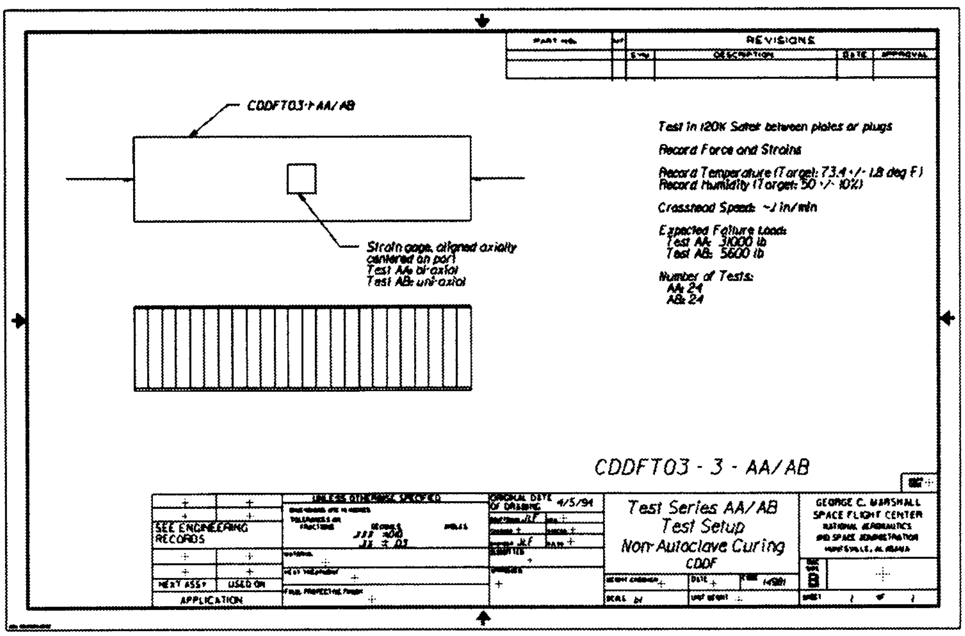

Figure 19. Eight-ply test setup AA and AB.

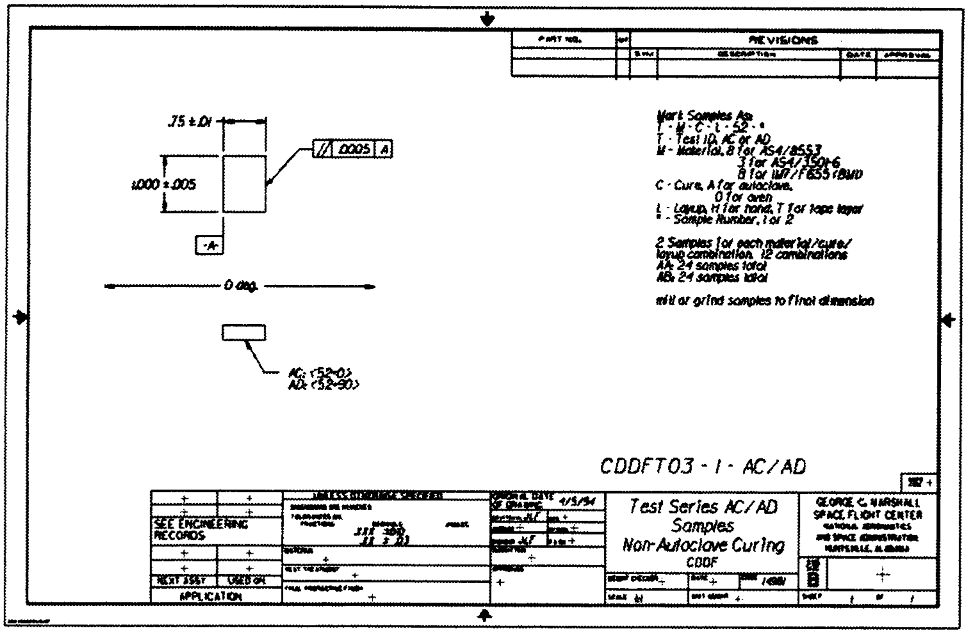

Figure 20. Fifty-two-ply test samples AC and AD.

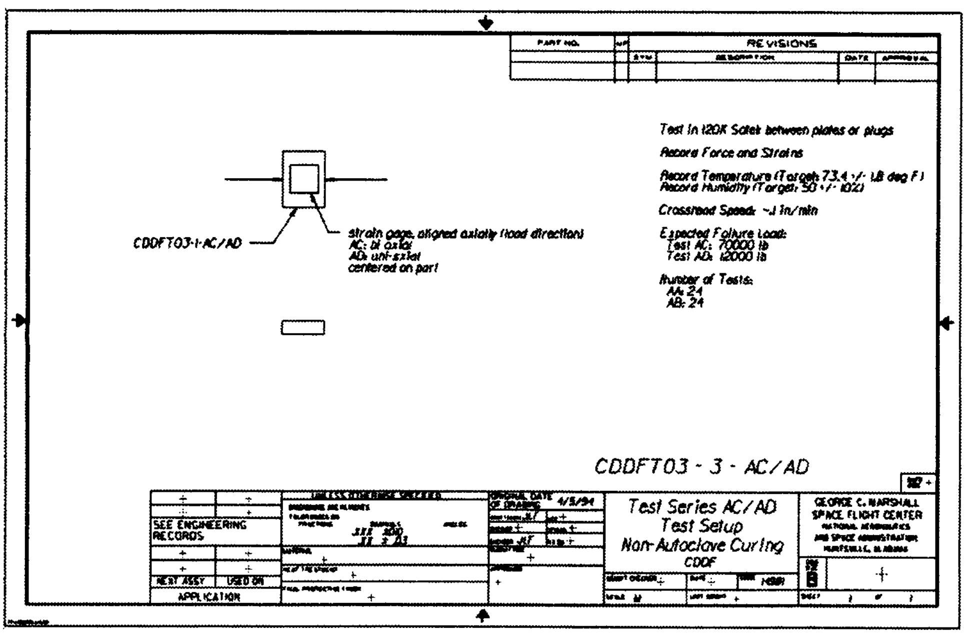

Figure 21. Fifty-two-ply test setup AC and AD.

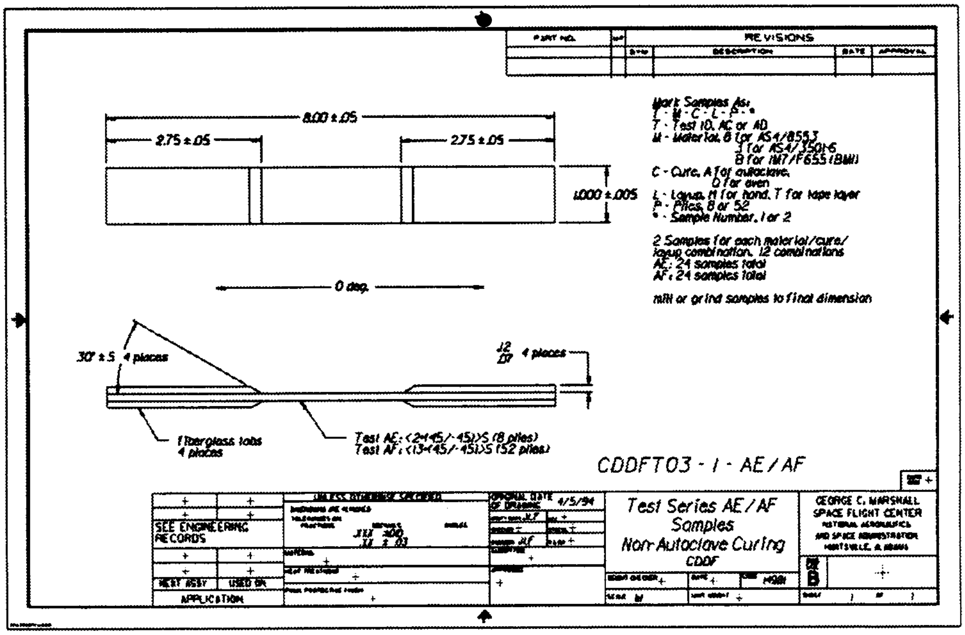

Figure 22. Tension-shear test samples AE and AF.

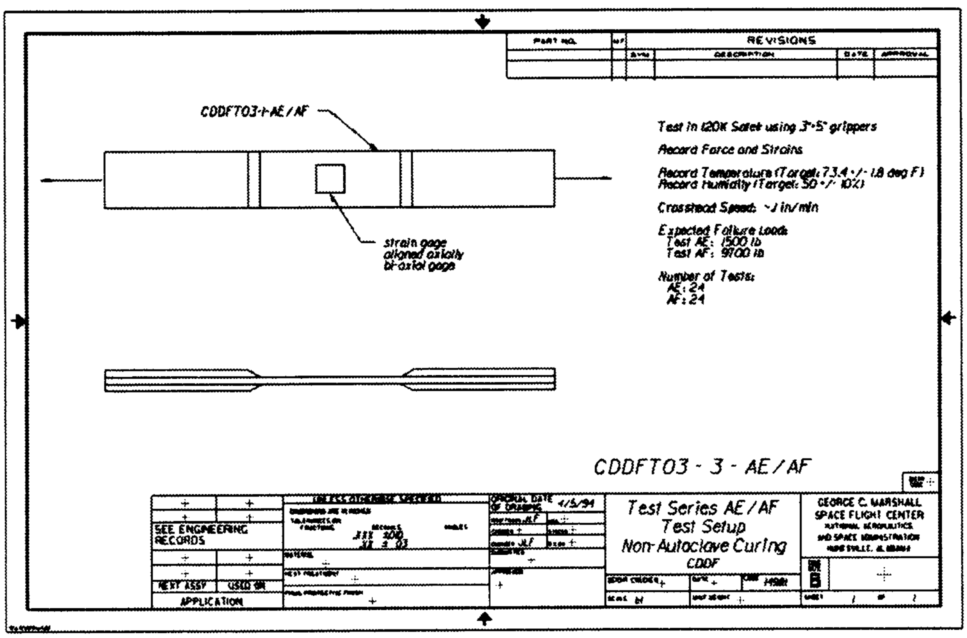

Figure 23. Tension-shear test setup AE and AF.

APPENDIX C—CURE CYCLES

The cure cycles for each material are shown in figures 24–27. The cycles shown are for the autoclave-cured samples. The oven-cured samples did not use any autoclave pressure and the vacuum pressure was not released.

The cure cycle used for AS4/3501–6 is as follows:

- Apply full vacuum
- Heat autoclave at 3–5 °F/min to 225 °F ± 10 °F
  - At 150 °F, pressurize to 15 ± 5 lb/in.^{2}
- Hold at 225 °F ± 10 °F for 60–70 min
  - Apply 100 ± 10 lb/in.^{2} pressure
  - Vent vacuum at 30 ± 5 lb/in.^{2} pressure
- Heat autoclave at 3–5 °F/min to 350 °F
- Hold at 350 °F ± 10 °F for 240 ± 15 min
- Cool down autoclave at 7–10 °F/min
- At 150 °F, dump pressure.

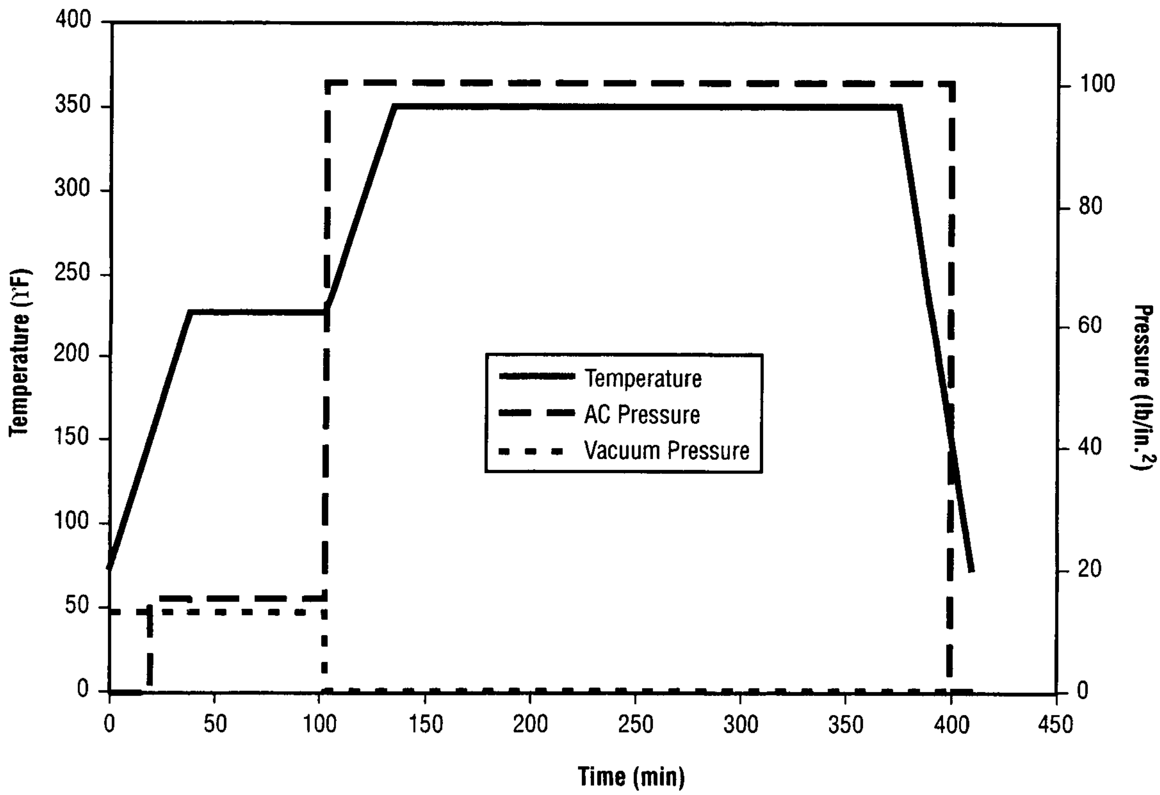

Figure 24. AS4/3501–6 cure cycle.

The cure cycle used for IM7/8551–7 is as follows:

- Apply full vacuum
- Heat autoclave at 3–5 °F/min to 225 °F ± 10 °F
  – At 150 °F, pressurize to 15 ± 5 lb/in.^{2}
- Hold at 225 °F ± 10 °F for 60–70 min
- Apply 100 ± 10 lb/in.^{2} pressure
  – Vent vacuum at 30 ± 5 lb/in.^{2} pressure
- Heat autoclave at 3–5 °F/min to 350 °F
- Hold at 350 °F ± 10 °F for 120 ± 15 min
- Cool down autoclave at 7–10 °F/min
- At 150 °F, dump pressure.

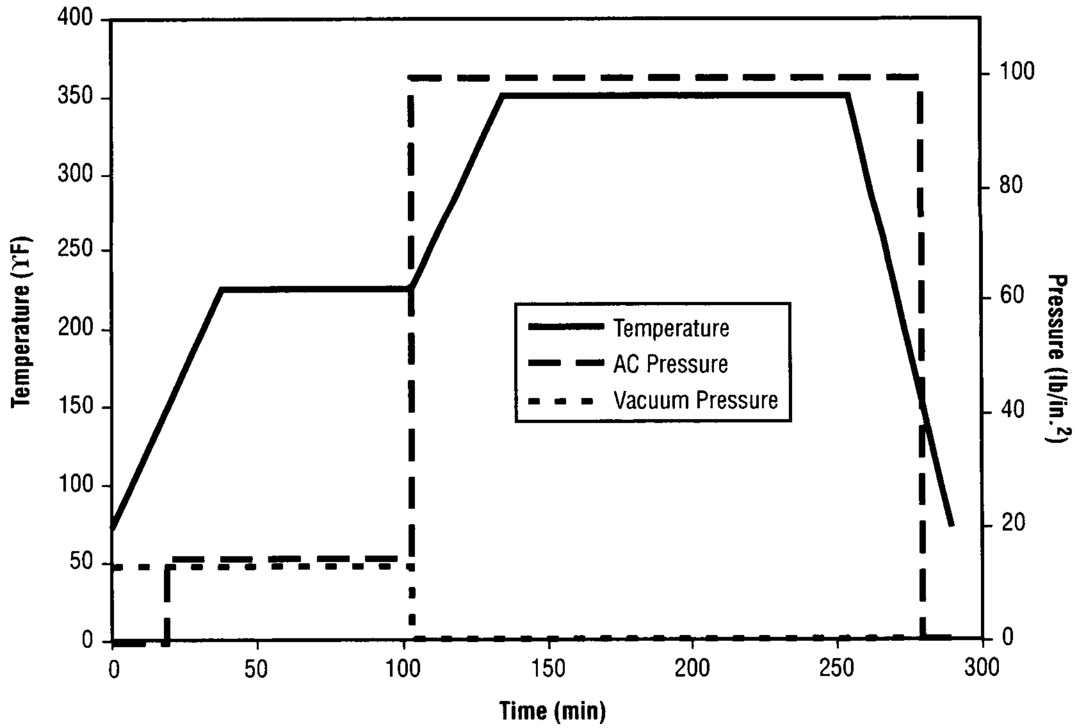

Figure 25. IM7/8551–7 cure cycle.

The cure cycle used for IM7/F584 is as follows:

- Apply vacuum of 22 in. Hg minimum
- Heat to 270 °F at 2–4 °F/min, apply 85 lb/in.^{2}
- Dwell at 270 °F for 30 min, release vacuum
- Heat to 375 °F at 2–4 °F/min, cure 4 hr
- Cool to 150 °F at ≤5 °F/min before releasing pressure.

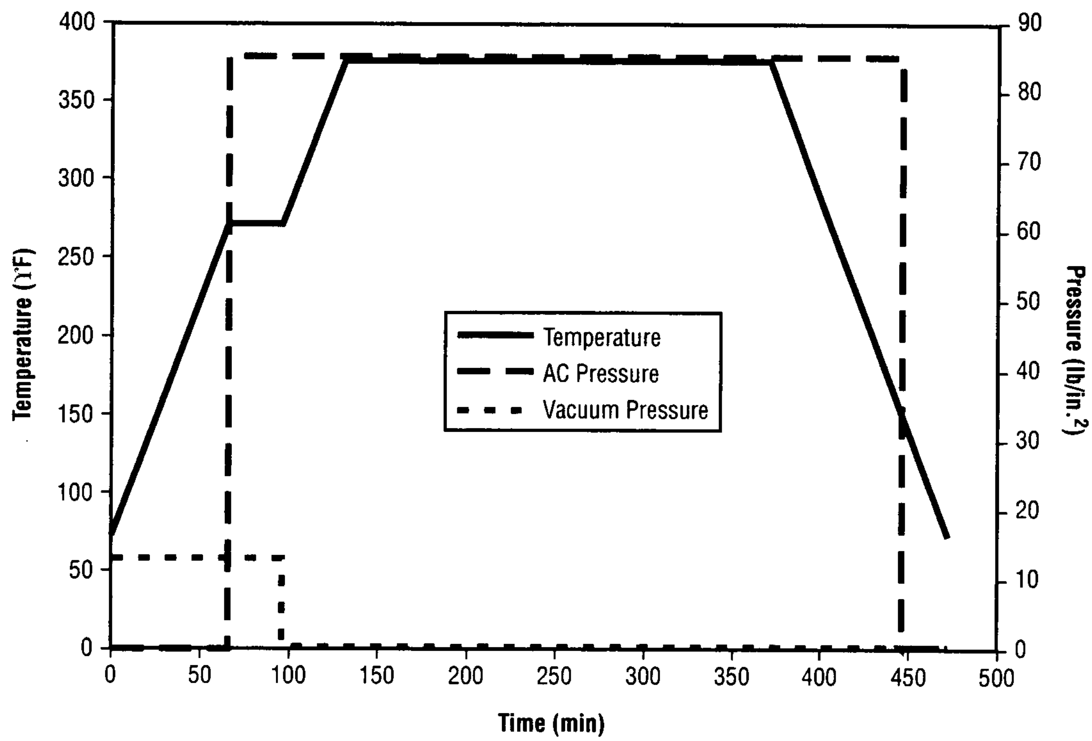

Figure 26. IM7/F584 cure cycle.

The cure cycle used for IM7/F655 is as follows:

- Apply vacuum of 22 in. Hg minimum
- Heat to 270 °F at 2–4 °F/min, apply 85 lb/in.^{2}
- Dwell at 270 °F for 30 min, release vacuum
- Heat to 375 °F at 2–4 °F/min, cure 4 hr
- Cool to 150 °F at ≤5 °F/min before releasing pressure
- Postcure in freestanding oven
  - Raise temperature from ambient to 375 °F at a rate of 5–10 °F/min and a rate of 1–2 °F/min above 375 °F.

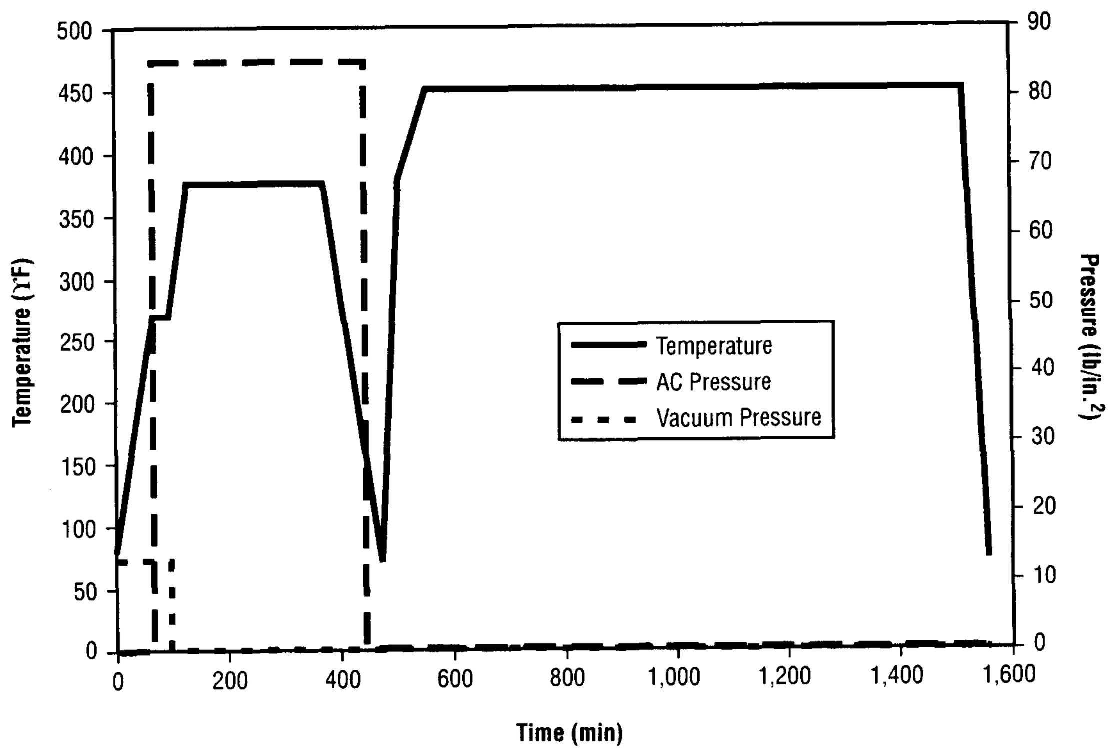

Figure 27. IM7/F655 cure cycle.

APPENDIX D—STRESS-STRAIN PLOTS

Stress-strain plots for various test series are shown in figures 28–47.

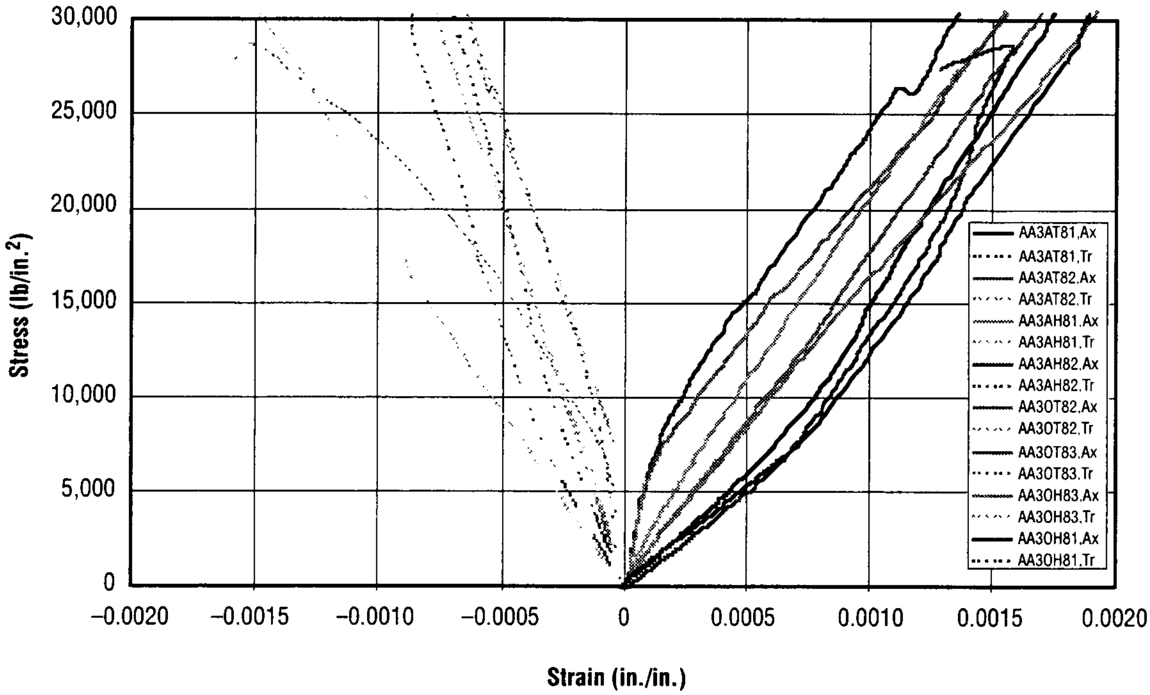

Figure 28. Stress versus strain, AS4/3501–6, test series AA.

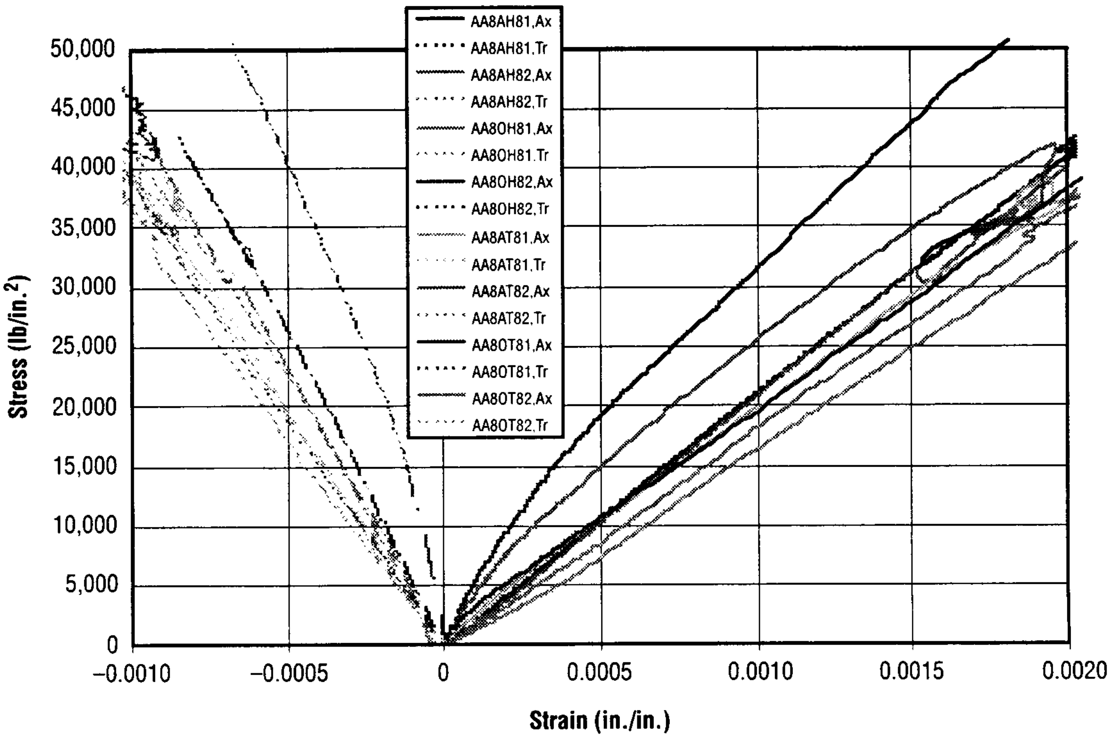

Figure 29. Stress versus strain, IM7/8551–7, test series AA.

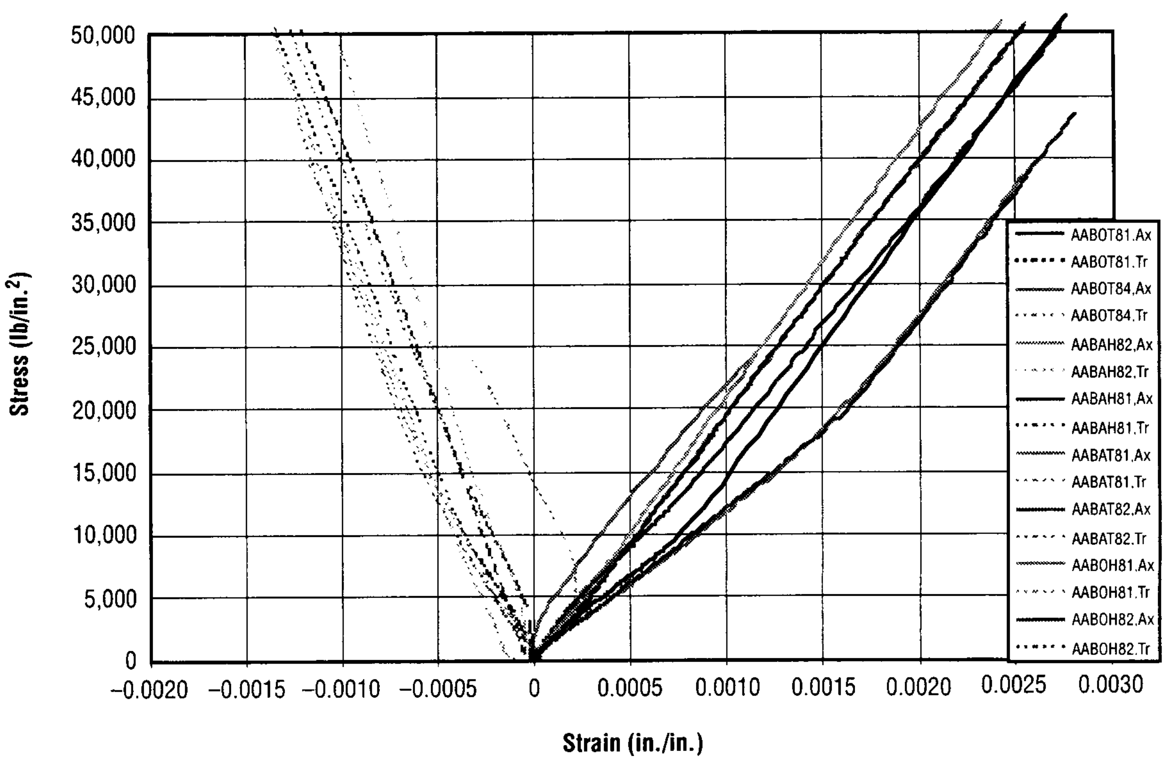

Figure 30. Stress versus strain, IM7/F655, test series AA.

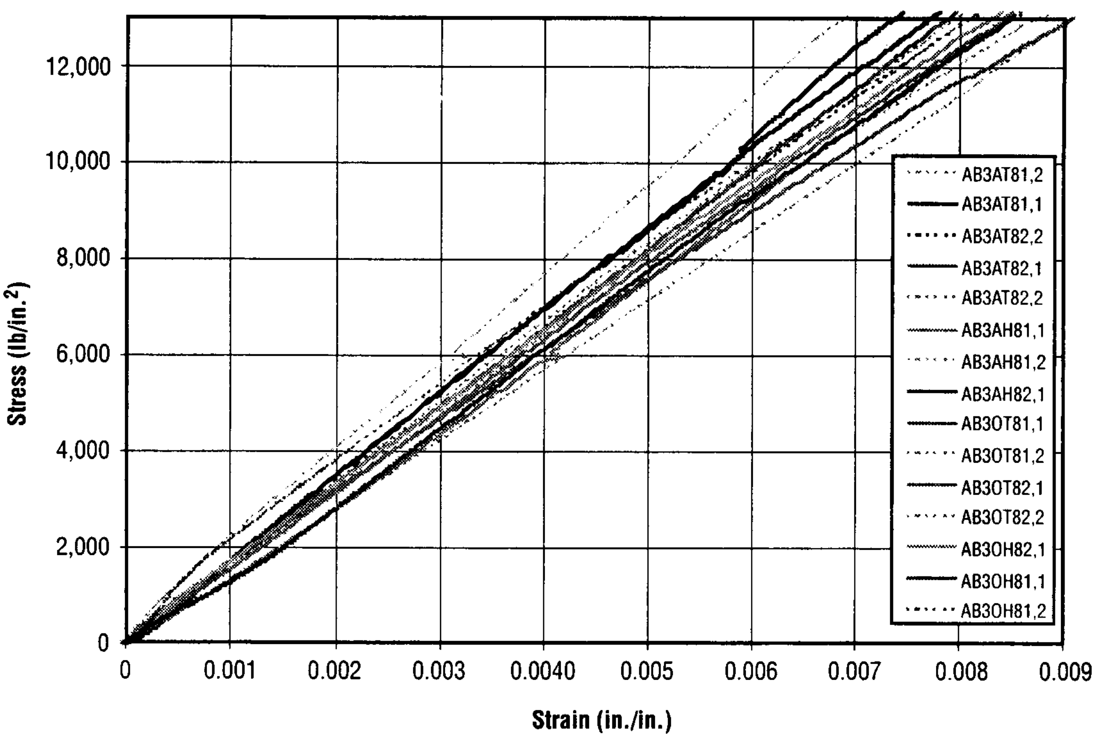

Figure 31. Stress versus strain, AS4/3501–6, test series AB.

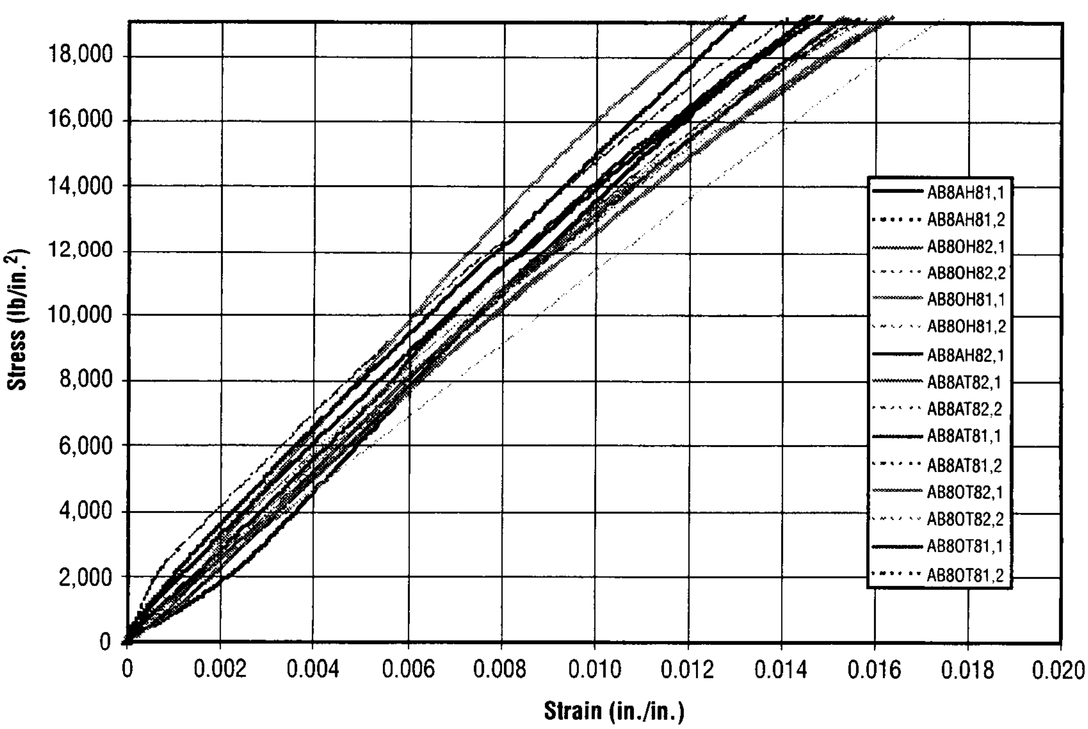

Figure 32. Stress versus strain, IM7/8551–7, test series AB.

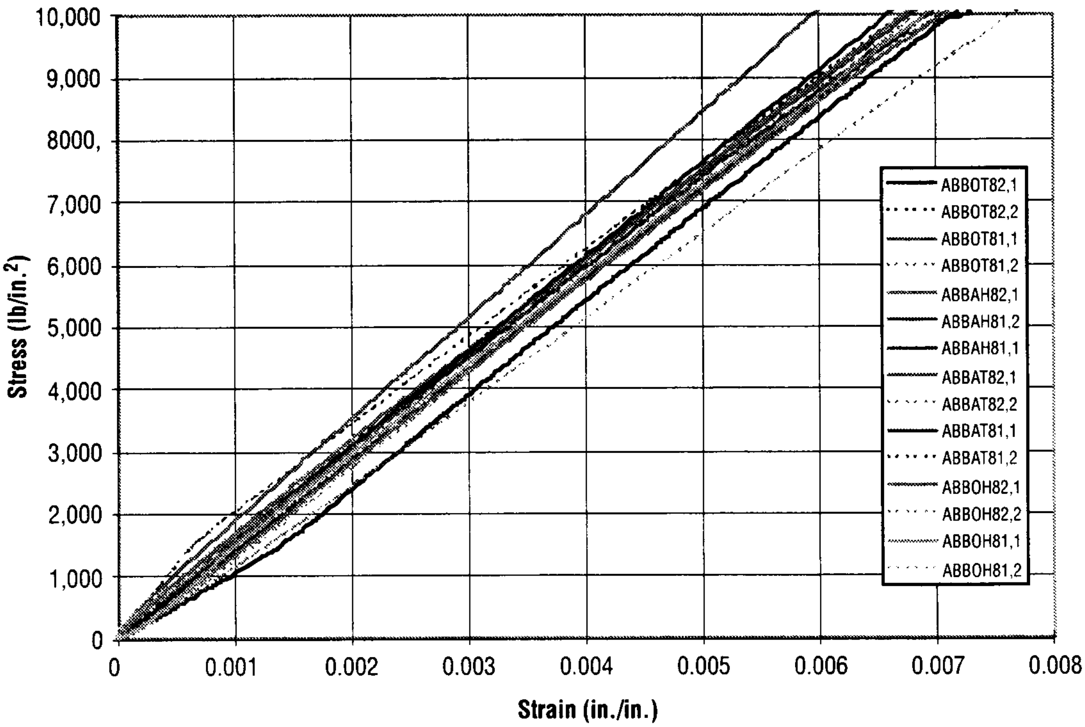

Figure 33. Stress versus strain, IM7/F655, test series AB.

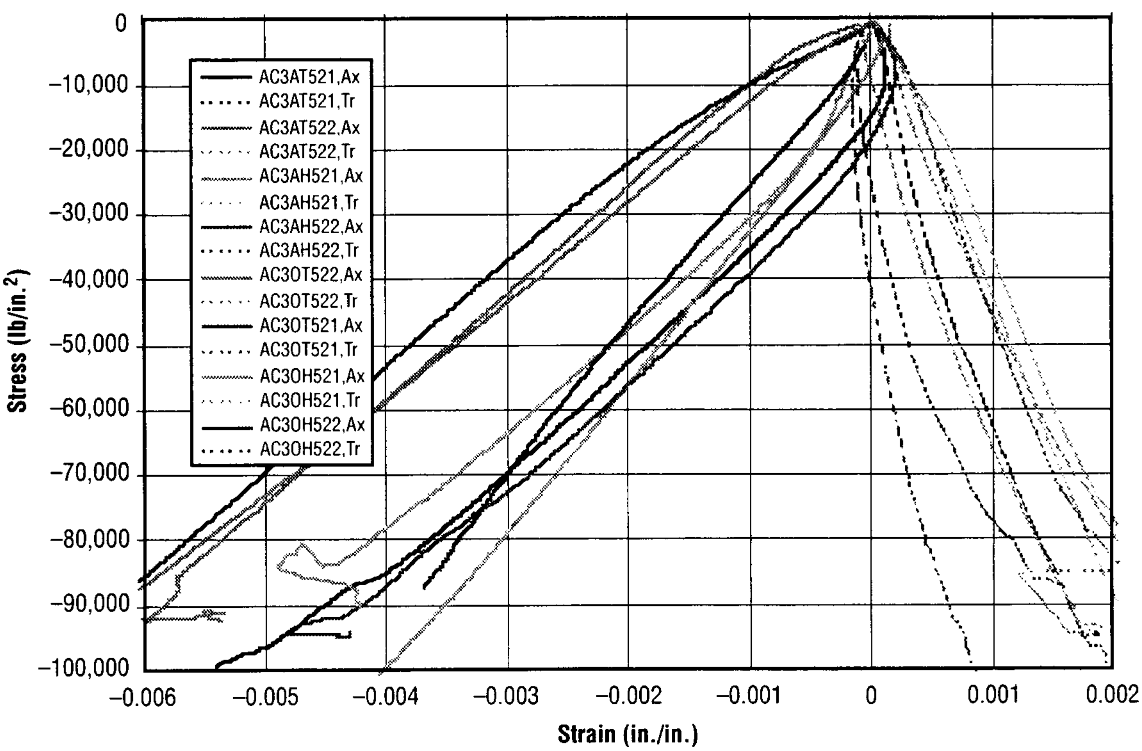

Figure 34. Stress versus strain, AS4/3501–6, test series AC.

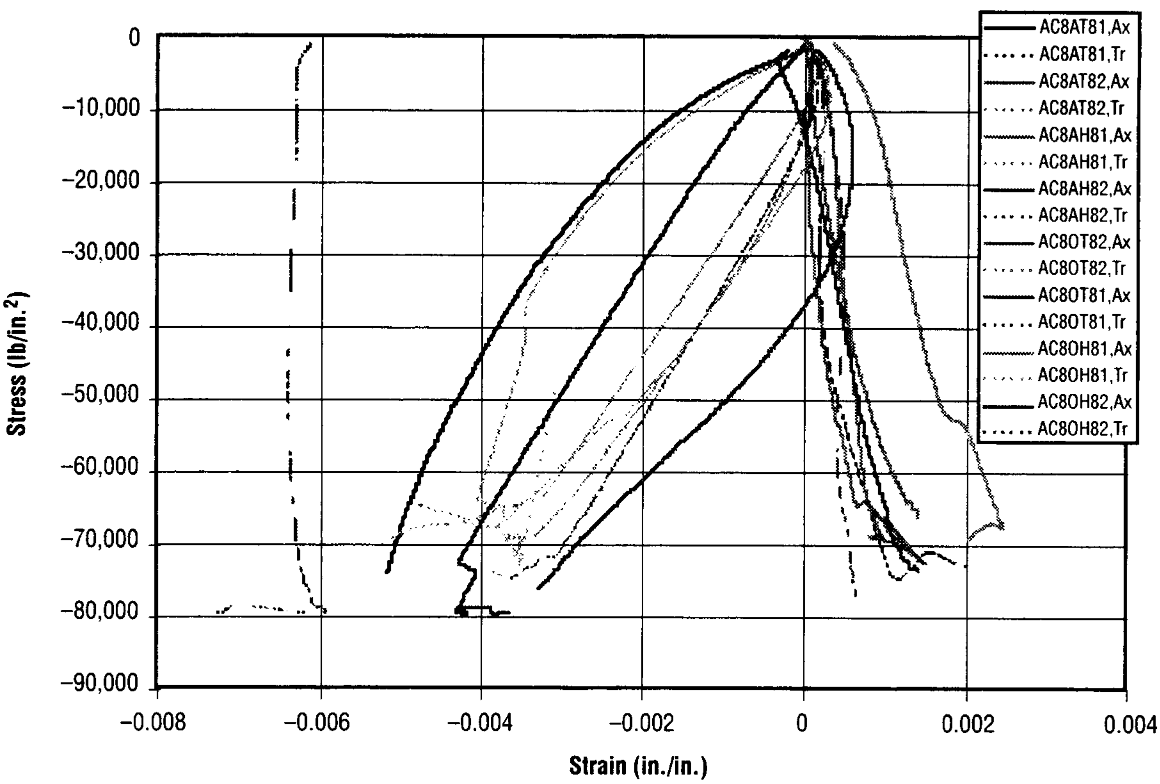

Figure 35. Stress versus strain, IM7/8551–7, test series AC.

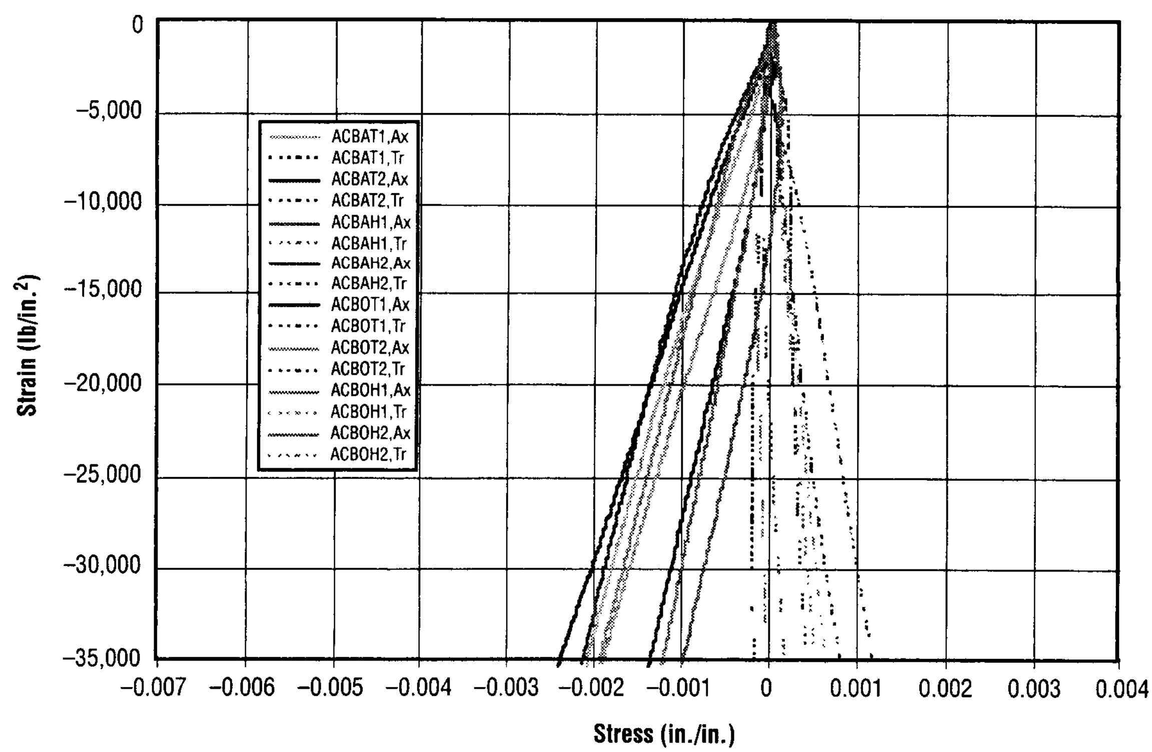

Figure 36. Stress versus strain, IM7/F655, test series AC.

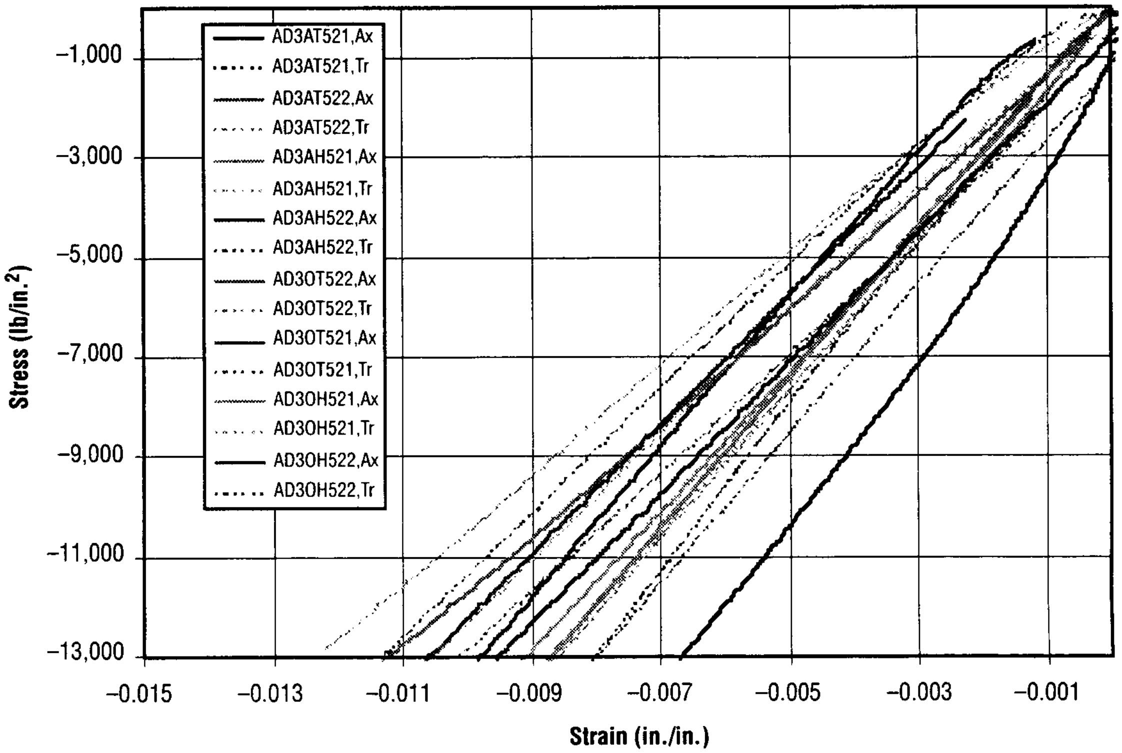

Figure 37. Stress versus strain, AS4/3501–6, test series AD.

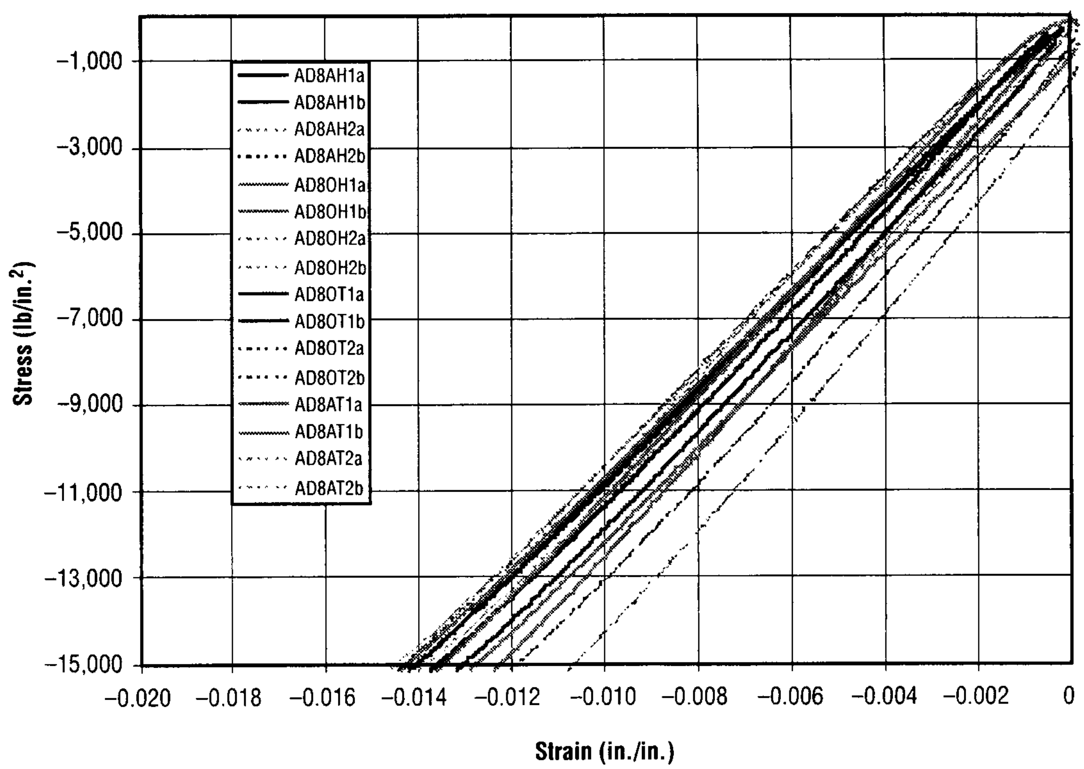

Figure 38. Stress versus strain, IM7/8551–7, test series AD.

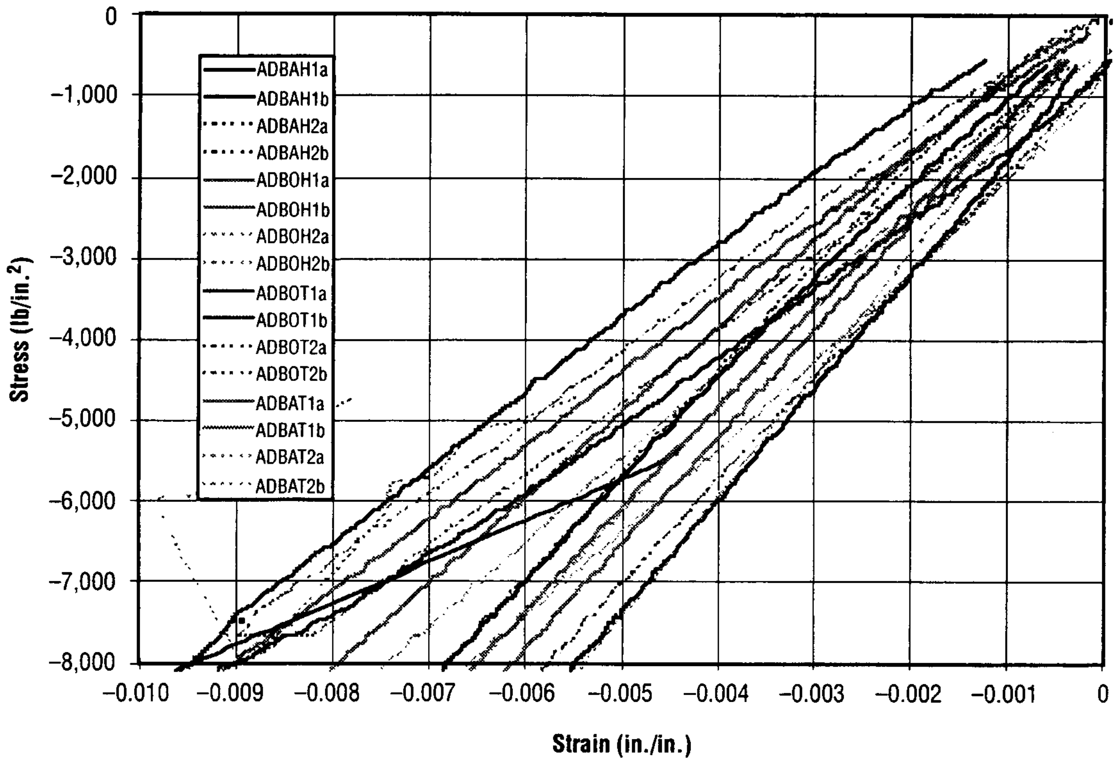

Figure 39. Stress versus strain, IM7/F655, test series AD.

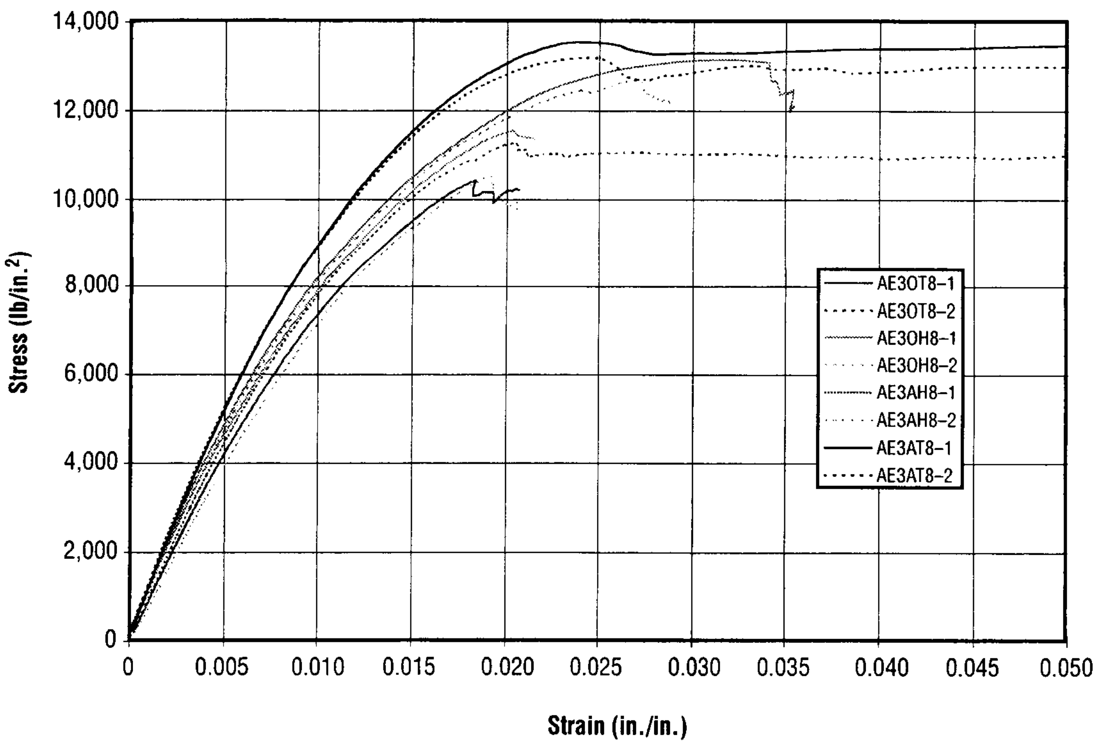

Figure 40. Shear stress versus strain, AS4/3501–6, series AE.

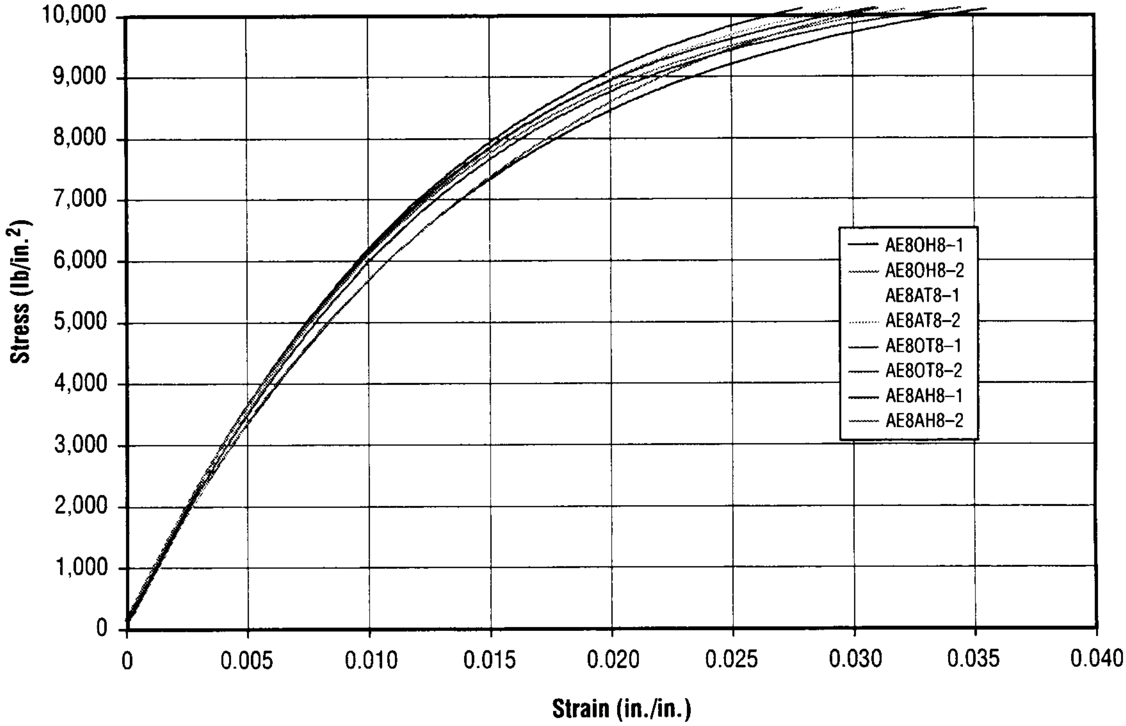

Figure 41. Shear stress versus strain, IM7/8551–7, series AE.

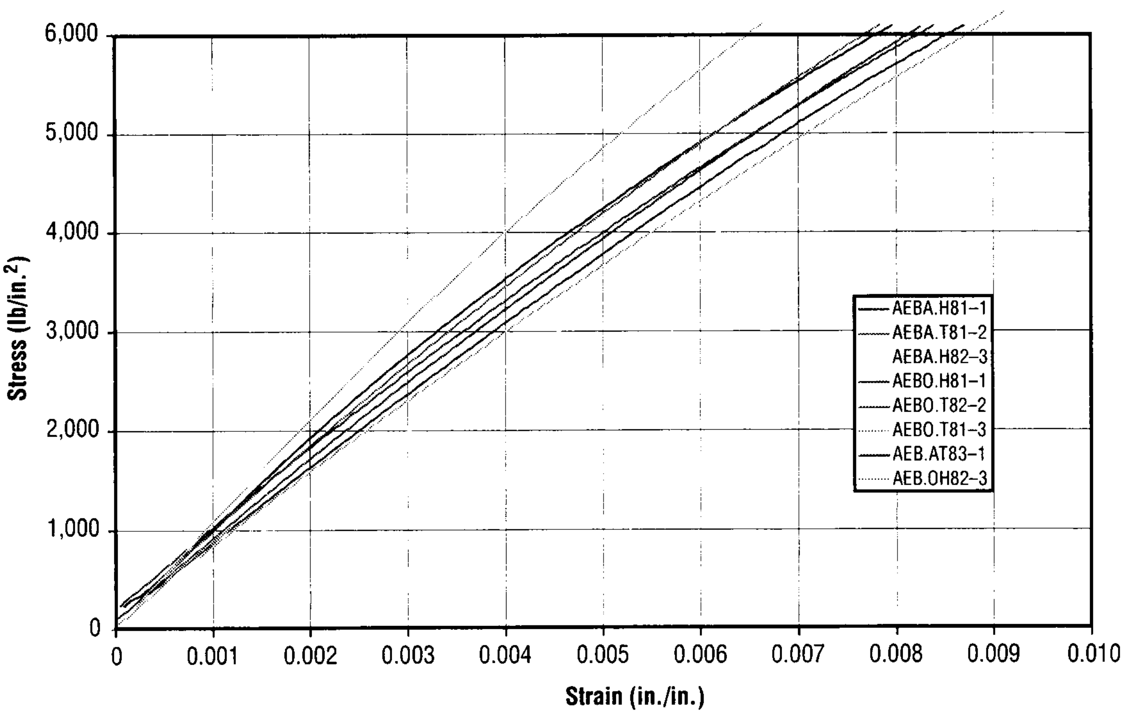

Figure 42. Shear stress versus strain, IM7/F655, series AE.

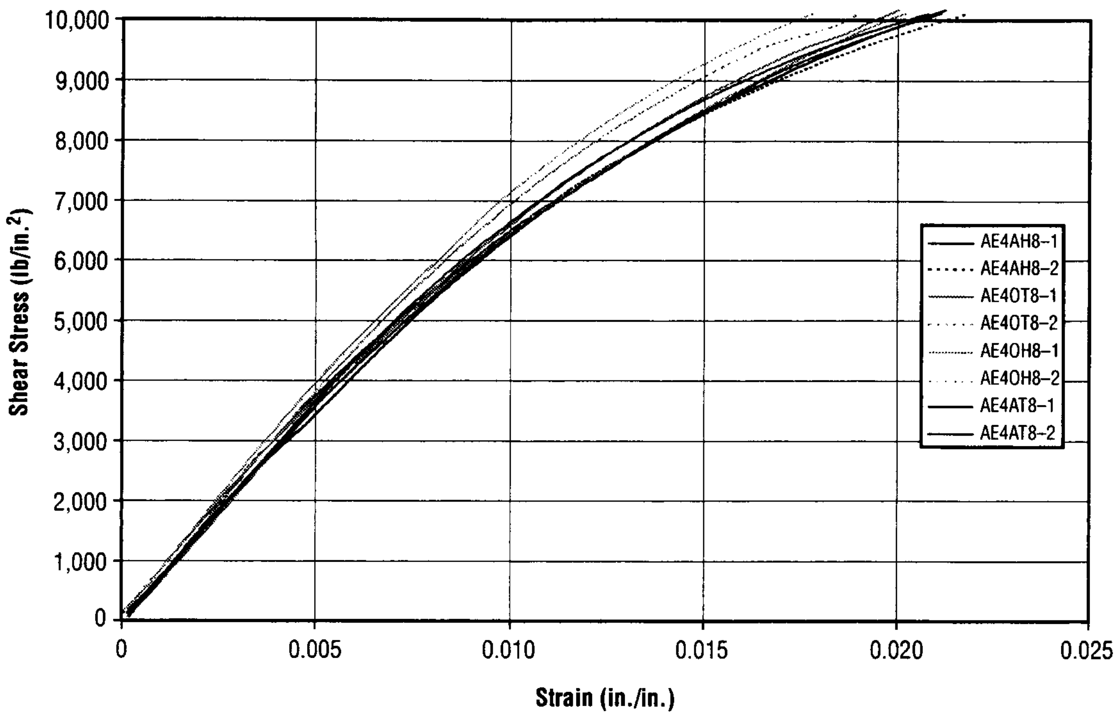

Figure 43. Shear stress versus strain, IM7/F584, series AE.

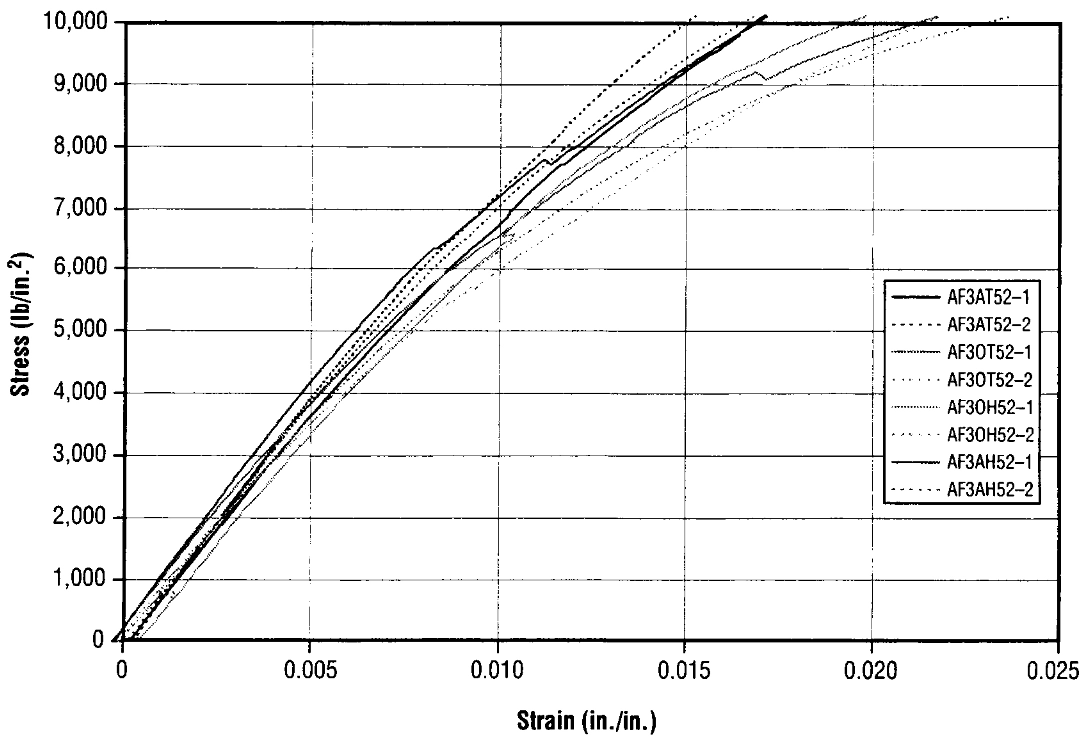

Figure 44. Shear stress versus strain, AS4/3501–6, series AF.

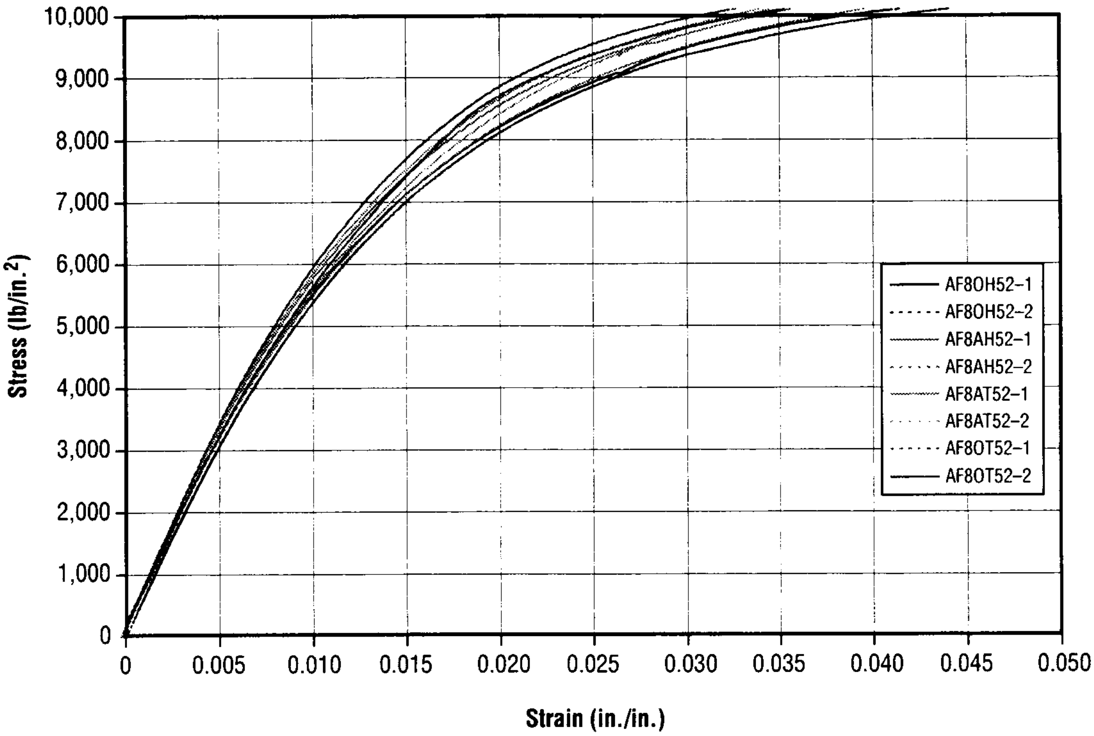

Figure 45. Shear stress versus strain, IM7/8551–7, series AF.

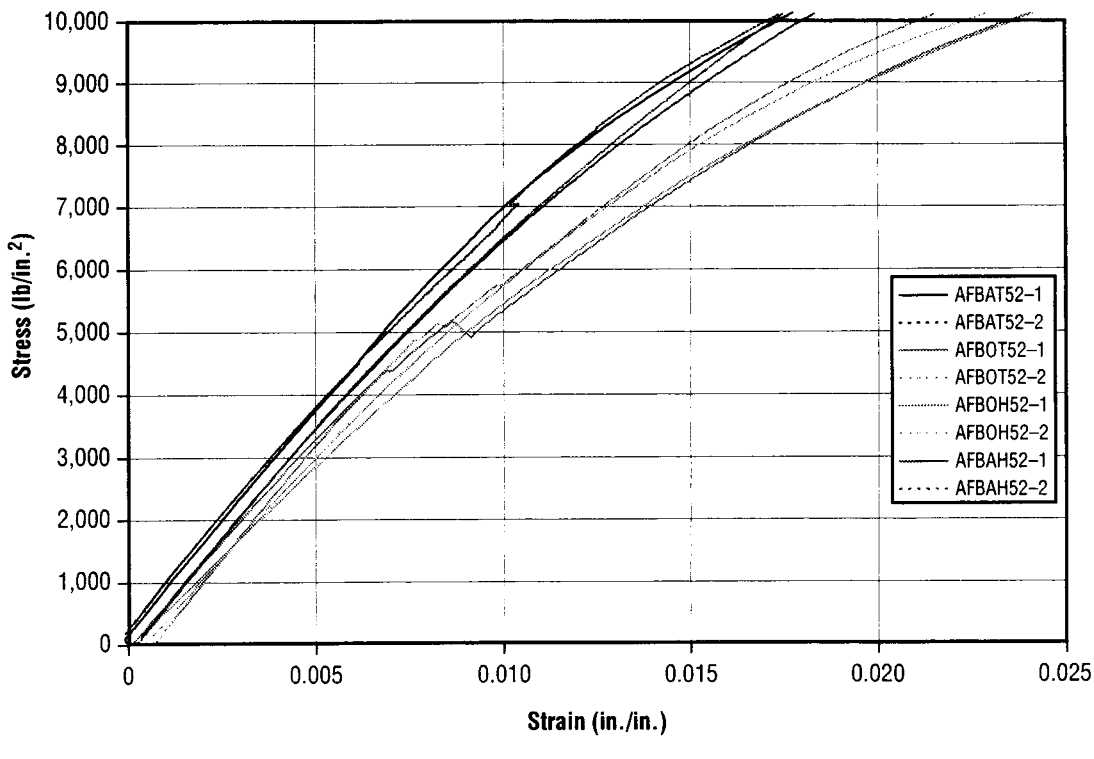

Figure 46. Shear stress versus strain, IM7/F655, series AF.

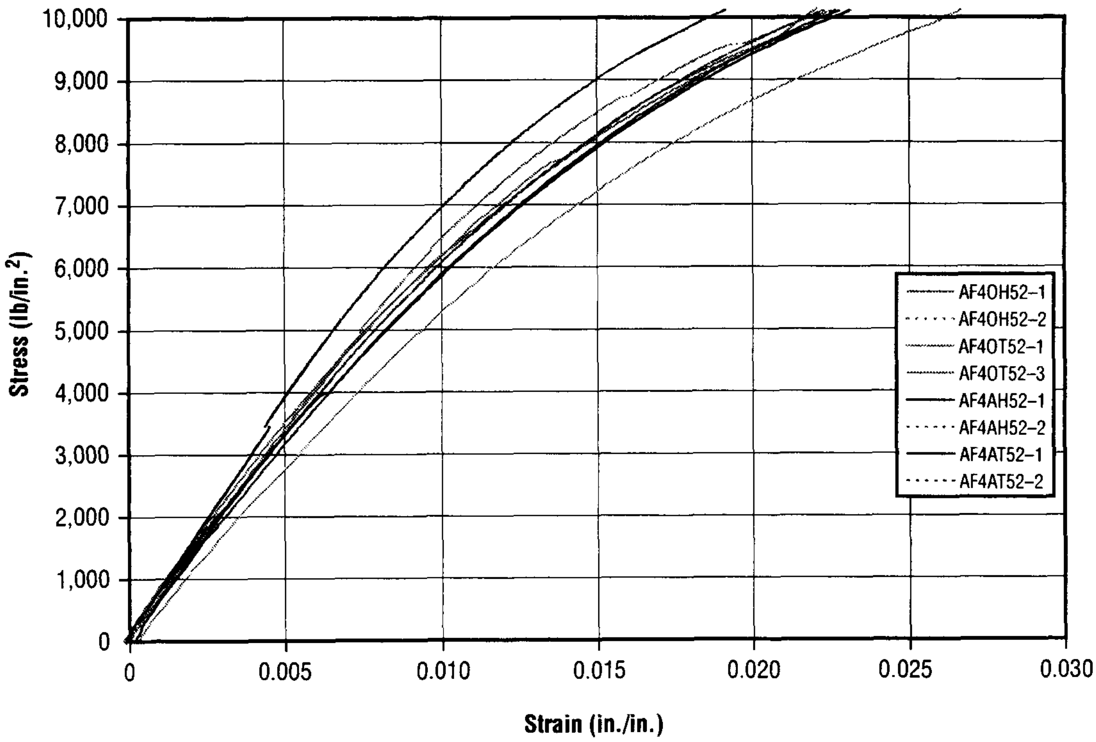

Figure 47. Shear stress versus strain, IM7/F584, series AF.

APPENDIX E—MATERIAL PROPERTY SPREADSHEETS

The statistical analysis spreadsheets use the strength and stiffness values to calculate the significant factors. Table 6 is for IM7/F584. Data for IM7/F655 are in table 7 for actual values, table 8 for normalized values, and table 9 for average ply thickness. Data for IM7/8551–7 are in table 10 for actual values, table 11 for normalized values, and table 12 for average ply thickness. The DOF column of the SS blocks of data includes, in parentheses, the DOF for the reduced ANOVA used for IM7/8551–7 E_1 and ν_{12}. Data for AS4/3501–6 are in table 13 for actual values, table 14 for normalized values, and table 15 for thickness.

By column, table 6 for IM7/F584 has the individual sample names; average ply thickness for test series AE and AF; actual shear moduli measured from 0.5 to 1, 3, 7, and 10 ksi; shear strength (invalid due to nonstandard samples); normalized shear moduli measured from 0.5 to 1, 3, 7, and 10 ksi; and normalized shear strength (invalid). By row, the blocks of data are the individual sample values; SS for each factor and interaction; statistical F-test evaluation; probability of significance; linear regression coefficients; and the percent effect of each factor and interaction.

By column, the actual value tables, tables 7, 10, and 13, have the individual sample name; average ply thickness for tests AE and AF; shear moduli; shear strength (invalid); average ply thickness for tests AA and AC; 0° elastic modulus; Poisson's ratio; 0° failure strength (invalid); average ply thickness for tests AB and AD; 90° elastic modulus; and 90° failure strength (invalid). The rows of data are the same as for table 6.

The normalized value tables, tables 8, 11, and 14, have the individual sample names; normalized shear moduli; shear strength (invalid); 0° modulus; 0° strength (invalid); 90° modulus; and 90° strength (invalid). The rows of data are the same as for table 6.

Tables 9, 12, and 15 address just the average ply thickness. The individual sample thickness data are included, followed by the SS, F-test, probability of significance, the linear regression, and the magnitude of the regression coefficient.

Table 6. IM7/F584 spreadsheet.

	Actual Values					Invalid	Normalized to Ply T of 0.00550				Invalid
Sample	t_p: AE,AF	G_{12} 0.5–1K	G_{12} 0.5–3K	G_{12} 0.5–7K	G_{12} 0.5–10K	S	G_{12} 0.5–1K	G_{12} 0.5–3K	G_{12} 0.5–7K	G_{12} 0.5–10K	S
AE-4-0-H-8-1	0.00563	794,584	741,380	640,821	533,512	12,420	812,642	758,229	655,385	545,637	12,702
AE-4-0-H-8-2	0.00538	789,679	803,724	709,064	599,742	14,247	771,731	785,458	692,949	586,111	13,923
AE-4-A-H-8-1	0.00563	713,162	701,928	631,021	558,089	12,997	729,370	717,881	645,362	570,773	13,292
AE-4-A-H-8-2	0.00563	768,442	745,481	621,517	492,786	12,700	785,907	762,423	635,642	503,985	12,989
AE-4-0-T-8-1	0.00550	725,146	740,621	670,876	590,636	12,506	725,146	740,621	670,876	590,636	12,506
AE-4-0-T-8-2	0.00538	799,340	790,532	703,912	612,352	12,534	781,173	772,565	687,914	598,435	12,249
AE-4-A-T-8-1	0.00563	770,455	755,941	671,205	537,596	12,789	787,966	773,121	686,460	549,814	13,080
AE-4-A-T-8-2	0.00538	795,576	728,119	628,486	529,703	13,023	777,495	711,571	614,202	517,665	12,727
AF-4-0-H-52-1	0.00596	708,450	670,789	586,213	470,580	19,482	767,901	727,079	635,406	510,069	21,117
AF-4-0-H-52-2	0.00606	716,432	675,456	639,091	515,161	18,601	789,078	743,946	703,894	567,398	20,487
AF-4-A-H-52-1	0.00588	663,364	581,519	553,851	459,480	21,550	709,753	622,185	592,582	491,611	23,057
AF-4-A-H-52-2	0.00585	688,966	620,574	577,341	479,388	21,050	732,327	659,632	613,677	509,559	22,375
AF-4-0-T-52-1	0.00588	630,861	576,486	513,521	416,453	17,732	674,977	616,800	549,431	445,575	18,972
AF-4-0-T-52-2	0.00579	675,831	680,210	609,715	488,302	20,576	711,276	715,885	641,693	513,912	21,655
AF-4-A-T-52-1	0.00583	683,564	691,235	562,159	466,856	21,598	724,195	732,323	595,574	494,606	22,881
AF-4-A-T-52-2	0.00581	737,673	745,507	713,593	572,470	21,102	778,942	787,214	753,514	604,496	22,283

		Actual Values					Invalid	Normalized to Ply T of 0.00550				Invalid
Sample		t_p: AE,AF	G_{12} 0.5–1K	G_{12} 0.5–3K	G_{12} 0.5–7K	G_{12} 0.5–10K	S	G_{12} 0.5–1K	G_{12} 0.5–3K	G_{12} 0.5–7K	G_{12} 0.5–10K	S
	DOF	Sum of Squares										
$SS_{corr}T$		5.20E–04	8.50E+12	7.91E+12	6.29E+12	4.33E+12	4.39E+09	9.09E+12	8.45E+12	6.73E+12	4.62E+12	4.77E+09
SS_C	1	1.44E–10	2.29E+07	7.41E+08	8.13E+08	1.06E+09	4.74E+06	3.97E+06	5.55E+08	6.32E+08	8.30E+08	5.14E+06
SS_L	1	4.17E–08	3.79E+07	1.76E+09	8.20E+08	6.97E+08	8.80E+04	1.18E+09	3.36E+08	3.83E+07	5.62E+07	8.05E+05
SS_T	1	5.38E–07	2.65E+10	3.67E+10	1.70E+10	2.14E+10	2.14E+08	5.00E+09	1.09E+10	2.58E+09	6.64E+09	3.01E+08
SS_{C-L}	1	9.77E–10	6.86E+09	8.78E+09	4.52E+09	1.03E+09	1.64E+05	8.10E+09	1.06E+10	5.63E+09	1.43E+09	2.77E+05
SS_{C-T}	1	3.08E–08	6.64E+08	2.04E+09	3.33E+09	5.84E+09	5.18E+06	8.91E+06	5.01E+08	1.41E+09	3.66E+09	3.66E+06
SS_{L-T}	1	2.83E–10	3.42E+08	9.36E+08	5.46E+07	2.78E+08	2.11E+05	4.18E+08	9.84E+08	7.86E+07	3.07E+08	7.56E+04
SS_{C-L-T}	1	8.79E–09	1.15E+08	4.68E+09	3.15E+09	3.44E+09	2.18E+05	6.70E+08	7.27E+09	4.96E+09	4.92E+09	2.95E+04
SS_E	8	8.05E–08	7.44E+09	1.21E+10	2.16E+10	1.39E+10	6.42E+06	6.70E+09	1.10E+10	2.28E+10	1.38E+10	5.10E+06
Total	15	7.01E–07	4.20E+10	6.78E+10	5.13E+10	4.77E+10	2.31E+08	2.21E+10	4.21E+10	3.81E+10	3.16E+10	3.16E+08
		F Test										
C		0.01	0.02	0.49	0.30	0.61	5.91	0.00	0.40	0.22	0.48	8.07
L		4.15	0.04	1.16	0.30	0.40	0.11	1.41	0.24	0.01	0.03	1.26
T		53.43	28.49	24.14	6.29	12.30	266.26	5.98	7.88	0.90	3.85	471.93
C–L		0.10	7.37	5.78	1.67	0.59	0.20	9.68	7.66	1.98	0.83	0.44
C–T		3.06	0.71	1.34	1.23	3.35	6.46	0.01	0.36	0.50	2.12	5.75
L–T		0.03	0.37	0.62	0.02	0.16	0.26	0.50	0.71	0.03	0.18	0.12
C–L–T		0.87	0.12	3.08	1.17	1.98	0.27	0.80	5.28	1.74	2.86	0.05

Table 6. IM7/F584 spreadsheet (Continued).

	Actual Values					Invalid	Normalized to Ply *T* of 0.00550				Invalid
Sample	t_p: **AE,AF**	G_{12} **0.5–1K**	G_{12} **0.5–3K**	G_{12} **0.5–7K**	G_{12} **0.5–10K**	*S*	G_{12} **0.5–1K**	G_{12} **0.5–3K**	G_{12} **0.5–7K**	G_{12} **0.5–10K**	*S*
	Probability of Being Significant										
C	0.0924	0.1207	0.4954	0.4018	0.5425	0.9588	0.0532	0.4566	0.3496	0.4929	0.9782
L	0.9240	0.1550	0.6869	0.4034	0.4553	0.2510	0.7313	0.3650	0.0895	0.1389	0.7064
T	0.9999	0.9993	0.9988	0.9636	0.9920	1.0000	0.9598	0.9770	0.6304	0.9148	1.0000
C–L	0.2367	0.9736	0.9571	0.7681	0.5351	0.3364	0.9856	0.9756	0.8026	0.6114	0.4721
C–T	0.8817	0.5774	0.7202	0.7010	0.8955	0.9653	0.0796	0.4367	0.4987	0.8169	0.9567
L–T	0.1291	0.4387	0.5450	0.1096	0.2999	0.3778	0.5003	0.5774	0.1278	0.3161	0.2606
C–L–T	0.6227	0.2658	0.8827	0.6882	0.8026	0.3835	0.6030	0.9493	0.7765	0.8705	0.1649
Regression: *Y*=Int+*C* *C+*L* *L+*TT+*CL**C*L+*CT**C*T+*LT**L*T+*CLT**C*L*T: *C*:–1=Oven/1=AC; *L*:–1=Hand/1=Tape; *T*:–1=8 Ply/1=52 Ply**											
Int	0.00570	728,845	703,094	627,024	520,194	16,557	753,742	726,683	648,410	537,518	17,268
C Coeff	0.00000	–1,195	–6,806	–7,128	–8,148	544	–498	–5,890	–6,284	–7,204	567
L Coeff	–0.00005	–1,540	10,488	7,159	6,602	–74	–8,596	4,579	1,548	1,875	–224
T Coeff	0.00018	–40,703	–47,872	–32,589	–36,608	3,655	–17,686	–26,050	–12,689	–20,364	4,335
C–L	0.00001	20,706	23,425	16,805	8,008	101	22,501	25,684	18,763	9,457	132
C–T	0.00000	–4,621	7,650	–1,848	–4,168	115	–5,112	7,843	–2,216	–4,381	69
L–T	–0.00004	6,444	11,293	14,428	19,110	569	746	5,595	9,399	15,119	478
C–L–T	0.00002	2,681	17,100	14,024	14,672	–117	6,471	21,323	17,613	17,532	–43
Percent Effect of Each Factor From Regression—2*Factor Coefficient/Intercept											
C	0	0	–2	–2	–3	7	0	–2	–2	–3	7
L	–2	0	3	2	3	–1	–2	1	0	1	–3
T	6	–11	–14	–10	–14	44	–5	–7	–4	–8	50
C–L	0	6	7	5	3	1	6	7	6	4	2
C–T	0	–1	2	–1	–2	1	–1	2	–1	–2	1
L–T	–2	2	3	5	7	7	0	2	3	6	6
C–L–T	1	1	5	4	6	–1	2	6	5	7	0

Table 7. IM7/F655 actual values spreadsheet.

	Actual Values					Invalid				Invalid			Invalid
Sample	t_p: AE,AF	G_{12} 0.5–1K	G_{12} 0.5–3K	G_{12} 0.5–7K	G_{12} 0.5–10K	S	t_p: AA,AC	E_1	ν_{12}	X_c	t_p: AB,AD	E_2	Y_c
B–O–H–8–1	0.00550	815,484	784,646	701,351	625,226	16,725	0.00625	20,264,858	0.4838	69,293	0.00625	1,440,267	19,919
B–O–H–8–2	0.00538	771,190	720,320	666,990	595,030	16,383	0.00625	21,019,136	0.4825	66,101	0.00625	1,456,385	17,005
B–A–H–8–1	0.00525	914,735	882,365	709,264	587,186	16,340	0.00619	18,632,861	0.4817	69,556	0.00613	1,458,339	20,844
B–A–H–8–2	0.00525	687,242	668,996	588,380	499,741	15,311	0.00606	21,440,589	0.4428	74,412	0.00613	1,482,570	22,152
B–O–T–8–1	0.00513	1,070,736	1,019,848	873,607	747,815	16,211	0.00531	20,866,451	0.4991	66,630	0.00531	1,569,147	17,630
B–O–T–8–2	0.00550	826,042	780,363	669,394	570,171	15,400	0.00531	16,898,822	0.5504	24,245	0.00550	1,446,311	16,378
B–A–T–8–1	0.00513	895,541	842,967	732,216	634,816	15,682	0.00525	16,480,002	0.4234	39,778	0.00519	1,486,333	17,124
B–A–T–8–2	0.00600	755,801	708,616	587,561	495,618	14,082	0.00519	15,471,181	0.3886	43,674	0.00556	1,398,827	16,217
B–O–H–52–1	0.00577	582,559	582,108	524,517	444,336	15,012	0.00611	18,807,848	0.3726	76,796	0.00585	985,644	12,272
B–O–H–52–2	0.00581	682,153	653,877	567,769	473,876	14,897	0.00611	25,577,350	0.1656	79,604	0.00581	1,057,246	16,781
B–A–H–52–1	0.00544	752,381	717,398	646,731	573,852	20,012	0.00533	24,143,824	0.3859	97,995	0.00513	1,320,860	29,035
B–A–H–52–2	0.00538	741,883	730,372	655,701	588,962	20,761	0.00521	18,486,487	0.2001	92,381	0.00525	1,283,418	25,499
B–O–T–52–1	0.00567	684,456	678,721	565,106	466,623	15,287	0.00639	15,214,110	0.4900	57,216	0.00623	880,641	8,351
B–O–T–52–2	0.00567	757,352	743,183	621,642	518,934	16,449	0.00676	15,555,784	0.3688	59,640	0.00640	880,559	7,905
B–A–T–52–1	0.00565	887,723	764,516	688,224	600,072	19,513	0.00537	16,462,328	0.0649	86,882	0.00535	1279,846	31,487
B–A–T–52–2	0.00567	778,770	724,028	649,419	585,594	20,430	0.00547	21,994,575	0.1608	82,166	0.00538	1383,988	29,145

		Actual Values					Invalid				Invalid			Invalid
Sample		t_p: AE,AF	G_{12} 0.5–1K	G_{12} 0.5–3K	G_{12} 0.5–7K	G_{12} 0.5–10K	S	t_p: AA,AC	E_1	ν_{12}	X_c	t_p: AB,AD	E_2	Y_c
	DOF	Sum of Squares												
$SS_{corr}T$		4.86E–04	9.93E+12	9.00E+12	6.82E+12	5.07E+12	4.51E+09	5.35E–04	5.90E+15	2.22E+00	7.38E+10	5.26E–04	2.71E+13	5.92E+09
SS_C	1	2.59E–08	3.14E+09	3.63E+08	2.82E+08	9.58E+08	1.55E+07	1.23E–06	7.46E+10	4.67E–02	4.77E+08	7.64E–07	1.19E+11	3.54E+08
SS_L	1	2.59E–08	3.14E+10	1.70E+10	6.66E+09	3.35E+09	3.56E+05	3.74E–07	5.41E+13	2.98E–04	1.72E+09	2.14E–07	1.58E+09	2.32E+07
SS_T	1	2.38E–07	4.73E+10	4.14E+10	2.32E+10	1.58E+10	1.65E+07	5.38E–08	1.67E+12	1.49E–01	2.00E+09	5.27E–08	4.44E+11	1.09E+07
SS_{C-L}	1	1.61E–07	4.41E+09	1.21E+10	2.80E+09	6.09E+08	5.81E+05	2.12E–08	1.46E+12	4.80E–02	3.08E+05	1.20E–08	1.74E+09	9.23E+06
SS_{C-T}	1	5.00E–08	2.93E+10	1.44E+10	2.68E+10	3.66E+10	3.13E+07	7.89E–07	1.05E+13	5.85E–03	4.52E+08	5.15E–07	1.50E+11	2.60E+08
SS_{L-T}	1	6.99E–10	6.43E+06	2.96E+08	2.82E+08	1.63E+08	1.20E+06	1.52E–06	2.36E+12	6.84E–06	1.22E+08	1.28E–06	5.08E+09	2.16E+06
SS_{C-L-T}	1	1.30E–09	4.09E+09	1.40E+09	5.44E+08	5.92E+06	3.22E+05	3.12E–08	1.23E+13	1.47E–02	7.32E+07	4.13E–08	1.66E+10	4.11E+07
SS_E	8	4.64E–07	8.02E+10	6.81E+10	4.25E+10	3.18E+10	3.58E+06	8.88E–08	6.69E+13	5.33E–02	9.56E+08	1.12E–07	2.05E+10	2.56E+07
Total	15	9.67E–07	2.00E+11	1.55E+11	1.03E+11	8.93E+10	6.93E+07	4.10E–06	1.49E+14	3.18E–01	5.80E+09	2.99E–06	7.59E+11	7.26E+08
		F Test												
C		0.45	0.31	0.04	0.05	0.24	34.73	110.43	0.01	7.01	3.99	54.46	46.35	110.82
L		0.45	3.13	2.00	1.25	0.84	0.80	33.73	6.47	0.04	14.39	15.27	0.62	7.26
T		4.11	4.72	4.86	4.37	3.99	36.78	4.85	0.20	22.35	16.75	3.76	173.49	3.41
C–L		2.78	0.44	1.42	0.53	0.15	1.30	1.91	0.18	7.21	0.00	0.85	0.68	2.89
C–T		0.86	2.92	1.70	5.04	9.22	69.93	71.10	1.26	0.88	3.78	36.72	58.65	81.27
L–T		0.01	0.00	0.03	0.05	0.04	2.68	136.78	0.28	0.00	1.02	91.24	1.99	0.67
C–L–T		0.02	0.41	0.16	0.10	0.00	0.72	2.81	1.47	2.21	0.61	2.94	6.49	12.86
		Probability of Being Significant												
C		0.4777	0.4090	0.1584	0.1762	0.3636	0.9996	1.0000	0.0729	0.9706	0.9190	0.9999	0.9999	1.0000
L		0.4777	0.8853	0.8052	0.7045	0.6146	0.6016	0.9996	0.9655	0.1623	0.9947	0.9955	0.5454	0.9727
T		0.9228	0.9383	0.9415	0.9300	0.9191	0.9997	0.9412	0.3332	0.9985	0.9965	0.9115	1.0000	0.8981
C–L		0.8661	0.4742	0.7329	0.5115	0.2944	0.7127	0.7953	0.3133	0.9723	0.0392	0.6174	0.5659	0.8725
C–T		0.6198	0.8742	0.7710	0.9450	0.9839	1.0000	1.0000	0.7049	0.6238	0.9122	0.9997	0.9999	1.0000
L–T		0.0848	0.0196	0.1432	0.1762	0.1554	0.8598	1.0000	0.3905	0.0248	0.6578	1.0000	0.8035	0.5647
C–L–T		0.1154	0.4593	0.3047	0.2427	0.0298	0.5789	0.8680	0.7408	0.8243	0.5434	0.8754	0.9657	0.9929

Table 7. IM7/F655 actual values spreadsheet (Continued).

	Actual Values					Invalid				Invalid			Invalid
Sample	t_p: AE,AF	G_{12} 0.5–1K	G_{12} 0.5–3K	G_{12} 0.5–7K	G_{12} 0.5–10K	S	t_p: AA,AC	E_1	ν_{12}	X_c	t_p: AB,AD	E_2	Y_c
Regression: Y=Int+C *C+L*L+T*T+CL*C*L+CT*C*T+LT*L*T+CLT*C*L*T: C:–1=Oven/1=AC; L:–1=Hand/1=Tape; T:–1=8 Ply/1=52 Ply													
Int	0.00551	787,753	750,145	652,992	562,991	16,781	0.00578	19,207,263	0.3726	67,898	0.00573	1,300,649	19,234
C Coeff	–0.00004	14,007	4,762	4,195	7,739	985	–0.00028	–68,282	–0.0540	5,457	–0.00022	86,124	4,704
L Coeff	0.00004	44,299	32,635	20,404	14,465	–149	–0.00015	–1,839,356	–0.0043	–10,369	–0.00012	–9,942	–1,204
T Coeff	0.00012	–54,343	–50,870	–38,103	–31,460	1,014	0.00006	323,025	–0.0965	11,187	–0.00006	–166,624	825
C–L	0.00010	–16,600	–27,511	–13,236	–6,170	–191	–0.00004	302,397	–0.0548	139	–0.00003	10,418	760
C–T	–0.00001	–634	–4,298	–4,195	–3,190	274	0.00031	–384,233	–0.0007	2,760	0.00028	–17,825	367
L–T	–0.00006	42,773	30,041	40,935	47,850	1,398	–0.00022	809,797	–0.0191	5,314	–0.00018	96,879	4,028
C–L–T	–0.00001	15,992	9,367	5,830	608	–142	–0.00004	877,840	–0.0303	2,138	–0.00005	32,238	1,602
Percent Effect of Each Factor From Regression—2*Factor Coefficient/Intercept													
C	–1	4	1	1	3	12	–10	–1	29	16	–8	13	49
L	1	11	9	6	5	–2	–5	–19	–2	–31	–4	–2	–13
T	4	–14	–14	–12	–11	12	2	3	–52	33	–2	–26	9
C–L	4	–4	–7	–4	–2	–2	–1	3	–29	0	–1	2	8
C–T	0	0	–1	–1	–1	3	11	–4	0	8	10	–3	4
L–T	–2	11	8	13	17	17	–8	8	–10	16	–6	15	42
C–L–T	0	4	2	2	0	–2	–2	9	–16	6	–2	5	17

Table 8. IM7/F655 normalized values spreadsheet.

	Normalized to Ply *T* of 0.00550				Invalid		Invalid		Invalid
Sample	G_{12} 0.5–1K	G_{12} 0.5–3K	G_{12} 0.5–7K	G_{12} 0.5–10K	S	E_1	X_c	E_2	Y_c
B–O–H–8–1	815,484	784,646	701,351	625,226	16,725	23,028,248	78,742	1,636,667	22,635
B–O–H–8–2	753,663	703,949	651,831	581,507	16,010	23,885,381	75,115	1,654,983	19,323
B–A–H–8–1	873,156	842,257	677,024	560,496	15,598	20,961,969	78,250	1,624,059	23,212
B–A–H–8–2	656,004	638,587	561,636	477,025	14,615	23,633,376	82,023	1,651,043	24,670
B–O–T–8–1	997,731	950,313	814,043	696,828	15,106	20,155,095	64,358	1,515,654	17,029
B–O–T–8–2	826,042	780,363	669,394	570,171	15,400	16,322,726	23,419	1,446,311	16,378
B–A–T–8–1	834,482	785,492	682,292	591,533	14,613	15,730,911	37,970	1,401,882	16,151
B–A–T–8–2	824,510	773,036	640,976	540,674	15,363	14,592,137	41,192	1,414,722	16,402
B–O–H–52–1	611,076	610,603	550,193	466,086	15,747	20,879,341	85,254	1,047,678	13,044
B–O–H–52–2	720,315	690,458	599,532	500,386	15,730	28,394,435	88,371	1,116,393	17,720
B–A–H–52–1	744,489	709,873	639,947	567,833	19,802	23,384,053	94,911	1,230,802	27,055
B–A–H–52–2	726,319	715,050	641,945	576,606	20,325	17,516,916	87,536	1,225,080	24,340
B–O–T–52–1	705,994	700,080	582,889	481,307	15,768	17,687,732	66,519	997,649	9,461
B–O–T–52–2	781,185	766,570	641,204	535,265	16,967	19,118,385	73,299	1,025,267	9,204
B–A–T–52–1	912,554	785,901	707,476	616,857	20,058	16,059,403	84,756	1,244,046	30,606
B–A–T–52–2	803,277	746,812	669,855	604,022	21,072	21,879,218	81,735	1,354,953	28,534

Table 8. IM7/F655 normalized values spreadsheet (Continued).

Sample		Normalized to Ply T of 0.00550				Invalid		Invalid		Invalid
		G_{12} 0.5–1K	G_{12} 0.5–3K	G_{12} 0.5–7K	G_{12} 0.5–10K	S	E_1	X_c	E_2	Y_c
	DOF	Sum of Squares								
$SS_{corr}T$		9.90E+12	8.98E+12	6.80E+12	5.05E+12	4.52E+09	6.53E+15	8.17E+10	2.91E+13	6.23E+09
SS_C	1	1.67E+09	6.28E+06	7.18E+06	3.83E+08	1.22E+07	1.54E+13	6.93E+07	3.12E+10	2.74E+08
SS_L	1	3.85E+10	2.20E+10	9.25E+09	4.95E+09	2.64E+03	1.01E+14	2.42E+09	3.86E+10	4.98E+07
SS_T	1	2.07E+10	1.78E+10	8.35E+09	5.44E+09	3.04E+07	2.73E+12	2.05E+09	6.02E+11	1.08E+06
SS_{C-L}	1	7.90E+07	3.09E+09	3.78E+07	2.31E+08	1.88E+05	2.01E+12	4.98E+05	1.51E+09	1.07E+07
SS_{C-T}	1	2.05E+10	8.55E+09	1.96E+10	2.94E+10	2.53E+07	9.50E+10	8.88E+07	6.63E+10	1.96E+08
SS_{L-T}	1	1.67E+07	1.34E+08	1.27E+08	5.05E+07	1.40E+06	5.38E+12	5.93E+08	3.90E+10	2.38E+07
SS_{C-L-T}	1	2.86E+09	7.10E+08	2.78E+08	4.08E+06	3.16E+05	1.11E+13	6.76E+07	1.07E+10	4.43E+07
SS_E	8	5.52E+10	4.47E+10	2.28E+10	1.59E+10	2.43E+06	7.53E+13	9.17E+08	1.19E+10	2.36E+07
Total	15	1.40E+11	9.69E+10	6.05E+10	5.64E+10	7.22E+07	2.13E+14	6.21E+09	8.01E+11	6.23E+08
		F Test								
C		0.24	0.00	0.00	0.19	40.25	1.64	0.60	20.89	92.83
L		5.58	3.94	3.24	2.49	0.01	10.69	21.16	25.91	16.90
T		3.00	3.18	2.93	2.74	99.84	0.29	17.93	403.76	0.37
$C–L$		0.01	0.55	0.01	0.12	0.62	0.21	0.00	1.01	3.62
$C–T$		2.97	1.53	6.87	14.79	83.03	0.01	0.78	44.46	66.57
$L–T$		0.00	0.02	0.04	0.03	4.60	0.57	5.18	26.17	8.08
$C–L–T$		0.41	0.13	0.10	0.00	1.04	1.18	0.59	7.15	15.02

Table 8. IM7/F655 normalized values spreadsheet (Continued).

Sample	Normalized to Ply *T* of 0.00550				Invalid		Invalid		Invalid
	G_{12} 0.5–1K	G_{12} 0.5–3K	G_{12} 0.5–7K	G_{12} 0.5–10K	S	E_1	X_c	E_2	Y_c
	Probability of Being Significant								
C	0.3637	0.0259	0.0388	0.3275	0.9998	0.7636	0.5409	0.9982	1.0000
L	0.9543	0.9175	0.8905	0.8467	0.0720	0.9886	0.9982	0.9991	0.9966
T	0.8787	0.8877	0.8745	0.8632	1.0000	0.3951	0.9971	1.0000	0.4389
C–L	0.0826	0.5214	0.0887	0.2578	0.5461	0.3435	0.0509	0.6564	0.9064
C–T	0.8770	0.7488	0.9694	0.9951	1.0000	0.0775	0.5957	0.9998	1.0000
L–T	0.0380	0.1195	0.1617	0.1226	0.9356	0.5286	0.9476	0.9991	0.9783
C–L–T	0.4625	0.2693	0.2372	0.0350	0.6620	0.6913	0.5355	0.9718	0.9953
Regression: *Y*=Int+*C* **C*+*L*L*+*T***T*+*CL***C***L*+*CT***C***T*+*LT***L***T*+*CLT***C***L***T*: *C*:–1=Oven/1=AC; *L*:–1=Hand/1=Tape; *T*:–1=8 Ply/1=52 Ply**									
Int	786,643	748,999	651,974	561,989	16,806	20,201,833	71,466	1,349,199	19,735
C Coeff	10,206	627	670	4,892	875	–982,085	2,081	44,124	4,136
L Coeff	49,079	37,071	24,042	17,593	–13	–2,508,632	–12,310	–49,139	–1,765
T Coeff	–35,991	–33,331	–22,844	–18,444	1,378	413,103	11,332	–193,966	260
C–L	–2,222	–13,887	–1,536	3,798	109	354,301	176	9,716	817
C–T	1,022	–2,899	–2,816	–1,776	296	579,881	6,089	49,384	1,220
L–T	35,802	23,114	35,006	42,892	1,256	77,047	2,356	64,363	3,502
C–L–T	13,377	6,662	4,170	–505	–140	833,863	2,055	25,818	1,664
Percent Effect of Each Factor From Regression — 2*Factor Coefficient/Intercept									
C	3	0	0	2	10	–10	6	7	42
L	12	10	7	6	0	–25	–34	–7	–18
T	–9	–9	–7	–7	16	4	32	–29	3
C–L	–1	–4	0	1	1	4	0	1	8
C–T	0	–1	–1	–1	4	6	17	7	12
L–T	9	6	11	15	15	1	7	10	35
C–L–T	3	2	1	0	–2	8	6	4	17

Table 9. IM7/F655 thickness spreadsheet.

O–H–8	0.00550	0.00538	0.00625	0.00625	0.00625	0.00625
A–H–8	0.00525	0.00525	0.00619	0.00606	0.00613	0.00613
O–T–8	0.00513	0.00550	0.00531	0.00531	0.00531	0.00550
A–T–8	0.00513	0.00600	0.00525	0.00519	0.00519	0.00556
O–H–52	0.00577	0.00581	0.00611	0.00611	0.00585	0.00581
A–H–52	0.00544	0.00538	0.00533	0.00521	0.00513	0.00525
O–T–52	0.00567	0.00567	0.00639	0.00676	0.00623	0.00640
A–T–52	0.00565	0.00567	0.00537	0.00547	0.00535	0.00538

Source Correction	DOF	Sum of Squares	*F* Test	Probability	Linear Regression	Percent of Intercept*
		0.00155			0.00568 +	
C	1	1.5E–06	15.95	0.9997	–0.00018 **C*+	–6
L	1	2.8E–07	2.90	0.9037	–0.00008 **L*+	–3
T	1	8E–08	0.84	0.6340	0.00004 **T*+	1
C–L	1	7.2E–09	0.07	0.2140	0.00001 **C***L*+	0
C–T	1	1.1E–06	11.63	0.9985	–0.00015 **C***T*+	–5
L–T	1	1.8E–06	18.98	0.9999	0.00019 **L***T*+	7
C–L–T	1	5.8E–08	0.60	0.5573	–0.00003 **C***L***T*	–1
E	40	3.84E–06	–	–		
Total	47	8.7E–06	–	–		

* 2*coefficient/intercept*100

C: –1=Oven, +1=Autoclave
L: –1=Hand, +1=Tape Layered
T: –1=8 Plies, +1=52 Plies

Table 10. IM7/8551–7 actual values spreadsheet.

	Actual Values					Invalid				Invalid			Invalid
Sample	t_p: AE,AF	G_{12} 0.5–1K	G_{12} 0.5–3K	G_{12} 0.5–7K	G_{12} 0.5–10K	S	t_p: AA,AC	E_1	ν_{12}	X_c	t_p: AB,AD	E_2	Y_c
8–O–H–8–1	0.00563	701,020	642,576	495,774	362,991	15,279	0.00581	16,671,847	0.4300	95,799	0.00588	1,406,853	21,926
8–O–H–8–2	0.00563	739,104	657,357	509,398	392,771	14,991	0.00569	25,288,448	0.3617	64,598	0.00581	1,365,366	21,800
8–A–H–8–1	0.00563	781,154	730,714	574,961	420,857	17,049	0.00563	20,506,425	0.3976	42,731	0.00600	1,471,501	24,813
8–A–H–8–2	0.00575	749,655	699,814	548,880	388,344	16,948	0.00563	20,984,729	0.4378	54,395	0.00575	1,486,763	25,254
8–O–T–8–1	0.00575	745,456	694,280	537,554	379,940	15,163	0.00581	18,241,855	0.4690	49,503	0.00588	1,384,822	21,307
8–O–T–8–2	0.00563	760,163	706,998	560,117	406,218	15,141	0.00594	17,519,059	0.4749	39,505	0.00588	1,345,861	19,396
8–A–T–8–1	0.00575	733,747	704,967	566,241	411,366	16,499	0.00606	18,921,587	0.4494	41,247	0.00600	1,358,902	21,533
8–A–T–8–2	0.00563	741,381	709,222	559,460	408,967	16,774	0.00613	20,476,153	0.4935	42,085	0.00594	1,307,224	20,009
8–O–H–52–1	0.00610	574,507	615,456	498,547	307,985	21,730	0.00608	–	–	69,278	0.00617	1,183,595	25,022
8–O–H–52–2	0.00604	625,043	607,766	474,535	256,180	21,845	0.00608	17,058,694	–	79,705	0.00620	1,176,416	23,609
8–A–H–52–1	0.00615	659,262	636,825	519,734	314,233	22,377	0.00597	–	–	72,858	0.00621	1,132,674	26,104
8–A–H–52–2	0.00615	656,336	617,710	472,930	273,840	22,463	0.00616	20,771,744	0.3864	74,686	0.00634	1,207,213	26,566
8–O–T–52–1	0.00598	586,751	621,880	512,412	329,206	22,015	0.00603	–	–	77,043	0.00625	1,132,948	26,736
8–O–T–52–2	0.00596	638,743	658,012	552,497	351,918	21,931	0.00628	16,997,873	0.2480	66,628	0.00613	1,205,710	27,325
8–A–T–52–1	0.00592	612,956	649,882	532,319	324,169	22,885	0.00606	–	–	74,721	0.00626	1,153,588	26,568
8–A–T–52–2	0.00596	654,742	612,226	492,334	316,423	22,610	0.00615	–	–	71,715	0.00618	1,098,078	26,841

Table 10. IM7/8551-7 actual values spreadsheet (Continued).

		Actual Values					Invalid				Invalid			Invalid
Sample		t_p: AE,AF	G_{12} 0.5–1K	G_{12} 0.5–3K	G_{12} 0.5–7K	G_{12} 0.5–10K	S	t_p: AA,AC	E_1	ν_{12}	X_c	t_p: AB,AD	E_2	Y_c
	DOF	Sum of Squares												
$SS_{corr}T$		5.48E–04	7.51E+12	6.98E+12	4.42E+12	1.99E+12	5.84E+09	5.70E–04	3.14E+15	1.54E+00	6.46E+10	5.87E–04	2.61E+13	9.25E+09
SS_C	1 (1)	3.61E–09	2.98E+09	1.54E+09	9.93E+08	3.15E+08	5.65E+06	3.25E–10	1.25E+12	2.28E–04	2.86E+08	1.44E–08	1.29E+07	6.98E+06
SS_L	1 (1)	1.50E–08	9.21E+06	1.39E+09	2.97E+09	2.78E+09	7.07E+03	1.26E–07	8.60E+12	8.43E–03	5.24E+08	1.48E–09	1.23E+10	1.81E+06
SS_T	1	5.24E–07	5.56E+10	1.73E+10	5.52E+09	3.04E+10	1.56E+08	2.81E–07	–	–	1.54E+09	4.31E–07	2.11E+11	6.70E+07
SS_{C-L}	1 (1)	7.91E–09	2.38E+09	1.74E+09	1.42E+09	4.38E+08	1.40E+04	2.33E–08	2.11E+12	2.48E–04	2.39E+08	5.78E–12	6.30E+09	6.49E+06
SS_{C-T}	1	5.78E–12	6.01E+08	1.06E+09	1.75E+09	6.79E+08	9.41E+05	5.73E–09	–	–	3.09E+08	2.31E–11	3.27E+09	8.99E+05
SS_{L-T}	1	3.43E–08	6.31E+07	2.69E+07	5.42E+07	1.02E+09	1.84E+05	5.72E–08	–	–	3.88E+08	7.49E–09	3.14E+09	1.96E+07
SS_{C-L-T}	1	6.99E–10	1.40E+08	2.94E+08	5.93E+07	1.28E+08	6.78E+04	3.65E–08	–	–	1.78E+08	3.61E–09	2.11E+09	4.09E+04
SS_E	8 (4)	2.60E–08	4.86E+09	2.25E+09	3.70E+09	3.77E+09	1.36E+05	7.19E–08	3.87E+13	4.13E–03	7.20E+08	5.30E–08	1.01E+10	4.41E+06
Total	15 (7)	6.11E–07	6.67E+10	2.56E+10	1.65E+10	3.95E+10	1.63E+08	6.02E–07	5.07E+13	1.30E–02	4.18E+09	5.11E–07	2.48E+11	1.07E+08
		F Test												
C		1.11	4.90	5.48	2.15	0.67	331.60	0.04	0.13	0.22	3.18	2.18	0.01	12.66
L		4.62	0.02	4.95	6.44	5.91	0.41	13.98	0.89	8.17	5.83	0.22	9.76	3.28
T		160.93	91.47	61.51	11.94	64.60	9168.75	31.24	–	–	17.07	65.01	167.69	121.50
C–L		2.43	3.91	6.18	3.06	0.93	0.82	2.59	0.22	0.24	2.65	0.00	5.01	11.78
C–T		0.00	0.99	3.75	3.79	1.44	55.22	0.64	–	–	3.43	0.00	2.60	1.63
L–T		10.53	0.10	0.10	0.12	2.17	10.78	6.36	–	–	4.31	1.13	2.50	35.59
C–L–T		0.21	0.23	1.05	0.13	0.27	3.97	4.06	–	–	1.98	0.55	1.68	0.07
		Probability of Being Significant												
C		0.6772	0.9423	0.9526	0.8191	0.5630	1.0000	0.1460	0.2630	0.3372	0.8874	0.8220	0.0782	0.9926
L		0.9362	0.0949	0.9432	0.9651	0.9589	0.4625	0.9943	0.6007	0.9540	0.9578	0.3508	0.9859	0.8923
T		1.0000	1.0000	0.9999	0.9914	1.0000	1.0000	0.9995	–	–	0.9967	1.0000	1.0000	1.0000
C–L		0.8425	0.9166	0.9622	0.8818	0.6370	0.6092	0.8539	0.3350	0.3505	0.8580	0.0228	0.9444	0.9911
C–T		0.0326	0.6507	0.9113	0.9125	0.7359	0.9999	0.5524	–	–	0.8988	0.0457	0.8542	0.7626
L–T		0.9882	0.2444	0.2351	0.2593	0.8214	0.9889	0.9643	–	–	0.9284	0.6813	0.8472	0.9997
C–L–T		0.3447	0.3558	0.6634	0.2705	0.3832	0.9187	0.9214	–	–	0.8030	0.5186	0.7686	0.2077

	Actual Values					Invalid				Invalid			Invalid
Sample	t_p: AE,AF	G_{12} 0.5–1K	G_{12} 0.5–3K	G_{12} 0.5–7K	G_{12} 0.5–10K	S	t_p: AA,AC	E_1	ν_{12}	X_c	t_p: AB,AD	E_2	Y_c
Regression: *Y*=Int+*C* **C*+*L***L*+*T***T*+*CL***C***L*+*CT***C***T*+*LT***L***T*+*CLT***C***L***T*: *C*:–1=Oven/1=AC; *L*:–1=Hand/1=Tape; *T*:–1=8 Ply/1=52 Ply													
Int	0.00585	685,001	660,355	525,481	352,838	19,106	0.00597	18,648,391	0.3754	63,531	0.00605	1,276,095	24,050
C Coeff	0.00002	13,653	9,815	7,877	4,437	594	0.00000	341,788	0.0516	–4,226	0.00003	898	661
L Coef	–0.00003	–759	9,328	13,636	13,188	21	0.00009	–3,451,541	0.0649	–5,725	0.00001	–27,703	–336
T Coeff	0.00018	–58,959	–32,886	–18,567	–43,594	3,126	0.00013	–6,696,544	–0.0638	9,798	0.00016	–114,817	2,046
C–L	–0.00002	–12,189	–10,424	–9,405	–5,232	–30	0.00004	1,546,075	–0.0056	3,862	0.00000	–19,842	–637
C–T	–0.00005	–1,986	–1,298	1,841	7,997	107	–0.00006	–164,438	0.0558	4,923	–0.00002	14,006	1107
L–T	0.00000	6,129	–8,124	–10,461	–6,515	–243	–0.00002	–1,551,004	0.0000	4,392	0.00000	–14,288	–237
C–L–T	–0.00001	2,958	4,287	1,925	–2,824	65	–0.00005	1,551,180	–	–3,337	–0.00002	11,483	51
Percent Effect of Each Factor From Regression—2*Factor Coefficient/Intercept													
C	1	4	3	3	3	6	0	4	28	–13	1	0	5
L	–1	0	3	5	7	0	3	–37	35	–18	0	–4	–3
T	6	–17	–10	–7	–25	33	4	–72	–34	31	5	–18	17
C–L	–1	–4	–3	–4	–3	0	1	17	–3	12	0	–3	–5
C–T	–2	–1	0	1	5	1	–2	–2	30	15	–1	2	9
L–T	0	2	–2	–4	–4	–3	–1	–17	0	14	0	–2	–2
C–L–T	0	1	1	1	–2	1	–2	17	–	–11	0	2	0

Table 11. IM7/8551–7 normalized values spreadsheet.

Sample	Normalized to Ply T of 0.00600				Invalid		Invalid		Invalid
	G_{12} 0.5–1K	G_{12} 0.5–3K	G_{12} 0.5–7K	G_{12} 0.5–10K	S	E_1	X_c	E_2	Y_c
8–O–H–8–1	657,206	602,415	464,788	340,304	14,324	16,150,852	92,806	1,377,543	21,469
8–O–H–8–2	692,910	616,272	477,561	368,223	14,054	23,971,341	61,233	1,322,698	21,119
8–A–H–8–1	732,332	685,044	539,026	394,553	15,983	19,224,773	40,060	1,471,501	24,813
8–A–H–8–2	718,420	670,655	526,010	372,163	16,242	19,673,184	50,995	1,424,815	24,201
8–O–T–8–1	714,396	665,352	515,156	364,110	14,531	17,671,797	47,956	1,355,971	20,863
8–O–T–8–2	712,653	662,811	525,109	380,829	14,195	17,336,569	39,094	1,317,822	18,992
8–A–T–8–1	703,174	675,593	542,648	394,226	15,811	19,118,687	41,676	1,358,902	21,533
8–A–T–8–2	695,045	664,896	524,493	383,406	15,726	20,902,740	42,962	1,293,607	19,801
8–O–H–52–1	583,714	625,319	506,537	312,920	22,078	–	70,166	1,217,737	25,743
8–O–H–52–2	629,050	611,662	477,576	257,823	21,985	17,277,395	80,727	1,216,007	24,403
8–A–H–52–1	676,167	653,153	533,061	322,290	22,951	–	72,508	1,172,608	27,025
8–A–H–52–2	673,165	633,548	485,057	280,862	23,039	21,337,641	76,721	1,274,926	28,056
8–O–T–52–1	584,871	619,887	510,770	328,151	21,944	–	77,413	1,180,154	27,850
8–O–T–52–2	634,649	653,794	548,955	349,662	21,790	17,787,838	69,724	1,232,761	27,938
8–A–T–52–1	605,098	641,550	525,495	320,013	22,592	–	75,439	1,203,502	27,717
8–A–T–52–2	650,545	608,301	489,178	314,395	22,465	–	73,554	1,131,513	27,658

Sample		Normalized to Ply T of 0.00600				Invalid		Invalid		Invalid
		G_{12} 0.5–1K	G_{12} 0.5–3K	G_{12} 0.5–7K	G_{12} 0.5–10K	S	E_1	X_c	E_2	Y_c
	DOF	Sum of Squares								
$SS_{corr}T$		7.11E+12	6.62E+12	4.19E+12	1.88E+12	5.61E+09	2.77E+15	6.41E+10	2.64E+13	9.47E+09
SS_C	1 (1)	3.74E+09	1.92E+09	1.20E+09	3.99E+08	6.13E+06	6.17E+12	2.66E+08	7.66E+08	9.65E+06
SS_L	1 (1)	2.44E+08	5.54E+08	1.85E+09	2.15E+09	1.60E+05	3.85E+13	3.74E+08	1.02E+10	1.25E+06
SS_T	1	2.17E+10	2.40E+09	9.10E+07	1.64E+10	2.10E+08	5.96E+14	2.01E+09	1.05E+11	1.19E+08
SS_{C-L}	1 (1)	3.30E+09	2.46E+09	1.91E+09	6.41E+08	1.68E+05	1.52E+13	2.57E+08	5.97E+09	6.62E+06
SS_{C-T}	1	6.36E+08	9.52E+08	1.61E+09	6.49E+08	7.26E+05	1.92E+13	2.69E+08	3.57E+09	7.16E+05
SS_{L-T}	1	7.75E+08	5.57E+08	4.85E+07	5.18E+08	5.32E+04	1.77E+13	3.01E+08	1.17E+09	1.67E+07
SS_{C-L-T}	1	5.26E+07	1.63E+08	1.75E+07	1.58E+08	1.16E+04	4.93E+13	2.03E+08	9.87E+08	9.97E+03
SS_E	8 (4)	4.07E+09	1.67E+09	3.34E+09	3.46E+09	1.58E+05	5.67E+14	6.94E+08	1.47E+10	4.94E+06
Total	15 (7)	3.45E+10	1.07E+10	1.01E+10	2.43E+10	2.17E+08	1.31E+15	4.38E+09	1.42E+11	1.59E+08
	F Test									
C		7.34	9.18	2.87	0.92	310.38	0.04	3.06	0.42	15.65
L		0.48	2.65	4.44	4.98	8.11	0.27	4.31	5.55	2.03
T		42.57	11.46	0.22	37.82	10,628.60	–	23.20	57.06	192.57
$C–L$		6.49	11.74	4.58	1.48	8.51	0.11	2.96	3.26	10.73
$C–T$		1.25	4.55	3.86	1.50	36.75	–	3.10	1.95	1.16
$L–T$		1.52	2.66	0.12	1.20	2.69	–	3.47	0.64	27.07
$C–L–T$		0.10	0.78	0.04	0.37	0.59	–	2.34	0.54	0.02

Table 11. IM7/8551–7 normalized values spreadsheet (Continued).

Sample	Normalized to Ply *T* of 0.00600				Invalid		Invalid		Invalid
	G_{12} 0.5–1K	G_{12} 0.5–3K	G_{12} 0.5–7K	G_{12} 0.5–10K	S	E_1	X_c	E_2	Y_c
	Probability of Being Significant								
C	0.9733	0.9837	0.8714	0.6349	1.0000	0.1551	0.8817	0.4638	0.9958
L	0.4920	0.8576	0.9318	0.9438	0.9784	0.3701	0.9286	0.9538	0.8080
T	0.9998	0.9904	0.3470	0.9997	1.0000	–	0.9987	0.9999	1.0000
C–L	0.9657	0.9910	0.9352	0.7419	0.9806	0.2404	0.8763	0.8912	0.9888
C–T	0.7039	0.9346	0.9150	0.7444	0.9997	–	0.8836	0.7995	0.6871
L–T	0.7476	0.8587	0.2580	0.6940	0.8604	–	0.9005	0.5529	0.9992
C–L–T	0.2440	0.5975	0.1573	0.4379	0.5340	–	0.8357	0.5160	0.0980
Regression: *Y*=Int+*C* **C*+*L* **L*+*T*T*+*CL* **C***L*+*CT***C***T*+*LT***L***T*+*CLT***C***L***T*: *C*:–1=Oven/1=AC; *L*:–1=Hand/1=Tape; *T*:–1=8 Ply/1=52 Ply**									
Int	666,462	643,141	511,964	342,746	18,732	18,549,337	63,315	1,284,504	24,324
C Coeff	15,281	10,952	8,657	4,993	619	355,803	–4,075	6,918	777
L Coeff	–3,908	5,882	10,762	11,603	–100	–3,162,257	–4,837	–25,225	–280
T Coeff	–36,805	–12,239	–2,385	–31,981	3,624	–6,169,080	11,217	–80,853	2,725
C–L	–14,369	–12,390	–10,929	–6,332	–103	1,469,684	4,006	–19,316	–643
C–T	–6,958	–5,901	–1,741	5,687	–58	–450,827	4,338	8,557	1,022
L–T	6,305	–7,715	–10,038	–6,367	–213	–1,697,087	4,099	–14,931	–211
C–L–T	1,814	3,196	1,047	–3,145	27	1,309,362	–3,566	7,854	–25
Percent Effect of Each Factor From Regression—2*Factor Coefficient/Intercept									
C	5	3	3	3	7	4	–13	1	6
L	–1	2	4	7	–1	–34	–15	–4	–2
T	–11	–4	–1	–19	39	–67	35	–13	22
C–L	–4	–4	–4	–4	–1	16	13	–3	–5
C–T	–2	–2	–1	3	–1	–5	14	1	8
L–T	2	–2	–4	–4	–2	–18	13	–2	–2
C–L–T	1	1	0	–2	0	14	–11	1	0

Table 12. IM7/8551–7 thickness spreadsheet.

O–H–8	0.00563	0.00581	0.00588	0.00563	0.00569	0.00581
A–H–8	0.00563	0.00563	0.00600	0.00575	0.00563	0.00575
O–T–8	0.00575	0.00581	0.00588	0.00563	0.00594	0.00588
A–T–8	0.00575	0.00606	0.00600	0.00563	0.00613	0.00594
O–H–52	0.00610	0.00608	0.00617	0.00604	0.00608	0.00620
A–H–52	0.00615	0.00597	0.00621	0.00615	0.00616	0.00634
O–T–52	0.00598	0.00603	0.00625	0.00596	0.00628	0.00613
A–T–52	0.00592	0.00606	0.00626	0.00596	0.00615	0.00618

Source	DOF	Sum of Squares	*F* Test	Probability	Linear Regression	Percent of Intercept*
corr		0.001704	–	–	0.00596 +	
C	1	1.31E–08	0.77	0.6141	0.00002 * *C*+	1
L	1	2.44E–08	1.43	0.7611	0.00002 * *L*+	1
T	1	1.22E–06	71.29	1.0000	0.00016 • *T*+	5
C–L	1	1.46E–09	0.09	0.2284	0.00001 * *C** *L*+	0
C–T	1	2.29E–09	0.13	0.2842	–0.00001 * *C** *T*+	0
L–T	1	8.70E–08	5.10	0.9705	–0.00004 * *L** *T*+	–1
C–L–T	1	2.57E–08	1.51	0.7732	–0.00002 * *C** *L** *T*	–1
E	40	6.82E–07	–	–		
Total	47	2.05E–06	–	–		

* 2*coefficient/intercept*100

C: –1=Oven, +1=Autoclave
L: –1=Hand, +1=Tape Layed
T: –1=8 Plies, +1=52 Plies

Table 13. AS4/3501–6 actual values spreadsheet.

	Actual Values					Invalid				Invalid			Invalid
Sample	t_p: AE,AF	G_{12} 0.5–1K	G_{12} 0.5–3K	G_{12} 0.5–7K	G_{12} 0.5–10K	S	t_p: AA,AC	E_1	ν_{12}	X_c	t_p: AB,AD	E_2	Y_c
3–O–H–8–1	0.00500	1,006,303	936,355	818,201	708,896	11,555	0.00506	2,1217,007	0.4559	46,254	0.00506	1,639,467	16,767
3–O–H–8–2	0.00500	807,162	827,141	736,416	628,393	10,529	0.00494	14,729,021	0.6170	45,178	0.00513	1,610,896	15,389
3–A–H–8–1	0.00438	1,144,537	1,014,724	882,889	779,707	13,151	0.00488	18,954,006	0.5133	43,922	0.00494	1,684,099	16,582
3–A–H–8–2	0.00438	1,057,746	968,134	872,776	765,543	12,684	0.00488	18,522,392	0.4624	40,565	0.00494	1,752,833	13,618
3–O–T–8–1	0.00525	906,245	856,927	774,254	646,628	10,436	0.00500	15,045,135	0.5499	28,730	0.00563	1,467,161	14,545
3–O–T–8–2	0.00500	973,113	945,631	804,294	684,206	11,281	0.00550	15,209,015	0.4407	36,477	0.00550	1,585,890	14,782
3–A–T–8–1	0.00450	1,121,078	1,083,951	955,871	845,105	13,760	0.00500	20,684,146	0.4004	42,248	0.00513	1,695,696	14,827
3–A–T–8–2	0.00450	1,108,007	1,077,214	945,072	850,498	13,367	0.00513	18,625,075	0.4213	46,278	0.00531	1,649,331	15,119
3–O–H–52–1	0.00527	742,562	733,733	657,355	553,536	17,027	0.00513	25,737,352	0.6335	90,026	0.00471	1,293,998	17,834
3–O–H–52–2	0.00519	737,639	689,689	565,154	476,751	17,396	0.00481	20,638,207	0.1717	88,082	0.00488	1,263,795	18,940
3–A–H–52–1	0.00510	840,339	805,621	734,657	619,272	20,949	0.00469	24,943,475	0.5238	109,854	0.00469	1,491,972	33,426
3–A–H–52–2	0.00510	794,169	789,620	715,613	617,354	19,947	0.00469	13,309,394	0.0411	100,287	0.00456	1,457,452	30,342
3–O–T–52–1	0.00579	777,901	740,419	620,248	488,218	19,693	0.00521	15,175,172	0.1998	94,924	0.00500	1,243,635	19,775
3–O–T–52–2	0.00587	729,440	715,940	592,459	437,251	13,821	0.00523	23,725,789	0.4039	94,373	0.00519	1,138,975	17,919
3–A–T–52–1	0.00531	781,625	756,549	688,528	615,443	19,693	0.00546	17,982,655	0.2031	99,107	0.00498	1,721,092	26,256
3–A–T–52–2	0.00517	880,376	830,023	766,019	695,517	19,979	0.00546	15,995,249	0.3200	92,359	0.00490	1,468,115	30,146

Table 13. AS4/3501–6 actual values spreadsheet (Continued).

		Actual Values					Invalid				Invalid			Invalid
Sample		t_p: AE,AF	G_{12} 0.5–1K	G_{12} 0.5–3K	G_{12} 0.5–7K	G_{12} 0.5–10K	S	t_p: AA,AC	E_1	ν_{12}	X_c	t_p: AB,AD	E_2	Y_c
	DOF	**Sum of Squares**												
$S_{corr}T$		4.08E–04	1.30E+13	1.19E+13	9.20E+12	6.78E+12	3.76E+09	4.11E–04	5.64E+15	2.53E+00	7.54E+10	4.05E–04	3.65E+13	6.25E+09
SS_C	1	9.71E–07	6.86E+10	4.84E+10	6.16E+10	8.48E+10	2.97E+07	3.00E–08	3.78E+11	2.15E–02	1.60E+08	1.69E–07	1.76E+11	1.23E+08
SS_L	1	2.45E–07	1.36E+09	3.65E+09	1.67E+09	8.04E+08	9.12E+04	5.34E–07	1.52E+13	1.44E–02	5.50E+07	4.69E–07	3.15E+09	5.68E+06
SS_T	1	1.43E–06	2.12E+11	1.70E+11	1.31E+11	1.23E+11	1.67E+08	5.92E–09	1.32E+13	1.16E–01	1.21E+10	4.60E–07	2.52E+11	3.33E+08
SS_{C-L}	1	5.11E–08	9.38E+07	5.96E+08	1.15E+09	7.05E+09	1.12E+05	5.11E–08	7.19E+12	4.84E–04	1.00E+04	7.49E–09	1.69E+10	2.04E+06
SS_{C-T}	1	6.99E–08	1.15E+10	4.76E+09	1.81E+08	2.28E+07	7.54E+05	1.94E–08	3.49E+13	1.88E–04	1.99E+07	7.91E–09	3.24E+10	1.38E+08
SS_{L-T}	1	6.01E–08	9.06E+07	2.33E+09	1.91E+09	1.90E+09	5.84E+05	8.60E–08	3.89E+12	2.96E–06	1.35E+07	4.21E–09	7.82E+09	7.07E+05
SS_{C-L-T}	1	5.11E–08	9.72E+07	2.04E+09	7.19E+08	3.12E+07	2.44E+05	8.32E–08	1.17E+12	3.35E–03	2.26E+08	1.02E–08	5.99E+09	7.37E+06
SS_E	8	4.62E–08	3.30E+10	1.51E+10	1.17E+10	1.15E+10	1.89E+07	1.91E–07	1.42E+14	2.71E–01	1.15E+08	7.12E–08	4.94E+10	2.01E+07
Total	15	2.93E–06	3.26E+11	2.47E+11	2.10E+11	2.30E+11	2.18E+08	1.00E–06	2.18E+14	4.27E–01	1.27E+10	1.20E–06	5.43E+11	6.30E+08
F Test														
C		168.10	16.60	25.64	42.05	58.88	12.55	1.25	0.02	0.64	11.13	18.98	28.44	49.03
L		42.44	0.33	1.93	1.14	0.56	0.04	22.35	0.85	0.42	3.83	52.73	0.51	2.26
T		248.00	51.24	89.97	89.62	85.79	70.75	0.25	0.74	3.43	839.89	51.62	40.73	132.78
$C–L$		8.84	0.02	0.32	0.78	4.90	0.05	2.14	0.40	0.01	0.00	0.84	2.74	0.81
$C–T$		12.10	2.79	2.52	0.12	0.02	0.32	0.81	1.96	0.01	1.38	0.89	5.24	55.12
$L–T$		10.40	0.02	1.23	1.30	1.32	0.25	3.60	0.22	0.00	0.94	0.47	1.27	0.28
$C–L–T$		8.84	0.02	1.08	0.49	0.02	0.10	3.48	0.07	0.10	15.73	1.15	0.97	2.94
Probability of Being Significant														
C		1.0000	0.9964	0.9990	0.9998	0.9999	0.9924	0.7047	0.1123	0.5516	0.9897	0.9976	0.9993	0.9999
L		0.9998	0.4177	0.7981	0.6837	0.5237	0.1508	0.9985	0.6178	0.4667	0.9140	0.9999	0.5047	0.8290
T		1.0000	0.9999	1.0000	1.0000	1.0000	1.0000	0.3679	0.5853	0.8988	1.0000	0.9999	0.9998	1.0000
$C–L$		0.9822	0.1160	0.4104	0.5977	0.9423	0.1672	0.8181	0.4570	0.0921	0.0204	0.6142	0.8635	0.6061
$C–T$		0.9917	0.8667	0.8490	0.2658	0.0971	0.4121	0.6066	0.8009	0.0575	0.7266	0.6266	0.9487	0.9999
$L–T$		0.9879	0.1140	0.7012	0.7131	0.7163	0.3674	0.9056	0.3473	0.0072	0.6394	0.4890	0.7070	0.3900
$C–L–T$		0.9822	0.1181	0.6715	0.4965	0.1134	0.2435	0.9010	0.1957	0.2385	0.9959	0.6842	0.6464	0.8751

	Actual Values					Invalid				Invalid			Invalid
Sample	t_p: AE,AF	G_{12} 0.5–1K	G_{12} 0.5–3K	G_{12} 0.5–7K	G_{12} 0.5–10K	S	t_p: AA,AC	E_1	ν_{12}	X_c	t_p: AB,AD	E_2	Y_c
Regression: Y=Int+C *C+L *L+T*T+CL *C*L+CT*C*T+LT*L *T+CLT*C*L *T: C:–1=Oven/1=AC; L:–1=Hand/1=Tape; T:–1=8 Ply/1=52 Ply													
Int	0.00505	900,515	860,729	758,113	650,770	15,329	0.00507	18,780,818	0.3974	68,667	0.00503	1,510,275	19,767
C Coeff	–0.00025	65,469	55,000	62,065	72,785	1,362	–0.00004	–153,769	–0.0367	3,161	–0.00010	104,798	2,773
L Coef	0.00012	9,208	15,102	10,230	7,088	–75	0.00018	–975,539	–0.0300	–1,855	0.00017	–14,039	–596
T Coeff	0.00030	–115,009	–103,030	–90,609	–87,852	3,234	0.00002	907,593	–0.0852	27,460	–0.00017	–125,396	4,563
C–L	–0.00006	–2,421	6,102	8,464	20,997	84	0.00006	670,271	0.0055	25	–0.00002	32,523	–357
C–T	0.00006	–2,379	–12,069	–10,921	–10,899	–191	0.00007	–493,157	–0.0004	919	–0.00002	22,114	–210
L–T	0.00007	–26,848	–17,246	–3,365	1,194	217	0.00003	–1,476,949	–0.0034	1,114	0.00002	44,980	2,940
C–L–T	–0.00006	2,465	–11,303	–6,704	1,396	–123	0.00007	–270,317	0.0145	–3,758	0.00003	19,347	–679
Percent Effect of Each Factor From Regression—2*Factor Coefficient/Intercept													
C	–10	15	13	16	22	18	–2	–2	–18	9	–4	14	28
L	5	2	4	3	2	–1	7	–10	–15	–5	7	–2	–6
T	12	–26	–24	–24	–27	42	1	10	–43	80	–7	–17	46
$C–L$	–2	–1	1	2	6	1	2	7	3	0	–1	4	–4
$C–T$	2	–1	–3	–3	–3	–2	3	–5	0	3	–1	3	–2
$L–T$	3	–6	–4	–1	0	3	1	–16	–2	3	1	6	30
$C–L–T$	–2	1	–3	–2	0	–2	3	–3	7	–11	1	3	–7

Table 14. AS4/3501–6 normalized values spreadsheet.

Sample	Normalized to Ply T of 0.00500 G_{12} 0.5–1K	G_{12} 0.5–3K	G_{12} 0.5–7K	G_{12} 0.5–10K	Invalid S	E_1	Invalid X_c	E_2	Invalid Y_c
3–O–H–8–1	1,006,303	936,355	818,201	708,896	11,555	21,482,219	46,832	1,659,960	16,977
3–O–H–8–2	807,162	827,141	736,416	628,393	10,529	14,544,909	44,613	1,651,169	15,774
3–A–H–8–1	1,001,470	887,883	772,528	682,244	11,507	18,480,156	42,824	1,663,047	16,375
3–A–H–8–2	925,527	847,118	763,679	669,850	11,099	18,059,332	39,551	1,730,922	13,448
3–O–T–8–1	951,557	899,773	812,967	678,960	10,958	15,045,135	28,730	1,650,556	16,363
3–O–T–8–2	973,113	945,631	804,294	684,206	11,281	16,729,916	40,124	1,744,479	16,260
3–A–T–8–1	1,008,970	975,556	860,284	760,594	12,384	20,684,146	42,248	1,738,088	15,198
3–A–T–8–2	997,206	969,492	850,565	765,448	12,030	19,090,702	47,435	1,752,414	16,064
3–O–H–52–1	782,546	773,242	692,751	583,342	17,944	26,380,786	92,277	1,219,345	16,805
3–O–H–52–2	766,010	716,215	586,890	495,087	18,065	19,844,430	84,694	1,232,200	18,467
3–A–H–52–1	856,500	821,114	748,785	631,181	21,352	23,408,492	103,094	1,400,159	31,369
3–A–H–52–2	809,441	804,805	729,375	629,226	20,331	12,490,354	94,115	1,328,524	27,658
3–O–T–52–1	900,570	857,177	718,056	565,207	22,799	15,817,198	98,940	1,243,635	19,775
3–O–T–52–2	855,689	839,853	695,001	512,928	16,213	24,820,825	98,728	1,182,782	18,608
3–A–T–52–1	829,725	803,106	730,899	653,316	20,905	19,642,592	108,255	1,714,473	26,155
3–A–T–52–2	910,851	858,754	792,535	719,592	20,671	17,471,733	100,885	1,439,882	29,566

Sample	DOF	Normalized to Ply T of 0.00500 G_{12} 0.5–1K	G_{12} 0.5–3K	G_{12} 0.5–7K	G_{12} 0.5–10K	Invalid S	E_1	Invalid X_c	E_2	Invalid Y_c
		Sum of Squares								
SS_{corr}		1.29E+13	1.18E+13	9.17E+12	6.72E+12	3.89E+09	5.78E+15	7.75E+10	3.71E+13	6.20E+09
SS_C	1	5.50E+09	1.86E+09	9.22E+09	2.68E+10	7.47E+06	1.78E+12	1.18E+08	8.75E+10	8.47E+07
SS_L	1	1.40E+10	1.79E+10	1.08E+10	6.09E+09	1.48E+06	1.81E+12	1.88E+07	2.11E+10	7.80E+04
SS_T	1	5.76E+10	4.15E+10	3.28E+10	3.89E+10	2.80E+08	1.55E+13	1.26E+10	5.00E+11	2.40E+08
SS_{C-L}	1	1.70E+09	1.18E+08	3.56E+07	4.25E+09	1.33E+05	1.28E+13	2.79E+07	1.34E+10	1.47E+06
SS_{C-T}	1	5.44E+08	5.68E+07	3.41E+09	5.59E+09	1.92E+06	3.13E+13	2.49E+07	4.27E+10	1.29E+08
SS_{L-T}	1	5.28E+08	1.47E+08	2.15E+08	4.80E+08	5.44E+04	7.04E+11	1.43E+08	3.03E+09	1.42E+05
SS_{C-L-T}	1	6.38E+08	5.62E+09	2.50E+09	7.78E+07	1.42E+06	2.93E+10	9.34E+07	1.20E+10	3.98E+06
SS_E	8	2.86E+10	1.13E+10	1.14E+10	1.08E+10	2.30E+07	1.51E+14	1.82E+08	4.91E+10	2.02E+07
Total	15	1.09E+11	7.85E+10	7.04E+10	9.29E+10	3.15E+08	2.15E+14	1.32E+10	7.29E+11	4.79E+08
		F Test								
C		1.54	1.31	6.46	19.82	2.60	0.09	5.18	14.27	33.60
L		3.91	12.66	7.57	4.51	0.51	0.10	0.82	3.44	0.03
T		16.14	29.31	22.98	28.79	97.55	0.82	551.64	81.61	95.18
$C–L$		0.48	0.08	0.02	3.15	0.05	0.68	1.22	2.19	0.58
$C–T$		0.15	0.04	2.39	4.14	0.67	1.66	1.09	6.97	51.09
$L–T$		0.15	0.10	0.15	0.36	0.02	0.04	6.29	0.49	0.06
$C–L–T$		0.18	3.97	1.75	0.06	0.49	0.00	4.10	1.96	1.58

Table 14. AS4/3501–6 normalized values spreadsheet (Continued).

Sample	Normalized to Ply T of 0.00500				Invalid		Invalid		Invalid
	G_{12} 0.5–1K	G_{12} 0.5–3K	G_{12} 0.5–7K	G_{12} 0.5–10K	S	E_1	X_c	E_2	Y_c
	Probability of Being Significant								
C	0.7505	0.7151	0.9653	0.9979	0.8547	0.2337	0.9476	0.9946	0.9996
L	0.9167	0.9926	0.9750	0.9335	0.5062	0.2358	0.6096	0.8993	0.1353
T	0.9961	0.9994	0.9986	0.9993	1.0000	0.6095	1.0000	1.0000	1.0000
C–L	0.4908	0.2201	0.1215	0.8862	0.1650	0.5657	0.6993	0.8227	0.5331
C–T	0.2937	0.1538	0.8393	0.9237	0.5629	0.7663	0.6732	0.9703	0.9999
L–T	0.2896	0.2442	0.2916	0.4324	0.1061	0.1484	0.9635	0.4978	0.1815
C–L–T	0.3164	0.9185	0.7779	0.1836	0.4979	0.0305	0.9225	0.8006	0.7559
Regression: Y=Int+C * C+L* L+T* T+CL*C* L+CT* C* T+LT* L* T+CLT* C* L* T; C:–1=Oven/1=AC; L:–1=Hand/1=Tape; T:–1=8 Ply/1=52 Ply									
Int	898,915	860,201	757,077	648,030	15,601	18,999,558	69,584	1,521,977	19,679
C Coeff	18,546	10,778	24,005	40,902	683	–333,619	2,717	73,961	2,300
L Coeff	29,545	33,467	25,998	19,502	304	–336,777	1,084	36,311	70
T Coeff	–59,999	–50,918	–45,290	–49,294	4,184	984,993	28,039	–176,852	3,872
C–L	–10,318	–2,718	1,491	16,304	–91	893,132	1,321	28,964	–303
C–T	5,747	–3,027	–3,662	–5,476	58	–209,687	2,995	13,757	–94
L–T	–5,833	1,884	14,607	18,692	346	–1,397,639	1,247	51,673	2,837
C–L–T	–6,315	–18,736	–12,509	–2,205	–298	–42,798	–2,417	27,386	–499
Percent Effect of Each Factor From Regression — 2*Factor Coefficient/Intercept									
C	4	3	6	13	9	–4	8	10	23
L	7	8	7	6	4	–4	3	5	1
T	–13	–12	–12	–15	54	10	81	–23	39
C–L	–2	–1	0	5	–1	9	4	4	-3
C–T	1	–1	–1	–2	1	–2	9	2	–1
L–T	–1	0	4	6	4	–15	4	7	29
C–L–T	–1	–4	-3	–1	–4	0	–7	4	–5

Table 15. AS4/3501–6 thickness spreadsheet.

O–H–8	0.00500	0.00506	0.00506	0.00500	0.00494	0.00513
A–H–8	0.00438	0.00488	0.00494	0.00438	0.00488	0.00494
O–T–8	0.00525	0.00500	0.00563	0.00500	0.00550	0.00550
A–T–8	0.00450	0.00500	0.00513	0.00450	0.00513	0.00531
O–H–52	0.00527	0.00513	0.00471	0.00519	0.00481	0.00488
A–H–52	0.00510	0.00469	0.00469	0.00510	0.00469	0.00456
O–T–52	0.00579	0.00521	0.00500	0.00587	0.00523	0.00519
A–T–52	0.00531	0.00546	0.00498	0.00517	0.00546	0.00490

Source Correction	DOF	Sum of Squares	*F* Test	Probability	Linear Regression	Percent of Intercept*
corr		0.001224			0.00505 +	
C	1	8.21E–07	11.68	0.9985	–0.00013 **C*+	–5
L	1	1.22E–06	17.32	0.9998	0.00016 **L*+	6
T	1	1.18E–07	1.69	0.7983	0.00005 **T*+	2
C–L	1	2.5E–09	0.04	0.1485	–0.00001 **C***L*+	0
C–T	1	8.09E–08	1.15	0.7103	0.00004 **C***T*+	2
L–T	1	7.48E–08	1.06	0.6914	0.00004 **L***T*+	2
C–L–T	1	8.91E–09	0.13	0.2763	0.00001 **C***L***T*	1
E	40	2.81E–06	–	–		
Total	47	5.14E–06	–	–		

* 2*coefficient/intercept*100

C: –1=Oven, +1=Autoclave
L: –1=Hand, +1=Tape Layed
T: –1=8 Plies, +1=52 Plies

REFERENCES

1. Yoon, K.J.; Kim, T.W.; Lee, W.I.; and Jun, E.J.: "Compaction Behavior of Graphite/Epoxy Laminate During Cure," Sixth International Conference on Composite Materials, Second European Conference on Composite Materials, Elsevier Applied Science Publishers, Ltd., Vol. 1, pp. 1.81–1.86, 1987.

2. Bratukhin, A.G.; and Bogolyubov, V.S.: *Composite Manufacturing Technology, Soviet Advanced Composites Technology Series*, Chapman & Hall, London, 1995.

3. Carpenter, J.F.: "Processing Science for AS/3501–6 Carbon/Epoxy Composites," *Report Number N00019–81–C–0184*, Department of the Navy, Naval Air Systems Command, Washington, DC, 1983.

4. Johnson, D.P.: "The Effect of Specimen Size on the Mechanical Response of Laminated Composite Coupons Loaded in Tension and Flexure," Dissertation, Virginia Polytechnic Institute and State University, 1994.

5. Camponeschi, E.T.: "Compression Response of Thick-Section Composite Materials," Dissertation, University of Delaware, 1990.

6. Gipple, K.: "A Comparison of the Compression Response of Thick (6.35 mm) and Thin (1.60 mm) Dry and Moisture Saturated AS4/3501–6 Laminates," DTRC–SME–90/74, David Taylor Research Center, Bethesda, MD, 1990.

7. Vannucci, R.D.: "Effect of Processing Parameters on Autoclaved PRM Polyimide Composites," *NASA–TM–73701*, Lewis Research Center, Cleveland, OH, 1977.

8. "Lightweight Composite Intertank Structure Phase IB Study Final Report," Vol. I, Secs. 6 and 7, *ALS–NLS ADP 3102*, Contract NAS8–37138, General Dynamics Space Systems, CA, and Marshall Space Flight Center, AL, 1993.

9. Montgomery, D.C.: *Design and Analysis of Experiments*, 3rd Edition, John Wiley & Sons, New York, 1991.

10. "Standard Test Method for Compressive Properties of Polymer Matrix Composite Materials with Unsupported Gage Section by Shear Loading," *ASTM D3410*, American Society for Testing and Materials, 1995.

11. "Standard Practice for In-Plane Shear Stress-Strain Response of Unidirectional Polymer Matrix Composites," *ASTM D3518*, American Society for Testing and Materials, 1991.

12. "Standard Test Methods for Void Content of Reinforced Plastics," *ASTM D2734*, American Society for Testing and Materials, 1994.

13. Kim, R.Y.; and Crasto, A.S.: "A Longitudinal Compression Test for Composites Using a Sandwich Specimen," *Journal of Composite Materials*, Vol. 26, No. 13, pp. 1992.

14. "Standard Test Method for Compressive Properties of Unidirectional Polymer Matrix Composite Using a Sandwich Beam," *ASTM D5467*, American Society for Testing and Materials, 1993.

15. "Standard Test Method for Compressive Properties of Rigid Plastics," *ASTM D695*, American Society for Testing and Materials, 1996.

16. "Standard Test Method for Tensile Properties of Polymer Matrix Composite Materials," *ASTM D3039*, American Society for Testing and Materials, 1995.

REPORT DOCUMENTATION PAGE

Form Approved
OMB No. 0704-0188

1. AGENCY USE ONLY *(Leave Blank)*	2. REPORT DATE	3. REPORT TYPE AND DATES COVERED
	July 2003	Technical Memorandum

4. TITLE AND SUBTITLE
Determination of Significant Composite Processing Factors by Designed Experiment
(MSFC Center Director's Discretionary Fund Final Report, Project No. 95–23)

5. FUNDING NUMBERS

6. AUTHORS
J.L. Finckenor

7. PERFORMING ORGANIZATION NAMES(S) AND ADDRESS(ES)
George C. Marshall Space Flight Center
Marshall Space Flight Center, AL 35812

8. PERFORMING ORGANIZATION REPORT NUMBER
M–1080

9. SPONSORING/MONITORING AGENCY NAME(S) AND ADDRESS(ES)
National Aeronautics and Space Administration
Washington, DC 20546–0001

10. SPONSORING/MONITORING AGENCY REPORT NUMBER
NASA/TM—2003–212633

11. SUPPLEMENTARY NOTES
Prepared for the Structures, Mechanics, and Thermal Department, Engineering Directorate

12a. DISTRIBUTION/AVAILABILITY STATEMENT
Unclassified-Unlimited
Subject Category 24
Nonstandard Distribution

12b. DISTRIBUTION CODE

13. ABSTRACT *(Maximum 200 words)*

To determine composite material properties' effects from processing variables, a 3 factorial designed experiment with two replicates was conducted. The factors were cure method (oven versus autoclave), layup (hand versus tape-laying machine), and thickness (8 versus 52 ply). Four material systems were tested: AS4/3501–6, IM7/8551–7, IM7/F655 bismaleimide (BMI), and shear tests on IM7/F584. Material properties were G_{12}, ν_{12}, E_{1C}, and E_{2C}. Since the samples were necessarily nonstandard, strengths, though recorded, cannot be considered valid. Void content was also compared.

Autoclave curing helped material properties for the low modulus fiber material but showed little benefit for higher stiffness fibers. The number of plies was very important for epoxy composites but not for the BMI. E_1 was generally unaffected by any factor.

Particularly high void content did correlate to reduced properties. Autoclave curing reduced void content over oven curing but a moderate amount of voids, <1 percent void content, did not correlate with material properties.

Oven cures and hand layups can produce high-quality parts. Part thickness of epoxy composites is important, though cure optimization may improve performance. Significant variations can be caused by processing and it is important that test coupons always reflect the layup and processes of the final part.

14. SUBJECT TERMS
composite materials, material properties, manufacturing processes, design of experiments

15. NUMBER OF PAGES
80

16. PRICE CODE

17. SECURITY CLASSIFICATION OF REPORT	18. SECURITY CLASSIFICATION OF THIS PAGE	19. SECURITY CLASSIFICATION OF ABSTRACT	20. LIMITATION OF ABSTRACT
Unclassified	Unclassified	Unclassified	Unlimited

NSN 7540-01-280-5500

Standard Form 298 (Rev. 2-89)
Prescribed by ANSI Std. 239-18
298-102